Excitations in the higher-lattice gauge theory model for topological phases. III. The (3+1)-dimensional case

Joe Huxford [1,2] and Steven H. Simon [1]

[1]*Rudolf Peierls Centre for Theoretical Physics, Clarendon Laboratory, Oxford OX1 3PU, United Kingdom*

[2]*Department of Physics, University of Toronto, Ontario, Canada M5S 1A7*

(Received 6 August 2022; revised 12 December 2023; accepted 15 December 2023; published 23 January 2024)

In this, the third paper in our series describing the excitations of the higher-lattice gauge theory model for topological phases, we will examine the (3+1)-dimensional case in detail. We will explicitly construct the ribbon and membrane operators which create the topological excitations, and use these creation operators to find the pattern of condensation and confinement. We also use these operators to find the braiding relations of the excitations, and to construct charge measurement operators which project to states of definite topological charge.

DOI: 10.1103/PhysRevB.109.035152

CONTENTS

I. INTRODUCTION

Over the past decade, there has been significant consideration given to topological phases in 3+1 dimensions, in addition to the (1+1)-dimensional [(1+1)D] and (2+1)-dimensional [(2+1)D] cases that have been more heavily studied in the past. So far, results for (3+1)-dimensional [(3+1)D] topological phases range from the construction of classes of commuting projector models [1–4] to a potential classification of the bosonic phases in the absence of symmetry [5,6]. (3+1)D phases are intriguing for several reasons. First, we live in a (3+1)D world, and so there is a natural interest in studying such phases. Second, the properties of (3+1)D topological phases are quite different from their

(2+1)D cousins. Unlike their (2+1)D counterparts, pointlike particles in (3+1)D are not expected to have nontrivial braiding with each other (outside of the usual bosonic and fermionic cases) [7,8]. However, in these higher-dimensional phases there exist looplike excitations with nontrivial loop-braiding properties, so that exchange processes involving the looplike excitations can result in a nontrivial transformation for the state of the system. Unfortunately, at present there are few examples of toy models where these looplike excitations are constructed explicitly and the properties of the excitations (both pointlike and looplike) are studied in more depth. In this series of papers, we study one such toy model [4], based on higher-lattice gauge theory [4,9–13], and aim to provide a detailed description of the excitations, and the conserved topological charge which they carry.

As we have already seen in Refs. [14,15], the Hamiltonian model for topological phases based on higher-lattice gauge theory [4] hosts rich physics, including nontrivial loop braiding [in the (3+1)D case], condensation, and confinement. In Ref. [14], we gave a brief qualitative description of these features, while in Ref. [15] we examined the (2+1)D model. Now we will give a more explicit and mathematically detailed treatment of the (3+1)D model, with full proofs presented in the Supplemental Material. Our approach focuses heavily on the so-called ribbon and membrane operators, which produce (as well as move and annihilate) the pointlike and looplike excitations of the model, respectively. Because loops are extended objects, they sweep through a surface as they move, rather than just a line as point particles would. Therefore, to produce and move loop excitations we need an operator that is defined across a general membrane rather than a line or ribbon. The ribbon and membrane operators can be used to find the braiding statistics [16,17] of the excitations, while closed ribbon and membrane operators can be used to measure topological charge [18]. In addition, certain properties of the excitations, such as whether they are confined or not, can be obtained directly from these operators. In this paper, we therefore aim to provide and justify the mathematical forms of the ribbon and membrane operators, and demonstrate how we can extract all of the previously mentioned information about the excitations from them.

A. Structure of this paper

In this paper, we will consider the (3+1)D model in various cases (a summary of these cases is presented in Sec. II, along with a brief reminder of the Hamiltonian model). For each case we define the membrane operators and find the effects of braiding in turn, before moving on to the next case. In Secs. III and IV we consider the case where one of the maps describing the model, $\triangleright$, is trivial (case 1 from Table I). In Sec. III we construct the ribbon and membrane operators for the theory and discuss the pattern of condensation and confinement exhibited by the excitations that they produce. In Sec. IV we use these operators to work out the braiding properties of these excitations, which involves passing loop or point particles through loops. In Secs. V and VI we repeat the construction of ribbon operators and the braiding for another special case, called the fake-flat case (case 3 from Table I), while in Secs. VII and VIII we repeat it for another special case (case 2 from Table I), which generalizes the $\triangleright$ trivial case.

Having found the membrane operators and effects of braiding, in Sec. IX we move on to consider the topological charges of the model. These topological charges are conserved quantities carried by the excitations of the model. In (2+1)D, to measure the topological charge in a spatial region, we simply put an operator on the boundary of that region. This boundary will be topologically equivalent to a circle (or multiple circles). However, in (3+1)D there are more topologically distinct surfaces which can enclose our regions of interest. We can use these different surfaces to measure the looplike and pointlike charge carried by the excitations. Using a sphere as our surface of measurement, we can determine the pointlike charge contained within the sphere. We present the corresponding charge measurement operators in Sec. IX A, and also find the charge carried by some simple excitations. However, to measure looplike charge we need some surface with noncontractible loops. An important example is the torus, which we look at in some detail in Sec. IX B. We compare the number of topological charges that we can measure with the torus to the ground-state degeneracy of the 3-torus and find that they are equivalent, in the broad cases that we look at, as previously reported in Ref. [19]. Finally, in Sec. X, we summarize our results and propose further avenues of research based on this work.

In the Supplemental Material [20], we present the proofs of our results that were too lengthy to include in the main text. We demonstrate the commutation relation between the energy terms and the ribbon and membrane operators in Sec. S-I [using some results from the (2+1)D case discussed in Ref. [15]]. Then in Sec. S-II we demonstrate that the nonconfined ribbon and membrane operators are *topological*, meaning that we can deform them through unexcited regions of space without affecting their action, provided that we keep the locations of any excitations they produce fixed. In Sec. S-III, we show that some of the magnetic loop excitations are condensed, and can be produced by operators only acting near the excitations (meaning that they cannot carry looplike topological charge). Next, in Sec. S-IV we find the braiding relations of the various excitations by explicitly calculating the appropriate commutation relations between the membrane and ribbon operators. Finally, in Sec. S-V we construct the measurement operators for topological charge and demonstrate that they are projectors.

II. SUMMARY OF THE MODEL

In this section we will remind the reader of the Hamiltonian model we are studying, the higher-lattice gauge theory model introduced in Ref. [4]. We hope that this will provide a convenient place for the reader to refer back to for definitions of the various terms in the Hamiltonian, along with several useful identities.

We are considering the model defined on a 3D lattice, representing the spatial degrees of freedom, with a Hamiltonian controlling the time evolution. The edges of the lattice are directed, while the plaquettes have a circulation and a base point (a privileged vertex which we can think of as the start of the circulation). The edges are labeled by elements of a group

G, and the plaquettes are labeled by elements of a second group E. These groups are part of a *crossed module*, which consists of the two groups and two maps, ∂ and $\triangleright$. Here ∂ is a group homomorphism from E to G, while $\triangleright$ is a group homomorphism from G to the automorphisms on E. That is, for each element $g \in G$, $g\triangleright$ is a group isomorphism from E to itself (so for $e \in E$, $g \triangleright e$ is an element of E). These maps satisfy two additional constraints, called the Peiffer conditions [4,9,21]:

$$\partial(g \triangleright e) = g\partial(e)g^{-1} \; \forall \; g \in G, \; e \in E, \tag{1}$$

$$\partial(e) \triangleright f = efe^{-1} \; \forall \; e, f \in E. \tag{2}$$

The Hamiltonian is given by a sum of projectors, with terms for the vertices, edges, plaquettes, and blobs (3-cells) of the lattice [4]:

$$H = -\sum_{\text{vertices, } v} A_v - \sum_{\text{edges, } i} \mathcal{A}_i - \sum_{\text{plaquettes, } p} B_p - \sum_{\text{blobs, } b} \mathcal{B}_b. \tag{3}$$

The vertex terms are a sum of vertex transforms, and can be thought of as projecting to states that are 1-gauge invariant. That is

$$A_v = \frac{1}{|G|} \sum_{g \in G} A_v^g,$$

where the vertex transforms have the algebra $A_v^g A_v^h = A_v^{gh}$, which implies that $A_v^g A_v = A_v$. This ensures that the ground states (which are eigenstates of A_v with eigenvalue one) are invariant under the vertex transforms:

$$A_v^g |GS\rangle = A_v^g A_v |GS\rangle = A_v |GS\rangle = |GS\rangle.$$

As for the specific action of the vertex transforms, they act on the edges adjacent to the vertex, as well as any plaquette whose base point is that vertex. For an edge i (initially labeled by g_i) or plaquette p (initially labeled by e_p), we have

$$A_v^g : g_i \to \begin{cases} g g_i & \text{if } v \text{ is the start of } i, \\ g_i g^{-1} & \text{if } v \text{ is the end of } i, \\ g_i & \text{otherwise,} \end{cases}$$

$$A_v^g : e_p \to \begin{cases} g \triangleright e_p & \text{if } v \text{ is the base point of } p, \\ e_p & \text{otherwise.} \end{cases} \tag{4}$$

Similarly, the edge term is a sum of edge transforms (2-gauge transforms)

$$\mathcal{A}_i = \frac{1}{|E|} \sum_{e \in E} \mathcal{A}_i^e,$$

which satisfy a similar algebra to the vertex transforms: $\mathcal{A}_i^e \mathcal{A}_i^f = \mathcal{A}_i^{ef}$. This ensures that individual edge transforms can be absorbed into the corresponding edge term, and into the ground state: $\mathcal{A}_i^e \mathcal{A}_i = \mathcal{A}_i$ and $\mathcal{A}_i^e |GS\rangle = |GS\rangle$. An edge transform $\mathcal{A}_i^e$ applied on an edge i acts on the label of edge i itself, as well as the labels of the adjacent plaquettes:

$$\mathcal{A}_i^e : g_j \to \begin{cases} \partial(e) g_j & \text{if } i = j, \\ g_j & \text{otherwise,} \end{cases}$$

$$\mathcal{A}_i^e : e_p \to \begin{cases} e_p \{ g(v_0(p) - s(i)) \triangleright e^{-1} \} & \text{if } i \text{ is on } p \text{ and aligned with } p, \\ \{ g(\overline{v_0(p) - s(i)}) \triangleright e \} e_p & \text{if } i \text{ is on } p \text{ and aligned against } p, \\ e_p & \text{otherwise.} \end{cases} \tag{5}$$

Here $s(i)$ is the source of edge i, which is the vertex attached to i that i points away from (with the vertex on the other end of i being called the target). $g[v_0(p) - s(i)]$ is the path element for the path from the base point of plaquette p to this source, running around the plaquette and aligned with the plaquette. On the other hand, $g(\overline{v_0(p) - s(i)})$ is the path element for the path around the plaquette from $v_0(p)$ to $s(i)$, but this time antialigned with the plaquette.

The next energy term is the plaquette term B_p, which enforces so-called *fake flatness*. This is similar to the plaquette term from Kitaev's quantum double model, in that it restricts which labels the boundary of a plaquette can have. Unlike the term from the quantum double model, however, the plaquette term in higher-lattice gauge theory relates the label of the boundary to the surface label of the plaquette itself, rather than requiring the boundary label to be trivial as for the quantum double model. For a plaquette whose boundary (starting at the base point and aligned with the circulation of the plaquette) has path label $\hat{g}_p$, and whose surface label is $\hat{e}_p$, the plaquette term B_p acts as

$$B_p = \delta(\partial(\hat{e}_p)\hat{g}_p, 1_G). \tag{6}$$

A plaquette which satisfies this Kronecker delta is called fake flat, and a surface made from fake-flat plaquettes is also called fake flat. Such a fake-flat surface will satisfy a similar condition on its surface and boundary labels. As we showed in Ref. [15], for a surface m whose constituent plaquettes satisfy fake flatness, the overall surface element will satisfy

$$\partial(\hat{e}(m))\hat{g}_{dm} = 1_G,$$

where $\hat{g}_{dm}$ is the group element associated to the boundary of m and the total surface element is constructed by combining individual surface elements, as explained in Ref. [4] and as we will summarize shortly. Note that this fake-flatness condition enables the presence of closed paths with nontrivial label in the ground state (indeed such closed paths are created by the edge transforms), indicating that some magnetic fluxes proliferate in the ground state and so are condensed.

The final energy term is the blob term $\mathcal{B}_b$, which enforces that the surface element of the boundary of the blob (calculated from the plaquettes on that blob using the rules for combining surfaces explained in Ref. [4], which we will

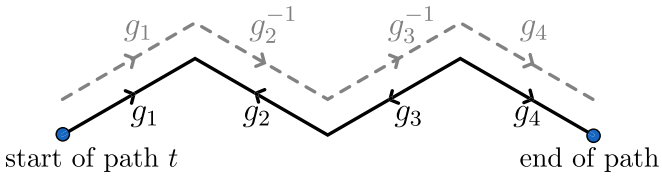

$$g(t) = g_1 g_2^{-1} g_3^{-1} g_4$$

FIG. 1. (Copy of Fig. 37 from Ref. [14]) An electric ribbon operator measures the value of a path and assigns a weight to each possibility, creating excitations at the two ends of the path. In order to find the group element associated to the path, we must first find the contribution of each edge to the path. In this example, the edges along the path are shown in black. Some of the edges are antialigned with the path and so we must invert the elements associated to these edges to find their contribution to the path. This is represented by the gray dashed lines, which are labeled with the contribution of each edge to the path.

describe shortly) is equal to the identity element 1_E. That is,

$$\mathcal{B}_b = \delta(\hat{e}(b), 1_E) \tag{7}$$

for blob b with surface element $\hat{e}(b)$.

A key idea in the higher-lattice gauge theory model is that we can compose edges into paths and plaquettes into surfaces, with composite objects appearing throughout the description of the model as well as in the ribbon and membrane operators. We will therefore briefly review the rules for this kind of combination. First, consider composing edges into paths. If two edges (or more general paths) lie end to end, then we can combine them into one path, with a group label given by the product of the elements for the two edges. Then to combine multiple edges into a path, we take a product of all of the constituent edge labels, with the first edge on the path appearing on the left of the product. If one or more of the edges points against the path (for example, the edges labeled by g_2 and g_3 in Fig. 1), then we include the edge label in the path element with an inverse.

Next consider composition of plaquettes or more generally surfaces. Surfaces have both an orientation and a privileged vertex, called the base point, which we can view as the start of the circulation. We represent this by drawing a circulating arrow in the plaquette which connects to the boundary at the base point, as illustrated in Fig. 2. When we combine two adjacent plaquettes, we must ensure that the base points and orientations of the plaquettes both agree. If they do, as in the example shown in Fig. 2, we can combine the plaquettes into a single surface whose label is a product of the two plaquettes. Contrary to the case of paths, the plaquette appearing first in the circulation is represented in the rightmost position of the product.

While this simple procedure works if the base points and orientations of the two plaquettes agree, we will often want to combine adjacent plaquettes for which this is not the case (similar to how we want to combine edges into paths even if their orientations are not all aligned). In this case, we need a procedure for changing the base point and orientation of a plaquette, and describing the label the plaquette would have with this new decoration. As described in Ref. [14], we can reverse the orientation of a plaquette (while keeping its base point

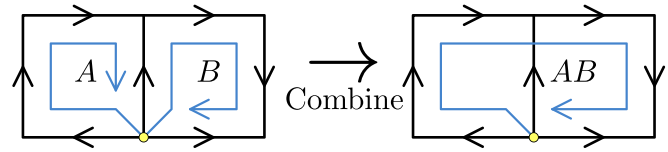

FIG. 2. Two adjacent surfaces can be combined into one if their base point (represented by the yellow dot) and circulation (represented by the blue arrow in the middle of each plaquette) match. The label of the combined surface is given by the product of the two individual elements in reverse order. That is, if the surfaces A and B have labels e_A and e_B, respectively, then the combined surface has label $e_{AB} = e_B e_A$. If two adjacent surfaces do not have the same base point and orientation, then we can still combine them by using a set of rules that describe what happens when we change the orientation or move the base point of a surface.

fixed) by inverting its group label, as shown in Fig. 3. If we want to move the base point along a path t, as shown in Fig. 4, then we must act on that plaquette element with $g(t)^{-1} \triangleright$, so that the plaquette label goes from e_p to $g(t)^{-1} \triangleright e_p$. When moving the base point in this way, we can either move it along the boundary of the plaquette, as shown in the bottom left of Fig. 4, or we can move it away from the boundary, as shown in the top right of Fig. 4. Combining these two procedures, we see that the general formula for the label of a composite surface m is

$$\hat{e}(m) = \prod_{p \in m} g(v_0(m) - v_0(p)) \triangleright e_p^{\sigma_p}, \tag{8}$$

where the $p \in m$ are the constituent plaquettes; $v_0(p)$ is the original base point of plaquette p; $v_0(m)$ is the base point of the combined surface; and σ_p is 1 if the circulation of plaquette p matches the surface and -1 otherwise. Note that this formula hides certain complexities, such as the order of the product and the precise definition of the paths $[v_0(m) - v_0(p))]$, but often we care about situations where these details do not matter (for example, if E is Abelian the order does not matter, and if the surface is also fake flat then the paths only need to be defined up to deformation).

One useful way of checking whether we have correctly composed two surfaces it to examine the boundary of the combined surface. The boundary of a surface made by composing two other surfaces is the product of the two individual boundaries, once we have ensured that the orientations and base points of the two surfaces agree. This product of the

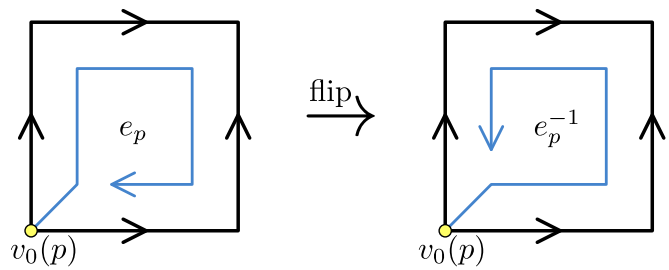

FIG. 3. Given a plaquette with label e_p, the label of the corresponding plaquette with the opposite orientation is e_p^{-1}. Note that when we reverse the orientation of a plaquette, we leave its base point, here $v_0(p)$, in the same position.

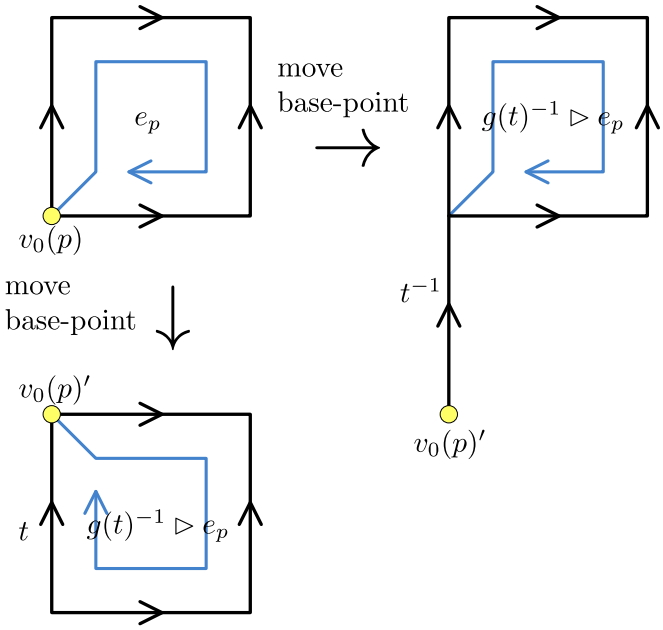

FIG. 4. We can move the base point of a surface, either along the boundary of the surface (resulting in the case shown in the bottom left) or away from the surface (in which case we say that we whisker the surface, and obtain the situation shown in the top right). When we move the base point of plaquette p along a path t in this way, the surface label goes from e_p to $g(t)^{-1} \triangleright e_p$.

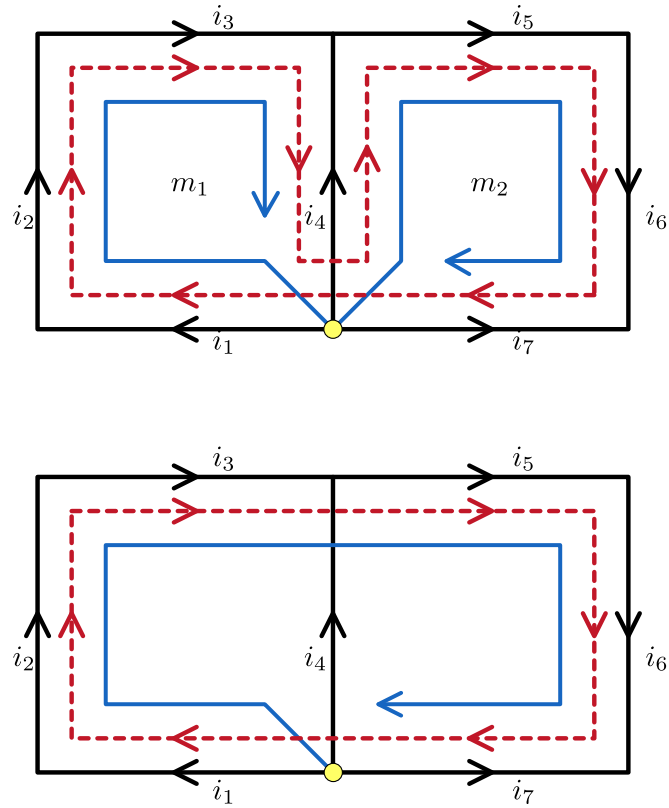

FIG. 5. When we combine two surfaces (top image) into one (bottom image), the boundary of the combined surface is the product of the two individual boundaries (here the boundary path is represented as the dashed red line). This boundary can be simplified by removing edges that appear twice consecutively in the boundary with opposite orientation. In this case the combined boundary includes $i_4^{-1}i_4$ in the top image (this is the section that dips down in the image), which can be removed to give the boundary shown in the bottom image.

boundaries follows from the rules for composing paths given previously. As an example, consider Fig. 5. The boundary of the left surface (m_1) in the top image is $i_1 i_2 i_3 i_4^{-1}$ (note that the boundary starts at the base point and follows the orientation of the plaquette), while the boundary of the right surface (m_2) is $i_4 i_5 i_6 i_7^{-1}$. Here i_x represents an edge, rather than an edge label. The boundary of the combined surface is therefore $i_1 i_2 i_3 i_4^{-1} i_4 i_5 i_6 i_7^{-1}$. This is the path shown in red in the upper image of Fig. 5. We can simplify this path by removing the section $i_4^{-1} i_4$, to give the boundary $i_1 i_2 i_3 i_4^{-1} i_4 i_5 i_6 i_7^{-1}$ shown in the lower image. This rule for combining boundaries ensures that the total surface satisfies fake flatness, if the two constituent surfaces do. If the surface label of surface m_x (for $x = 1$ or 2) is e_x, and the boundary bd$[m(x)]$ has label t_x, then the surface m_1 satisfies fake flatness when

$$\partial(e_1)t_1 = 1_G,$$

and the surface m_2 satisfies fake flatness when

$$\partial(e_2)t_2 = 1_G.$$

The combined surface has label $e_2 e_1$ and boundary label $t_1 t_2$ (note the opposite order of composition for the paths and surfaces). If the two constituent surfaces satisfy fake flatness, then the combined surface label satisfies

$$\begin{aligned}\partial(e_2 e_1)t_1 t_2 &= \partial(e_2)(\partial(e_1)t_1)t_2 \\ &= \partial(e_2)1_G t_2 \\ &= 1_G,\end{aligned}$$

so the total surface satisfies a fake-flatness condition, as we claimed earlier.

Next, we want to remind the reader of the various special cases in which we consider the model. In the most general case of the model, the projectors in the Hamiltonian (specifically the edge and blob terms) no longer commute [4]. Furthermore, there are inconsistencies with regards to changing the branching structure of the lattice (reversing the orientation of edges or plaquettes, or moving the base points of plaquettes around), as we showed in the Appendix of Ref. [14]. This only occurs when $\triangleright$ is nontrivial and there are fake-flatness violations (i.e., plaquette excitations), so the ground-state space is always well defined. This may be similar to how the plaquette terms in the string-net model become poorly defined when neighboring vertex terms are not satisfied and are usually set to zero in such cases [17]. Regardless, these inconsistencies make it difficult to define the plaquette excitations, which form flux tubes. We therefore consider the higher-lattice gauge theory model in various special cases that remove these inconsistencies, or at least make them more manageable. In the first such special case (case 1 in Table I), we take the map $\triangleright$ to be trivial, so that each map $g\triangleright$ is the identity map ($g \triangleright e = e$ for all $g \in G$ and $e \in E$). This leads to a model very similar in character to a (3+1)D version of

TABLE I. A reminder of the special cases of the model.

Case	E	$\triangleright$	$\partial(E)$	Full Hilbert space
1	Abelian	Trivial	$\subset$ center(G)	Yes
2	Abelian	General	$\subset$ center(G)	Yes
3	General	General	General	No

Kitaev's quantum double model, but with some additional excitations (and with condensation and confinement). Because of the Peiffer conditions, taking this form for $\triangleright$ enforces that E be an Abelian group and ∂ maps onto the center of G. In the second special case (case 2 in Table I), we instead take these properties as our starting point, allowing $\triangleright$ to be general, subject to the constraint that E is Abelian and ∂ maps to the center of G. In the final case (case 3 in Table I), we do not place any conditions on our crossed module, but instead restrict the Hilbert space to only include fake-flat states (states where all of the plaquette terms are satisfied). This prevents any inconsistencies, but means that some of the excitations are missing.

We mentioned that when $\triangleright$ is trivial, the higher-lattice gauge theory model becomes similar to a (3+1)D version of Kitaev's quantum double model, i.e., to regular lattice gauge theory. Indeed, there are two subcases where the model is equivalent to lattice gauge theory. The first of these is when the group E is the trivial group $\{1_E\}$ and so ∂ maps to the identity of G. In this case, the blob and edge energy terms become trivial, while the vertex and plaquette terms become the corresponding lattice gauge theory terms. This directly gives the lattice gauge theory Hilbert space and Hamiltonian. The other limit is where the group G is trivial (which also implies that ∂ maps to the identity element because G only has one element). In this case, the vertex and plaquette terms become trivial. Under a change of basis from group elements of E to irreps of E, the remaining energy terms become the lattice gauge theory terms on the dual lattice, where the group is the group of irreps of E. Specifically, the blob energy term of higher-lattice gauge theory becomes the vertex term of lattice gauge theory, while the edge term becomes the plaquette term. More generally, if both groups G and E are nontrivial, but $\triangleright$ is trivial and ∂ maps to the identity of G, we can see that each of the energy terms given in Eqs. (4)–(7) only affects the variables corresponding to one group. This means that these variables decouple and we can think of higher-lattice gauge theory as two decoupled lattice gauge theory models in this case. This also helps us to interpret more general cases of the model. If we change ∂ to map to a larger subgroup, the two lattice gauge theories interact and produce condensation and confinement, as we will discuss later.

III. RIBBON AND MEMBRANE OPERATORS IN THE $\triangleright$ TRIVIAL CASE

First, we consider case 1 from Table I, the case where $\triangleright$ is trivial ($g \triangleright e = e \;\; \forall\, e \in E,\; g \in G$), which enforces that E is Abelian.

A. Electric excitations

The first type of excitation to consider is the electric excitations. The ribbon operators that produce the electric excitations in (3+1)D have the same form as the ones for the (2+1)D case that we considered in Ref. [15]. That is, an electric ribbon operator measures the group element of a path and assigns a weight depending on the measured group element. As we claimed in Ref. [14], an electric ribbon operator applied on a path t has the form

$$\hat{S}^{\vec{\alpha}}(t) = \sum_{g\in G} \alpha_g \delta(\hat{g}(t), g), \tag{9}$$

where α is an arbitrary set of coefficients for each group element $g \in G$ and different choices for these coefficients describe different operators in a space of ribbon operators. A useful basis for this space has basis operators that are labeled by irreps of the group G and the matrix indices for that irrep. These basis electric ribbon operators have the form

$$\hat{S}^{R,a,b}(t) = \sum_{g\in G} [D^R(g)]_{ab} \delta(\hat{g}(t), g), \tag{10}$$

where R is an irrep of G, $D^R(g)$ is the associated matrix representation of element g, and a and b are the matrix indices. As we proved in Ref. [15] [in the (2+1)D case, although the proof also holds for (3+1)D], the operators labeled by nontrivial irreps excite the vertices at the ends of the path, whereas the operator labeled by the trivial irrep is the identity operator (which of course does not create any excitations). In addition, just as in the (2+1)D case discussed in Ref. [15], the irreps that have nontrivial restriction to the image of ∂ label confined excitations. The electric ribbon operators labeled by such irreps cause the edges along the path to be excited, so the excitations produced at the ends of the ribbon are confined.

B. Magnetic excitations

Unlike the electric excitations, the magnetic excitations in (3+1)D are significantly different from their counterparts in (2+1)D. Whereas in (2+1)D the magnetic excitations are point particles that are produced in pairs by a ribbon operator (as we described in Ref. [15]), in (3+1)D the elementary magnetic excitation is a "flux tube" at the boundary of a membrane. That is, the magnetic excitations are looplike. We can see that the magnetic excitations must be looplike by trying to excite a single plaquette. We try changing the value of a single edge belonging to that plaquette. However, as shown in Fig. 6, in (3+1)D each edge belongs to multiple plaquettes (as opposed to two plaquettes when there are only two spatial dimensions). Therefore, changing the label of an edge excites all of the plaquettes around that edge. We can then put one of these plaquettes back into a lower-energy state by changing the label of another edge on that plaquette, but this in turn excites all of the other plaquettes attached to that edge (see the second image in Fig. 6). We see that these excited plaquettes lie on a closed loop that pierces their centers, as shown by the blue loops in Fig. 6. This is made more clear by considering changing more edges. Instead of changing edges along a line, we consider changing edges across some surface (such as the four edges shown in the third image of Fig. 6, which lie on a

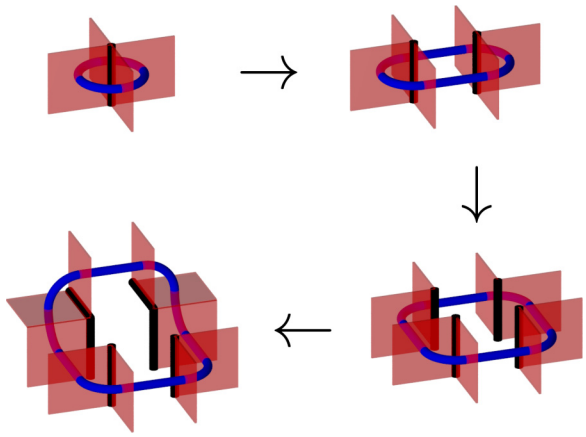

FIG. 6. (Copy of Fig. 40 from Ref. [14]) In order to excite one of the plaquettes in the lattice and produce a magnetic excitation, we change the label of one of the edges (black cylinders) on the boundary of the plaquette. However, this excites all of the plaquettes (the excited plaquettes are the squares, shown in red) adjacent to that edge, as shown in the first image. Note that these plaquettes lie on a closed loop through their centers. If we change another edge label to try to prevent some of the plaquette excitations, we will excite the other plaquettes adjacent to that edge, as shown in the second image. Repeating the process, by changing the edges shown in black excites plaquettes along a closed loop (blue). Changing more edges simply changes the shape of this loop (unless we change the edge labels back and shrink the loop to nothing). This tells us that the magnetic excitations are looplike.

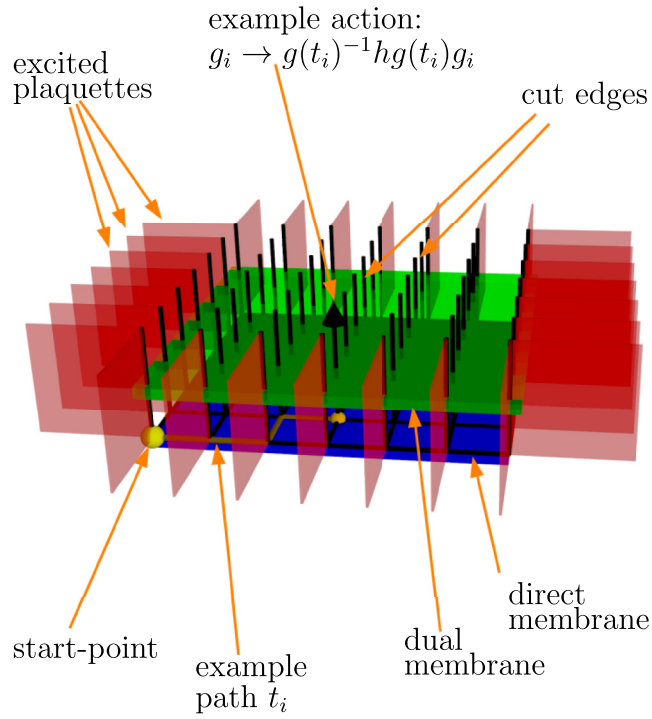

FIG. 7. (Copy of Fig. 41 from Ref. [14]) Here we give an example of the membranes for the flux creation operator (magnetic membrane operator). The dual membrane (green) cuts through the edges changed by the operator. The direct membrane (blue) contains a vertex at the end of each of these cut edges (such as the orange sphere). A path from a privileged start point to the end of the edge (such as the example path, t_i) determines the action on the edge. This action leads to the plaquettes around the boundary of the membrane being excited.

square). Changing these edges excites the plaquettes on the boundary of that surface, much as the ribbon operators in (2+1)D excite particles at the ends of some path.

The fact that we produce a loop excitation by changing edges across a surface rather than just along a path indicates that our creation operator is a membrane operator. While we have given a rough idea of the action of the membrane operator in the above discussion, we will now be more specific. In order to define the operator that produces a magnetic excitation, we must specify the region (the "membrane") that this operator acts on. First we specify a membrane that passes through the centers of plaquettes and cuts through edges. The edges cut by the membrane ("cut edges") are acted on by the operator, as shown in Fig. 7. This membrane is called the dual membrane, and is analogous to the dual path for the magnetic ribbon operator in (2+1)D. In addition to the dual membrane, we must specify a "direct membrane." The cut edges terminate on this membrane. That is, the direct membrane contains one vertex at the end of each of the cut edges, as shown in Fig. 7 (in special cases, with tightly folded membranes, both ends may be on the direct membrane and an edge may be cut twice by the dual membrane). We must also specify a set of paths to the vertices on the direct membrane. These paths go from a common start point to the base of each cut edge (that is, to the vertex that lies on the direct membrane). We call this common start point of the paths the start point of the membrane or of the membrane operator. These features of the membrane operator are illustrated in Fig. 7.

The fact that we specify two membranes as part of the magnetic membrane operator indicates that our "membrane operator" really acts on a "thickened" membrane, much as the ribbon operators in (2+1)D can be considered as acting on thickened strings, that is on ribbons (i.e., their support has some finite thickness). Regardless, we will continue to refer to these operators as membrane operators. This unfortunately means that our use of the term membrane is somewhat ambiguous. Sometimes we mean a "thickened membrane" and sometimes just an unthickened membrane. Generally we try to use membrane to refer to the region on which our membrane operators act, whether those regions are thickened or otherwise. If we want to refer to a surface that may not be part of a membrane operator, we will call this a surface. If we want to refer to part of a thickened membrane, we will use the terms direct and dual membranes.

Having specified these features of the membrane, we can now describe the action of the magnetic membrane operator. The membrane operator acts on the edges cut by the dual membrane, in a way that depends on the direct membrane and the paths we defined. This is analogous to how the action of the magnetic ribbon operator in the (2+1)D case depends on a direct path and a dual path (see Ref. [15]). The membrane operator is labeled by a group element $h \in G$, but the label of each cut edge i is left multiplied by $g(\text{s.p.} - v_i)^{-1} h g(\text{s.p.} - v_i)$ or right multiplied by the inverse, where $g(\text{s.p.} - v_i)$ is the group element associated to the path specified from the start-point s.p. to the vertex v_i on the direct membrane that is

attached to the cut edge i. Whether left multiplication or right multiplication by the inverse is used depends on the orientation of the edge. The edge label is left multiplied if the edge points away from the direct membrane (as with the example edge in Fig. 7) and is right multiplied by the inverse element if it points towards the membrane. That is, the action of the membrane operator on an edge i with initial label g_i is given by

$$C^h(m) : g_i = \begin{cases} g(\text{s.p.} - v_i)^{-1} h g(\text{s.p.} - v_i) g_i & \text{if } i \text{ points away from the direct membrane,} \\ g_i g(\text{s.p.} - v_i)^{-1} h^{-1} g(\text{s.p.} - v_i) & \text{if } i \text{ points towards the direct membrane.} \end{cases} \tag{11}$$

The only difference compared to the action of the magnetic ribbon operator in (2+1)D is that the operator acts on a general membrane, rather than just a ribbon. In particular, this means that instead of having a direct path along a ribbon, we have multiple paths across a membrane. For a given edge i, there are many potential choices for the path from the start point to the edge. However, the action of the membrane operator is unaffected by deforming any of these paths over a region satisfying fake flatness. This is because deforming the path in this way only changes the path element $g(\text{s.p.} - v_i)$ by an element $\partial(e)$ in $\partial(E)$. This factor of $\partial(e)$ is in the center of G and so it does not affect the expression $g(\text{s.p.} - v_i)^{-1} h g(\text{s.p.} - v_i)$, which just gains a factor of $\partial(e)$ and a factor of $\partial(e)^{-1}$ which can be moved together and canceled.

Now that we have described the action of the membrane operator, we can discuss which of the energy terms are excited by the membrane operator. First, note that if the membrane operator is labeled by 1_G, then the membrane operator is just the identity operator and so will not excite any of the energy terms. From now on we will assume that we are talking about a membrane operator labeled by some nontrivial element of G. In this case the membrane operator excites the "boundary plaquettes," which are plaquettes where only one edge on the plaquette is changed by the membrane operator (rather than two for the "bulk" plaquettes). These boundary plaquettes lie around the perimeter of the membrane (they are the red plaquettes in Fig. 7) and we can construct a closed path around the boundary of the dual membrane which passes through these plaquettes.

In addition to these plaquettes, the magnetic membrane operator may also excite the privileged start-point vertex that we defined previously, just as we saw in the (2+1)D case for the magnetic ribbon operator in Ref. [15]. In order for the magnetic membrane operator to produce an eigenstate of this vertex energy term when acting on an initially unexcited region, we need to construct a linear combination of the magnetic membrane operators labeled by elements of G. If the coefficients for this linear combination are a function of conjugacy class (that is, we have an equal sum over all elements of the conjugacy class), the vertex is not excited. On the other hand, if the coefficients within each conjugacy class sum to zero, then the vertex is excited. In any other case (such as when we do not take a superposition of our operators), the start point is neither definitely excited nor definitely unexcited because we do not produce an energy eigenstate. While in Fig. 7 the start point is next to the looplike excitation (at the edge of the membrane), the start point can be displaced any distance from the excited loop (or even away from the membrane). The position of the start point can be interpreted in terms of the picture of the ribbon and membrane operators creating and moving excitations. We can think of the membrane as corresponding to the process where we nucleate a loop at the start point and then grow and move the loop along the membrane to its final position. The fact that the start point may be excited far from the loop suggests that it can be treated as an additional particle. Therefore, when we produce a loop, we may also have to produce a point particle. This is similar to how pointlike charges must be produced in pairs in order to conserve topological charge. Indeed, we will see in Sec. IX A that some looplike excitations carry a nontrivial "pointlike" conserved charge, which must be balanced by the charge carried by the additional excitation at the start point.

The magnetic membrane operator described above is a creation operator for our flux tube, which runs around the perimeter of the membrane. The membrane operator creates a flux tube (and its associated vertex excitation) from the vacuum. Another relevant operator is the one that moves an existing flux tube to a new position. The movement operator can be thought of as an ordinary membrane operator, but with an additional hole whose boundary fits the loop that we wish to move. To see that this is a movement operator, consider splitting a creation operator into two parts, an inner part, which is another creation operator, and an outer part applied on a membrane equivalent to a tube or annulus, as shown in Fig. 8. We know that the overall membrane operator produces and moves an excitation to the boundary of the outer part, while the inner part produces and moves an excitation to the boundary of the inner part. Because the overall membrane operator is a combination of the inner membrane operator and outer membrane operator, this means that the outer membrane operator must take the excitation from the boundary of the inner part and move it to the boundary of the outer part, to match the action of the total membrane operator.

For instance, consider the example shown in Fig. 8. In this figure, the yellow membranes indicate the membrane on which the operator is applied (so that if we zoomed in we would see the structure from Fig. 7). The yellow spheres are the start points for the membranes (note that they are all in the

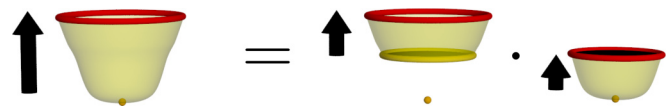

FIG. 8. Given a flux creation operator (left), we can split it into two parts. One of these parts (the rightmost picture, comprised of the inner part of the original membrane) is another flux creation operator that nucleates the loop and moves it part way along the membrane. The second part (the outer part) takes that existing loop and moves it to the final position.

same position). The opaque tori indicate the excitations they create. The two membranes on the right are displaced horizontally to indicate an order in which operators are applied, rather than spatial displacement. On the left-hand side of the figure, we have an operator that simply creates and moves an excitation to the final position (indicated by the red torus). We can split this operator into the two operators shown on the right-hand side. The rightmost operator on the right-hand side is the inner part of the original membrane operator and so is another flux creation operator. Therefore, this operator also creates an excitation and moves it to its boundary, the lower red torus. In order for this decomposition of operators to agree with the total operator on the left-hand side, we see that the middle operator, which represents the outer part of the original membrane operator, must move an excitation from the lower position (the yellow torus) to the final position (the red torus). While in this context the outer membrane operator moves an existing excitation, we can also apply it when there are no existing excitations. In this case, the operator instead creates two opposite fluxes at the two ends of the operator. We therefore do not need to distinguish between movement and creation operators because the movement operators are also creation operators, although they create multiple looplike excitations.

More generally, we can put many holes in the membrane to produce many loop excitations. Indeed, we can think of the membrane operator that we originally defined as a closed, topologically spherical membrane with a single hole in it. Then the excited loops (or single loop in the ordinary case) are at the boundaries of these holes. A topologically spherical membrane operator would produce no excitations. Indeed, as we prove in Sec. S-II D in the Supplemental Material [20], such a spherical membrane operator will act trivially if it is contractible and encloses no other excitations.

When producing an excitation in a given location, there are many choices for the position of the membrane. This is because the excitation is produced at the boundary of the membrane and many different membranes share the same boundary. However, the membrane operator is *topological* in the following sense. We can freely deform the membrane on which the operator is applied through the lattice, while keeping the positions of any excitations produced by the operator fixed, as long as we do not deform the membrane over any existing excitations. When we do this, the action of the membrane operator is preserved. That is, given an initial state $|\psi\rangle$ and a magnetic membrane operator $C^h(m)$ applied on a membrane m, if we can deform the membrane m into a new membrane m' without crossing any excitations in $|\psi\rangle$, or moving the excitations produced by $C^h(m)$, then we have $C^h(m)|\psi\rangle = C^h(m')|\psi\rangle$. This means that, like the ribbons in (2+1)D, the membrane is invisible when acting on the ground state; it does not matter precisely where we put the membrane. However, when we act on a state that already has excitations, the position may matter. Indeed this fact is vital when considering braiding and leads to the nontrivial braiding relations that we will see in Sec. IV.

It is not just the magnetic membrane operators that have this property under deformation, but all of the nonconfined membrane and ribbon operators, as we will prove in Sec. S-II in the Supplemental Material [20]. We therefore call the nonconfined ribbon and membrane operators topological.

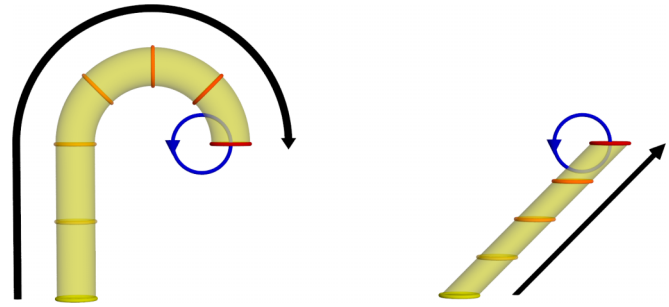

FIG. 9. Two membranes that would move a loop excitation from the same initial location to the same final location. The membrane on the left flips the loop during its motion (intermediate positions of the loop are shown along the membrane), whereas the right membrane moves the loop without flipping it. For the same original loop, measuring the flux along the blue path in the left figure gives us the inverse of the flux along the blue path on the right.

However, in reality this topological nature is a combined property of the ground state and the operators because we can only freely deform the membranes over a space that does not contain any excitations.

Having obtained the membrane operators, we can find their algebra, which can give us the fusion rules for the excitations (although to formally obtain the fusion rules we should organize our excitations according to their topological charge first). Just as in (2+1)D, two magnetic operators applied on the same space combine by multiplication of their flux labels. The precise way in which this occurs depends on the position of the start point of the common membrane m. We may have $C^g(m)C^h(m) = C^{gh}(m)$, but we could also have $C^g(m)C^h(m) = C^{hg}(m)$ if the paths from the start point to the membrane m themselves intersect with the dual membrane. This is because in this case the action of the membrane operator $C^h(m)$ affects the path labels $g(\text{s.p.}(m) - v_i)$ that determine the action of $C^g(m)$ [see Eq. (11)], leading to the membrane operator $C^g(m)$ instead acting like $C^{hgh^{-1}}(m)$. We also note that, just as we described for the E-valued membrane operators in (2+1)D in Ref. [15] (see Sec. III D), we can have partial fusion of the excitations. In this case the two magnetic membrane operators share part of their membrane and boundary, but the membranes are not completely identical [i.e., we have some $C^g(m_2)$ instead of $C^g(m)$], which can lead to only sections of the excited strings merging.

As well as fusion, loop excitations have another important relationship between the different excitations. We can flip the orientation of a loop excitation and ask what the resulting label should be in terms of an unflipped loop. By flip the loop, we mean that we turn the loop over during its motion using its membrane operator. Then we determine what membrane operator would produce an equivalent flux tube by producing a loop without flipping it over during its motion. An example of the relevant membranes is shown in Fig. 9. In the case of the magnetic excitations, flipping the loop over gives a loop labeled by the inverse of the original label. This indicates that to specify a flux, the orientation of the flux tube is important. This is a feature not seen in point particles and highlights that measuring the topological charge of a loop excitation is not as simple as it is for point excitations.

C. E-valued loop excitations

Magnetic excitations are not the only looplike excitations that we find in this model. In Ref. [15], we showed that in (2+1)D we could have looplike excitations that arise when our group E is nontrivial, which we called E-valued loop excitations. These excitations persist in the (3+1)D case, and the membrane operators that produce these excitations in (3+1)D are very similar to the operators in (2+1)D. Just as in (2+1)D, the membrane operator measures the surface label $\hat{e}(m)$ of some membrane m and assigns a weight depending on the value measured. It is convenient to consider a basis for this space of membrane operators where the weights are given by the irreducible representations of the group E. That is, we can define basis operators

$$L^{\mu}(m) = \sum_{e\in E} \mu(e)\delta(\hat{e}(m), e), \tag{12}$$

where μ is an irrep of E and $\mu(e)$ is the phase representing the element $e \in E$. Note that the irreps of E are 1D because E is Abelian when $\triangleright$ is trivial. Then any of these operators that are labeled by nontrivial representations produce a loop of excited edges on the boundary of the membrane, whereas the operator labeled by the trivial irrep is the identity operator. We can fuse these excitations, with the resulting label being given by the product of the irreps under the multiplication $(\mu\nu)(e) = \mu(e)\nu(e)$ for irreps μ and ν of E.

Unlike in (2+1)D, there are many different membranes that have the same boundary and so produce a loop excitation in the same location. However, much like the magnetic membrane operators, the E-valued membrane operators are topological, meaning that we can deform the membrane without changing the action of the membrane operator. For the E-valued membrane the topological nature is relatively intuitive and derives from the fact that closed, contractible surfaces are forced to have trivial label in the ground state by the blob condition in the Hamiltonian. The E-valued membrane measures the value of some surface. Given two such surfaces with the same boundary, we can consider the difference between their labels by inverting the orientation of one surface and combining it with the other surface by gluing the surfaces along their common boundary. If the two surfaces can be deformed into one another, this gluing procedure produces a contractible closed surface that encloses no excitations. However, in the ground state such a surface must have trivial label, due to the blob energy terms. Therefore, the two original surfaces must have the same label and so the two original operators give the same result. This is shown in Fig. 10. In the leftmost diagram we have one surface, the boundary of which is our loop excitation. This surface is labeled by e_1. In the next diagram, we have another surface with the same boundary, labeled by e_2. We can invert this surface, reversing its orientation and changing the label from e_2 to e_2^{-1} as shown in the third picture. Then we can glue these surfaces together to obtain a sphere labeled by $e_1e_2^{-1}$. However, this resulting surface is contractible, so its label must be 1_E if it encloses no excitations. Therefore, $e_1e_2^{-1} = 1_E$. This indicates that the two different surfaces have the same label. From this, we see that deforming the surface, without crossing an excitation, does not affect the action of the membrane operator.

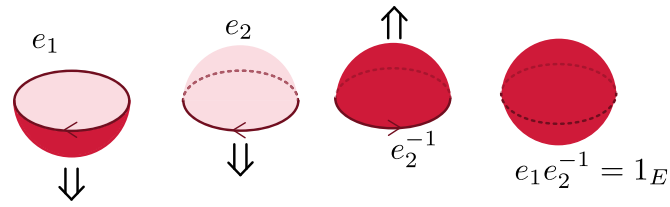

FIG. 10. Given two different surfaces with the same boundary, such as the first two surfaces in the figure, their labels must be the same if we can deform one into another without crossing any excitations. This is because the volume over which we deform them must have trivial boundary surface label.

D. Blob excitations

In addition to the three types of excitation we have considered so far [and which we already saw in the (2+1)D case discussed in Ref. [15]], we have a fourth simple excitation in (3+1)D, called the blob excitation (or 2-flux excitation). The blob excitations correspond to violations of the 2-flatness of blobs, also called 3-cells (i.e., to violations of the blob energy terms). As we described in Ref. [14] (in Sec. III B), we can consider creating two blob excitations by changing a chain of plaquettes along a dual path in the lattice. The blob energy term forces the total surface label around the blob (which is a certain product of surface elements around the blob) to be 1_E when the blob is unexcited. Then to excite a blob the naive thing to do is to multiply a single plaquette by some group element, e^{-1} for example. However, each plaquette belongs to two adjacent blobs, both of which will be excited by changing the plaquette, as is shown in Fig. 11. We can correct the 2-holonomy of one of these blobs by changing the label of another plaquette on that blob, but this excites yet another blob, as shown in Fig. 11. We can repeat this process with another plaquette, this only moves one of the blob excitations around. That is, by changing the labels of a series of plaquettes appropriately, we can produce a pair of blob excitations and move one of these excitations along a path. This is exactly the behavior we expect of a *ribbon operator*.

Having discussed the rough idea behind the blob ribbon operator, we will now be somewhat more precise about the action of the operator. Each blob ribbon operator is labeled by an element of E, for example e. We must also specify a (dual)

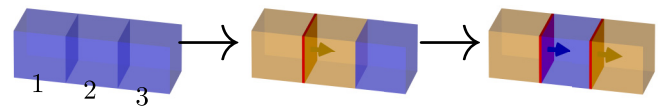

FIG. 11. (Copy of Fig. 38 from Ref. [14]) We consider a series of blobs in the ground state (leftmost image). In the ground state, all of the blob terms are satisfied, which we represent here by coloring the blobs blue (dark gray in grayscale). Changing the label of the plaquette between blobs 1 and 2 excites both adjacent blobs, as can be seen in the middle image (we represent excited blobs by coloring them orange, or lighter gray in grayscale). Multiplying another plaquette label on blob 2 to try to correct it just moves the right-hand excitation from blob 2 to blob 3 (rightmost image). In each step, the plaquettes whose labels we changed are indicated by the (red) squares and their orientations are indicated by an arrow.

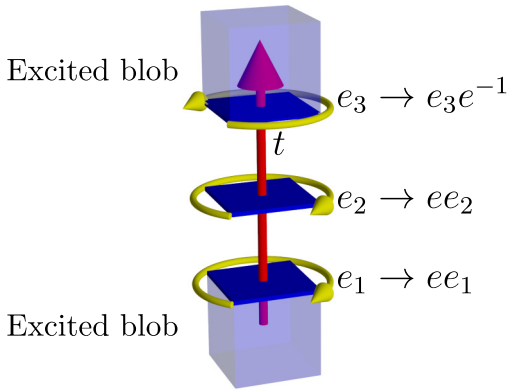

FIG. 12. In the $\triangleright$ trivial case, the blob ribbon operator multiplies the labels of the plaquettes pierced by the ribbon by e or e^{-1}, depending on the orientation of the plaquette. Here the circulation of a plaquette is shown by the curved (yellow) arrows, and this can be converted into a direction using the right-hand rule. The plaquette label is multiplied by e^{-1} if the orientation of the plaquette matches that of the ribbon and by e if the orientation is antialigned with the ribbon (note that the order of multiplication does not matter when $\triangleright$ is trivial, because E is Abelian, but the order is chosen in this figure to match the more general case).

path for the blob ribbon operator to act on. We denote the blob ribbon operator labeled by e and acting on the path t by $B^e(t)$. The path passes between the centers of blobs, much as a path on the lattice passes from one vertex to the next. Because the path travels between blobs, the path will pierce plaquettes and it is these pierced plaquettes that the operator will act on. The operator does so by multiplication of the plaquette label by e^{-1} if the orientation of the plaquette is aligned with the direction of the ribbon and e if it is aligned with the ribbon, where we use the right-hand rule to convert the clockwise or anticlockwise circulation of the plaquette into a direction in order to compare it with the orientation of the ribbon. An example of the action of the blob ribbon operator is illustrated in Fig. 12. This action excites the blob in which the ribbon originates and the blob in which it terminates. If the label of the operator e is in $\ker(\partial)$ then these two blob terms are the only excited energy terms. However, if e is not in the kernel the plaquettes pierced by the ribbon are also excited, so the particles produced are confined (there is an energy cost that increases with the length of the ribbon). The plaquettes are excited because the plaquette operator checks that the image under ∂ of the plaquette element matches the path around the plaquette. Therefore, multiplying the plaquette label by an element e with nontrivial $\partial(e)$ (i.e., an element outside the kernel of ∂) will cause this plaquette condition to be violated.

Much like the other operators we have considered so far, blob ribbon operators can be combined by applying one after the other on the same path. This process leads to fusion of the simple excitations produced by the operators. The excitations fuse in a similar way to the magnetic ones: the ribbon algebra is given by $B^e(t)B^f(t) = B^{ef}(t)$.

Before we move on to summarize the excitations, it is worth mentioning that the blob excitations in (3+1)D replace the single-plaquette excitations from (2+1)D. Recall from Ref. [15] that we create the single-plaquette excitations by multiplying a plaquette label by an element of E. Because there are no blobs to excite in (2+1)D (where the lattice is two dimensional) this creates no excitations other than the plaquette. However, in (3+1)D such an action produces blob excitations, as we saw from the action of the blob ribbon operator.

E. Condensation and confinement

In Refs. [14,15], we described a type of transition between different higher-lattice gauge theory models called condensation-confinement transitions. During this transition, some particle types become confined, so that it costs energy to separate a confined particle from its antiparticle, and others become "condensed." A condensed excitation can be produced *locally* and so carries trivial topological charge in the condensed phase. We can consider a model with no confinement where $\partial \to 1_G$. Note that in this uncondensed model, with both $\triangleright$ and ∂ trivial, the two gauge groups (G and E) decouple and the model can be treated as a tensor product of two independent lattice gauge theories, as we discussed in Sec. II. Then changing this ∂ so that it maps onto a nontrivial subgroup of G, while keeping the groups G and E constant, results in certain topological charges condensing. In particular, the magnetic excitations labeled by $h \in \partial(E)$ and the E-valued loop excitations that are labeled by trivial irreps of the kernel become condensed. To see what we mean by this, consider the E-valued membrane operators, which have the form

$$\sum_{e\in E} \alpha_e \delta(e, \hat{e}(m)).$$

If the membrane m satisfies fake flatness, the surface label of the membrane is related to the label of its boundary $\mathrm{bd}(m)$ through $\partial(\hat{e}(m))\hat{g}(\mathrm{bd}(m)) = 1_G$. Then, if the coefficients α_e are only a function of $\partial(e)$, and so are not sensitive to the kernel of ∂, we can write the membrane operator (when acting on a fake-flat state) as

$$\sum_{e\in E} \alpha_e \delta(e, \hat{e}(m)) = \sum_{e_k \in \ker(\partial)} \sum_{q\in E/\ker(\partial)} \alpha_q \delta(q e_k, \hat{e}(m)),$$

where the q are representative elements from the cosets of $\ker(\partial)$ in E and $\alpha_{qe_k} = \alpha_q$ because the coefficient is not sensitive to factors in the kernel. Then

$$\begin{aligned}
\sum_{e\in E} \alpha_e \delta(e, \hat{e}(m)) &= \sum_{q\in E/\ker(\partial)} \alpha_q \sum_{e_k\in\ker(\partial)} \delta(q e_k, \hat{e}(m)) \\
&= \sum_{q\in E/\ker(\partial)} \alpha_q \delta(\partial(q), \partial(\hat{e}(m))) \\
&= \sum_{q\in E/\ker(\partial)} \alpha_q \delta(\partial(q), \hat{g}(\mathrm{bd}(m))^{-1}) \\
&= \sum_{g\in\partial(E)} \beta_g \delta(g, \hat{g}(\mathrm{bd}(m))),
\end{aligned}$$

where $\beta_{\partial(e)^{-1}} = \alpha_e$. This is just an electric ribbon operator applied on the boundary of m and so is local to the excitation produced by the membrane operator. Rather than local in the usual sense of being restricted to a small spatial region, we mean that the operator only acts near the excitation. We see

that the excitation produced by the membrane operator can be produced locally and so is condensed. That is, the E-valued membrane operators which are not sensitive to the kernel of ∂ produce condensed excitations. When we consider the irrep basis for the membrane operators, the operators labeled by irreps with trivial restriction to the kernel correspond to condensed excitations. For the magnetic excitations, it is the fluxes with label in $\partial(E)$ that are condensed. It is slightly more complicated to show directly that the membrane operators associated to these condensed excitations are equivalent to local operators, so we postpone this proof until Sec. S-III of the Supplemental Material [20]. However, as we discussed in Sec. II, the plaquette terms allow for closed paths with label in $\partial(E)$ in the ground state rather than just closed paths with trivial label and these nontrivial paths are created by the edge transforms. Therefore, it is no surprise that fluxes with label in $\partial(E)$ should be condensed. We note that this condensation of fluxes is similar to that for a related field-theory model used to discuss condensation and confinement in regular gauge theory [11], where fluxes in the subgroup $\pi_1(H)$ [equivalent to $\partial(E)$] are condensed. This reinforces the connection between the higher-lattice gauge theory model and (partially) condensed lattice gauge theory

As these magnetic and E-valued loops condense, some of the pointlike particles in the model become confined. As we showed in Sec. S-I A of the Supplemental Material of Ref. [15] [with the proof being the same for the (2+1)D and (3+1)D cases], the confined electric ribbon operators $\sum_g \alpha_g \delta(\hat{g}(t), g)$ are those for which $\sum_{e\in E} \alpha_{\partial(e)g} = 0$ for all $g \in G$. This means that a basis ribbon operator, given by

$$S^{R,a,b}(t) = \sum_{g\in G} [D^R(g)]_{ab} \delta(\hat{g}(t), g),$$

for irrep R of G and matrix indices a and b, is confined if R has a nontrivial restriction to the subgroup $\partial(E)$ of G. Similar to the condensation of fluxes, this confinement is equivalent to that in Ref. [11], where the electric operators are confined if they are sensitive to factors in a subgroup $\pi_1(H)$ [which is equivalent to $\partial(E)$ here]. So far, this pattern of condensation and confinement is analogous to the (2+1)D case described in Ref. [15], but in the (3+1)D case we have an extra type of excitation, the blob excitation. As we discussed in the previous subsection, the blob excitations with label outside the kernel of ∂ are also confined because the corresponding ribbon operators multiply the plaquette labels of the plaquettes pierced by the ribbon by a factor which breaks the fake-flatness condition. These confined blob excitations are important when discussing the condensation of the magnetic excitations. The magnetic condensation is slightly different when there are three spatial dimensions compared to the case where there are only two because the magnetic excitations in (3+1)D are loops. Rather than being equivalent to strictly local (i.e., unextended) operators when acting on the ground state, the magnetic membrane operator is instead equivalent to a (confined) blob excitation operator acting on a path that runs around the boundary of the magnetic membrane. This blob ribbon operator is not local in the usual sense, given that the operator is linearly extended, but it is instead local to the excitation. This is analogous to how the condensed E-valued membrane operators act equivalently to (confined) electric ribbon operators applied around the boundary of the membrane.

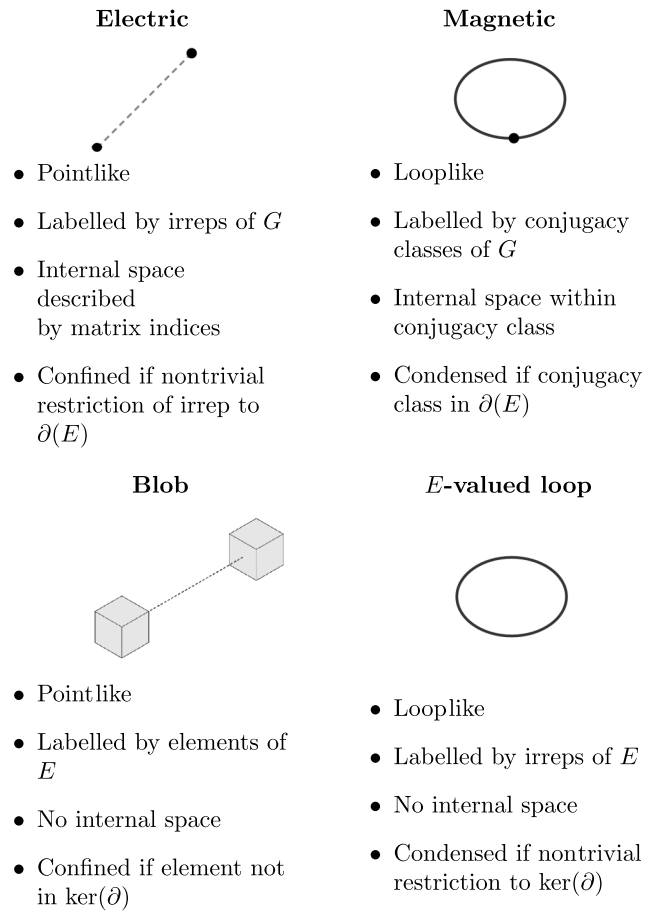

FIG. 13. A summary of the excitations when $\triangleright$ is trivial.

F. Summary of excitations

Given the large number of excitations that we have seen so far, it may be useful to briefly summarize them. The simple excitations and their confinement and condensation properties for the case described above are summarized in Fig. 13.

IV. BRAIDING IN THE $\triangleright$ TRIVIAL CASE

Now that we have obtained the membrane and ribbon operators that produce the various excitations of our theory, we can use these operators to obtain the braiding relations of the excitations. We find that the nontrivial braiding is between the magnetic flux tubes and the electric charges; between the flux tubes and other flux tubes (though this is only nontrivial if G is non-Abelian); and between the blob excitations and E-valued loops. We will describe all of these in more detail in the following sections. First, we will look at the relations involving the magnetic fluxes and electric charges. To describe this braiding, it is convenient to separately consider the cases where G is Abelian and non-Abelian, starting with the Abelian case.

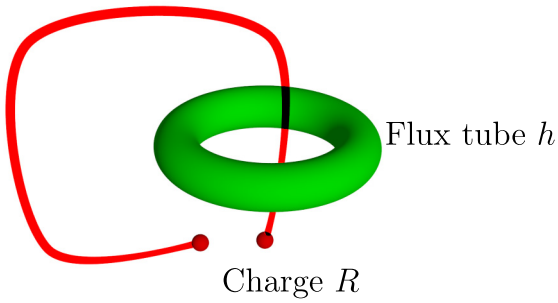

FIG. 14. (Copy of Fig. 35 from Ref. [14]) Schematic view of braiding a charge through a loop. The red line tracks the motion of the charge.

A. Abelian case

1. Flux-charge braiding

The first nontrivial braiding that we consider is the braiding involving our magnetic fluxes and electric charges. Recall that the magnetic fluxes are looplike particles, whereas the electric charges are pointlike. Because of this, the appropriate braiding between these two types of particle is to pass the electric charge through the loop and back around to its original position, as shown in Fig. 14. It is also possible to pass the electric charge around the loop (without passing through), just as if the loop were a point particle, but this process is found to be trivial in this model. Indeed, generally we find that in the higher-lattice gauge theory model, any braiding where one particle (looplike or otherwise) is moved around another particle (but not through a loop particle) is trivial. This is because such an operation can always be performed by membrane (and ribbon) operators which never intersect and so commute. This means that each excitation is oblivious to the presence of the other and so the motion has the same result as moving through the vacuum.

Now that we have discussed what the relevant braiding move is, we need to find how the excitations transform under such a move. The braiding relation is conveniently calculated by considering a commutation of operators as follows. Consider starting with a state that has no excitations and then applying a magnetic membrane operator that produces a flux tube. Then consider acting with an electric string operator to produce a pair of electric charges and move one along the path of the string, with this path passing through the loop excitation. In this case the electric excitation has undergone the braiding move we described earlier. We want to compare this situation to a similar one in which the electric excitation has not braided with the loop excitation. To do so, consider reversing the order of operators that we apply. Instead of first acting with the magnetic membrane and then with the electric string operator, we first apply the electric operator. This produces a pair of electric excitations and moves one of them along the ribbon. However, there is no magnetic excitation present at this stage, so no braiding occurs. Then we act with the magnetic membrane to produce our flux tube. In this situation, the excitations end up in the same location as when we applied the operators in the original order, but no braiding has occurred. Comparing these two situations therefore gives us the braiding relation. This means that to describe the braiding, we just need to find the relationship between the two possible orderings of the operators. That is, we need to calculate the commutation relations of the magnetic membrane operator and the electric ribbon operator.

In the case where G is Abelian, it is simple to calculate the commutation relation described above. Let the path of the electric ribbon operator be t and consider a magnetic membrane operator $C^h(m)$ applied on a membrane which intersects with the path t. The path t intersects with the membrane m at some edge i in t. The label of the path up to edge i is not affected by the magnetic membrane because it does not intersect with it. We denote this part of the path by t_1. The path after i, which we call t_2, is similarly unaffected. However, the label of the edge i itself is multiplied by either h or h^{-1}, depending on the relative orientation of the edge and the membrane. Then the total path t is the composition of t_1, the edge i and t_2, which we write as $t = t_1 i t_2$ (if the edge i points along the path, otherwise $t = t_1 i^{-1} t_2$). This means that the path label operator satisfies the following commutation relation with the magnetic membrane operator:

$$\begin{aligned}\hat{g}(t)C^h(m) &= \hat{g}(t_1)\hat{g}_i\hat{g}(t_2)C^h(m)\\ &= C^h(m)\hat{g}(t_1)h^{\pm 1}\hat{g}_i\hat{g}(t_2),\end{aligned}$$

where the inverse depends on the orientation of the membrane. Because we are looking at the case where G is Abelian, we can extract the factor $h^{\pm 1}$ to the front of the path operator and combine the sections of path to obtain

$$\hat{g}(t)C^h(m)|GS\rangle = C^h(m)h^{\pm 1}\hat{g}(t)|GS\rangle.$$

Now consider an electric ribbon operator, which has the form

$$\sum_{g\in G}\alpha_g\delta(g,\hat{g}(t)),$$

where α_g is an arbitrary set of coefficients. This ribbon operator then satisfies the commutation relation

$$\begin{aligned}&\sum_g \alpha_g\delta(g,\hat{g}(t))C^h(m)|GS\rangle\\ &\quad= C^h(m)\sum_g \alpha_g\delta(g,h^{\pm 1}\hat{g}(t))|GS\rangle\\ &\quad= C^h(m)\sum_{g'=h^{\mp 1}g}\alpha_{h^{\pm 1}g'}\delta(g',\hat{g}(t))|GS\rangle \qquad (13)\end{aligned}$$

with the magnetic membrane operator. This relation is simplified when we consider an electric ribbon operator whose coefficients are described by an irrep R of G. As discussed in Sec. III A, the electric ribbon operators labeled by irreps of G form a basis for the space of electric ribbon operators, and so we can decompose any electric ribbon operator into a sum of such irrep-labeled ribbon operators. When G is Abelian, all of the irreps are 1D, and so the basis ribbon operator labeled by irrep R is given by

$$S^R(t) = \sum_{g\in G} R(g)\delta(g,\hat{g}(t)),$$

where $R(g)$ is the representation of element g in the irrep, and is a phase because the irreps are 1D when G is Abelian.

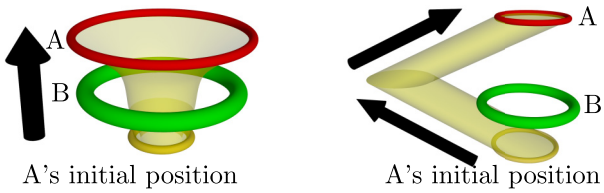

FIG. 15. Schematic of a braid move (left) and a permutation move (right). The translucent membrane is the surface swept by the red loop (the loop at the top of each image), which is also the membrane on which we apply the corresponding membrane operator.

Substituting this into Eq. (13), we see that the electric ribbon operator labeled by an irrep R and the magnetic membrane operator satisfy the commutation relation

$$\begin{aligned} S^R(t)C^h(m)|GS\rangle &= \sum_g R(g)\delta(g,\hat{g}(t))C^h(m)|GS\rangle \\ &= C^h(m)\sum_{g'=h^{\mp 1}g} R(h^{\pm 1}g')\delta(g',\hat{g}(t))|GS\rangle \\ &= C^h(m)\sum_{g'} R(h^{\pm 1})R(g')\delta(g',\hat{g}(t))|GS\rangle \\ &= R(h^{\pm 1})C^h(m)\sum_{g'} R(g')\delta(g',\hat{g}(t))|GS\rangle \\ &= R(h^{\pm 1})C^h(m)S^R(t)|GS\rangle. \end{aligned} \tag{14}$$

This is the same as the unbraided version $C^h(m)S^R(t)$, except that we have gained a phase of $R(h)$ or $R(h^{-1})$. Therefore, under braiding the state obtains a simple phase $R(h)$ (or the inverse) and so the braiding is Abelian. The phase is $R(h)$ if the electric ribbon's path meets the direct membrane before the dual membrane, and the inverse otherwise, as we show in Sec. S-IV A 1 of the Supplemental Material [20]. Note that this is the same result that we would expect for conventional discrete gauge theory (see, e.g., Refs. [22,23] and our discussion of how this relates to higher gauge theory in Sec. II of Ref. [14]).

2. *Flux-flux braiding*

Just as a point particle can be braided with a looplike excitation in two ways, so can two loops be braided in multiple ways. The allowed patterns of motion can be built from two types of movement. First, we can move the loops around each other (in the same way as we can move two point particles around each other), which we call permutation. Second, we can pull a loop through another loop (or over it, which is equivalent to pulling the second loop through the first), just as we saw when braiding point particles with loops. These two moves are shown in Fig. 15. In this figure, in each case the red loop is moved, with the path of its motion being represented by the yellow membrane. The arrows indicate the direction of motion. In this model, the permutation move is trivial in that it is the same regardless of whether the green loop is present or not. This is because the motion can be performed by membrane operators acting on membranes that never intersect. Then because the membranes do not intersect, the membrane operators commute. Even if we choose

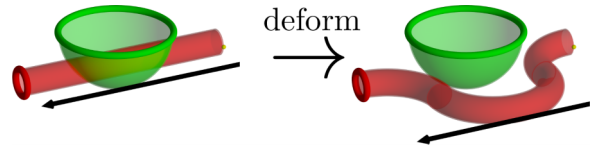

FIG. 16. Exchange of two excitations is implemented by membranes which can be freely deformed so that they do not intersect. This means that the corresponding commutation relation of operators is trivial.

to use membrane operators that do intersect, as in Fig. 16, the membranes can be deformed so that they do not intersect, by using the topological property of membrane operators. In the example shown in Fig. 16, a loop (shown as a small red torus in the figure) is moved along a surface (indicated by the red surface attached to the loop) that intersects twice with a green membrane. Although the red loop intersects the green membrane, the red loop does not pass through the larger green loop excitation created by this green membrane. This motion is performed by an operator placed on the red surface. The red and green membranes can be deformed so that one goes around the other, using the topological property of the membrane operators. Then because the membranes do not intersect (and indeed can be deformed so that they never come close), the corresponding membrane operators commute and so permutation is trivial. This is also true for permutation involving nonconfined point particles or the E-valued loops: in (3+1)D the permutation can be performed by ribbon or membrane operators which do not intersect.

As we did with the flux-charge braiding, we can express the braiding relation between two loops in terms of the commutation relation between creation operators. The flux tubes are created and moved by membrane operators, so the appropriate commutation relation is between two membrane operators, as indicated in Fig. 17. In the Abelian case, the two magnetic membrane operators commute, and so the loop braiding between two magnetic fluxes is trivial. This is because in this case, the magnetic membrane operator simply multiplies each cut edge by the label of the magnetic operator. This is in contrast to the non-Abelian case, where the action of the

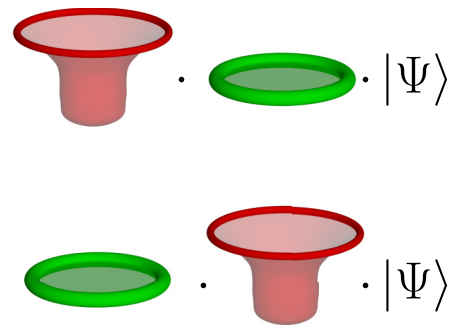

FIG. 17. (Copy of Fig. 43 from Ref. [14]) The commutation of operators used to calculate the braiding. The partially transparent surfaces indicate the membranes for the operators, while the opaque loops indicate the excited regions, which are the boundaries of the membranes.

membrane operator on each edge depends on the value of the path from the start point to that edge. This means that, in the Abelian case, the two membrane operators only share support when their membranes cut some of the same edges, so that the two membrane operators directly change the same edge label. Even then, the action on a shared edge is the same regardless of the order in which the operators act. Consider the action of two membrane operators $C^{h_1}(m_1)$ and $C^{h_2}(m_2)$ on such a shared edge i (i.e., one cut by the dual membranes of both operators). If we first act with the membrane operator labeled by h_2 and then by the operator labeled by h_1, the edge label goes from g_i to $h_1 h_2 g_i$ (possibly with inverses on h_1 or h_2, depending on the relative orientation of the membranes and the edge). On the other hand, when $C^{h_1}(m_1)$ acts first on the edge, followed by $C^{h_2}(m_2)$, the total effect on the edge label is given by $g_i \to h_2 h_1 g_i$. This is the same as $h_1 h_2 g_i$ (because G is Abelian), so the two membrane operators commute and the braiding is trivial.

B. Non-Abelian case

1. Flux-charge braiding

In the case where G is non-Abelian, the braiding relations between the magnetic fluxes and electric charges are a little more complex, although they still match our expectations from conventional gauge theory (see, e.g., Refs. [22,23] and our discussion in Sec. II of Ref. [14]). Recall from the Abelian case that the electric string operator fails to commute with the magnetic membrane operator because the latter operator changes the label of one (or possibly more) of the edges along the path of the electric ribbon. In the Abelian case, the action on the path element was simple. The affected edge was multiplied by a fixed element h or the inverse, and this factor could be brought to the front of the product of group elements that make up the path element, so that the entire path element was also multiplied by h or the inverse. In the non-Abelian case, this is no longer true. First, any changes to the edge cannot simply be extracted to the front of the path element by commutation. Second, the action of the membrane on the individual edge that is changed is more complex, depending on the path from the start point of the magnetic membrane to the affected edge. This means that, rather than multiply the affected edge label by a fixed element h, we multiply the label by an element within the conjugacy class of h, with this element depending on the path element from the start point of the membrane to the edge. However, this path element depends on the state that we act on, and even in the ground state the element is not generally fixed (the ground state is made of a superposition of states with different values of this path element) and so we must leave this path element as an operator. Therefore, the braiding relation is not generally well defined. To illustrate this idea, consider performing exactly the same braiding as in the Abelian case, by passing an electric ribbon operator through a magnetic membrane operator. Again we split the path t of the electric ribbon into the path t_1 before the intersection; the edge i along which the ribbon and membrane intersect; and the path t_2 after the intersection. Of these parts, only the group element $\hat{g}_i$ assigned to the edge i is affected. For now, assume that the edge i points along the path t, so that $t = t_1 i t_2$. If this path passes through the direct membrane of the magnetic membrane operator before the dual membrane (i.e., for a particular choice of relative orientation of ribbon and membrane), we have that

$$\hat{g}_i C^h(m) = C^h(m)\hat{g}(t_s)^{-1} h \hat{g}(t_s)\hat{g}_i,$$

where t_s is the path from the start point of the membrane to the crossing point and we have assumed that the ribbon is aligned so that the path reaches the direct membrane of the magnetic membrane operator before the dual membrane. Then for the entire path element, we have that

$$\begin{aligned}\hat{g}(t)C^h(m) &= \hat{g}(t_1)\hat{g}_i\hat{g}(t_2)C^h(m)\\ &= C^h(m)\hat{g}(t_1)\hat{g}(t_s)^{-1}h\hat{g}(t_s)\hat{g}_i\hat{g}(t_2).\end{aligned}$$

If we had taken edge i to point against the path, we would have a similar result because the edge element $\hat{g}_i$ would appear with an inverse in the path element, but the edge element would be right multiplied by the inverse factor $\hat{g}(t_s)^{-1}h^{-1}\hat{g}(t_s)$ by the membrane operator, so we would obtain

$$\begin{aligned}\hat{g}(t)C^h(m) &= \hat{g}(t_1)\hat{g}_i^{-1}\hat{g}(t_2)C^h(m)\\ &= C^h(m)\hat{g}(t_1)[\hat{g}_i\hat{g}(t_s)^{-1}h^{-1}\hat{g}(t_s)]^{-1}\hat{g}(t_2)\\ &= C^h(m)\hat{g}(t_1)\hat{g}(t_s)^{-1}h\hat{g}(t_s)\hat{g}_i^{-1}\hat{g}(t_2).\end{aligned}$$

We can combine these cases by introducing $\hat{g}_i^{\sigma_i}$, where σ_i is 1 if the edge and path align and -1 otherwise. Then we have

$$\begin{aligned}\hat{g}(t)C^h(m) &= \hat{g}(t_1)\hat{g}_i\hat{g}(t_2)C^h(m)\\ &= C^h(m)\hat{g}(t_1)\hat{g}(t_s)^{-1}h\hat{g}(t_s)\hat{g}_i^{\sigma_i}\hat{g}(t_2).\end{aligned}$$

By inserting the identity in the form $\hat{g}(t_1)^{-1}\hat{g}(t_1)$, we can write the commutation relation as

$$\begin{aligned}\hat{g}(t)C^h(m) &= C^h(m)\hat{g}(t_1)\hat{g}(t_s)^{-1}h\hat{g}(t_s)\hat{g}(t_1)^{-1}\hat{g}(t_1)\hat{g}_i^{\sigma_i}\hat{g}(t_2)\\ &= C^h(m)[\hat{g}(t_s)\hat{g}(t_1)^{-1}]^{-1}h[\hat{g}(t_s)\hat{g}(t_1)^{-1}]\hat{g}(t).\end{aligned} \quad (15)$$

This is similar to the commutation relation from the Abelian case, except that the path element gains a factor of

$$[\hat{g}(t_s)\hat{g}(t_1)^{-1}]^{-1}h[\hat{g}(t_s)\hat{g}(t_1)^{-1}],$$

instead of simply h. This factor is an operator and has no definite value in general, so the effect on the electric excitation depends on which configuration within the ground state we consider and we cannot extract a definite braiding relation. However, there is one special case where we can obtain a definite braiding relation. When the electric string starts at the start point of the magnetic membrane, then the path sections t_s and t_1 start and end at the same points as each other. Provided that these path sections can be deformed into one another without crossing over any excitations, the fake-flatness condition imposed by the plaquette energy terms ensures that $\hat{g}(t_s) = \hat{g}(t_1)$ up to a potential factor of $\partial(e)$ for some $e \in E$. Such factors of $\partial(e)$ do not affect

$$[\hat{g}(t_s)\hat{g}(t_1)^{-1}]^{-1}h[\hat{g}(t_s)\hat{g}(t_1)^{-1}]$$

because $\partial(e)$ is in the center of G, so the factor of $\partial(e)$ and $\partial(e)^{-1}$ from $\hat{g}(t_s)$ and $\hat{g}(t_s)^{-1}$ cancels. Therefore,

$$\begin{aligned}[\hat{g}(t_s)\hat{g}(t_1)^{-1}]^{-1}h[\hat{g}(t_s)\hat{g}(t_1)^{-1}]\hat{g}(t) &= \partial(e)^{-1}h\partial(e)\hat{g}(t)\\ &= h\hat{g}(t).\end{aligned} \quad (16)$$

This relation then gives us a simple braiding relation in the "same-site" (or same start-point) case. Note that we gave this braiding relation for a particular choice of relative orientation for the ribbon and membrane operator, and if we reversed this relative orientation then the element $g(t)$ would instead be multiplied by h^{-1} (as we show in Sec. S-IV A 1 in the Supplemental Material [20]). This braiding relation is a simple extension of the Abelian case. Having said that, the non-Abelian nature of the group does still have some relevance when we use our irrep basis for the electric operators. Recall that the electric excitations are labeled by irreps of the group G, combined with matrix indices for the irrep. When G is Abelian, these representations are 1D and we need not worry about matrix indices. However, when G is non-Abelian some of these irreps are not 1D. We can look at the effect of braiding on an electric ribbon labeled by a representation R and its indices, for which we find that

$$\begin{aligned}
&\sum_{g\in G}[D^R(g)]_{ab}\delta(g,\hat{g}(t))C^h(m)|GS\rangle \\
&= \sum_{g\in G} C^h(m)[D^R(g)]_{ab}\delta(g,h\hat{g}(t))|GS\rangle \\
&= \sum_{g\in G} C^h(m)[D^R(g)]_{ab}\delta(h^{-1}g,\hat{g}(t))|GS\rangle \\
&= \sum_{g'=h^{-1}g} C^h(m)[D^R(hg')]_{ab}\delta(g',\hat{g}(t))|GS\rangle \\
&= C^h(m)\sum_{c=1}^{|R|}[D^R(h)]_{ac}\sum_{g'\in G}[D^R(g')]_{cb}\delta(g',\hat{g}(t))|GS\rangle. \quad (17)
\end{aligned}$$

We see from Eq. (17) that the braiding mixes electric ribbon operators labeled by different matrix indices but the same representation. The fact that the representation is left invariant suggests that the representations label the purely electric topological sectors, given that braiding cannot mix different sectors.

The importance of the start points of the membrane and ribbon operators when it comes to braiding can be interpreted in terms of gauge theory. Just as we discussed for the (2+1)D case in Ref. [15], the start point of the magnetic membrane can be seen as a unique point in that the flux tube produced by the magnetic membrane operator has a definite flux label with respect to this point even within the conjugacy class. When we give a flux tube a flux label, we must specify the path with respect to which we measure this flux. The path must link with the flux tube, but smoothly deforming the path should not change the flux label measured (where by smoothly deform, we mean pulling through the space represented by the lattice to another position on the lattice). An exception to this is the start point of the path. Moving this start point can change the flux label that we would assign to the flux tube (see, e.g., Ref. [24]). Suppose that the flux label measured with respect to a particular start point is h. Then if we measure the flux label of the flux tube starting from a different point, the result is related to h by conjugation by a path element for a path between the two start points. In our model this path element is not usually well defined because the energy eigenstates are usually linear combinations of states with different group elements assigned to the path. We say that the path element is generally operator valued. Therefore, the flux tube does not generally have definite flux with respect to points other than the start point (with an exception if the flux label is in the center of G). This nondefinite flux is reflected in the flux-flux braiding. This idea is explained more clearly in the context of field theory in Ref. [24].

A second interpretation of the start-point dependent fusion comes from anyon theory. We only have definite fusion in the case where the membrane operators share a start point. Then, as in the (2+1)D case, we may expect that we only have definite braiding when the fusion channel is definite: that is, when the operators involved have a common start point.

2. Flux-flux braiding

As with the flux-charge braiding, the general result of braiding two magnetic fluxes is more complicated when G is non-Abelian. However, as with the flux-charge braiding, there is a special case with simple braiding relations, when the two magnetic membrane operators have the same start point. This makes sense if we think of the base point as the point of definite flux because we only expect a definite braiding result if the two flux tubes have definite flux when measured with respect to the same point.

We consider the case where one flux tube (which we will call the inner loop) is passed through another loop (which we call the outer loop). The inner loop takes the role of the red loop in the left diagram of Fig. 15. Then in the same start-point case the label of the inner loop is conjugated by the label of the outer loop, while the label of the outer loop is unchanged. That is, if the label of the inner membrane operator is k and the outer membrane operator is labeled by h, under braiding the label of the excitation from the inner membrane becomes $h^{-1}kh$ and the label of the outer membrane is unchanged. The simplest way to obtain this braiding relation is to use the topological nature of the operators. We can freely deform the membranes, as long as they do not cross an excitation and no excitations are moved in doing so. We can therefore pull the membrane that produces the inner loop fully through the other membrane (as there are no excitations within the membrane itself). However, when we do this we must keep the start point fixed (because it may be excited), so the start point is not moved through the outer membrane. However, recall that the action of the magnetic membrane operator depends on a set of paths from the start point to the edges being changed by the membrane operator. As we deform the membrane, the start of these paths (the start point) is fixed, while the ends are pulled through the outer membrane (if these ends were not already on the other side of the membrane). Therefore, all of these paths intersect the outer membrane. This means that the group elements of these paths will be changed by the action of the outer membrane operator, which will in turn affect the action of the inner membrane operator. To see how the inner membrane operator changes under the commutation relation we need to know how the labels of these paths are affected.

As an example, consider Fig. 18. In the left side of the figure we have the membranes in their original position, with the red membrane nucleating a loop at the common start point and moving the red loop through the green one. To calculate

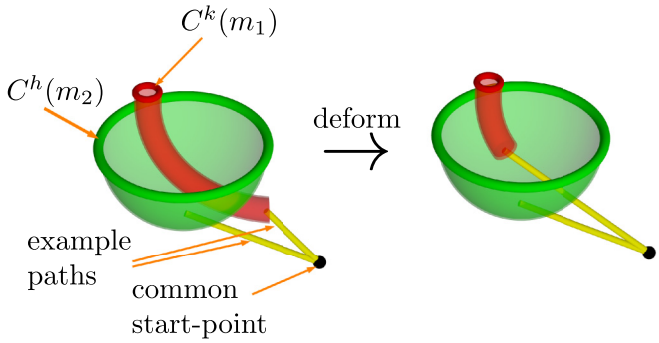

FIG. 18. To calculate the braiding of two loops, we consider the situation shown on the left where we first apply a magnetic membrane operator $C^h(m_2)$, then apply a membrane operator $C^k(m_1)$ which intersects with the first membrane and pushes a loop excitation through that first membrane. We choose the start points of these two membranes to be the same. Example paths from the common start point to the two membranes are shown as (yellow) cylinders. We can use the topological property of the membrane operators to deform the inner (red) membrane m_1, and pull it through the green membrane m_2 to obtain the image on the right-hand side. However, when we do so we must leave the start point fixed. Therefore, the paths from the start point to each point on the membrane m_1, such as the example path shown here, must pass through m_2. This leads to a nontrivial braiding relation in general.

the commutation relation, we deform the red membrane so that it is entirely pulled through the green membrane, as in the right side of Fig. 18. However, when we deform a membrane we must keep any excitations fixed, including the potentially excited start point. Therefore, the start point is fixed. This means that the paths from the start point to the red membrane, like the example path to the red membrane in the right-hand side of the figure, pass through the green membrane and so can be affected by the green membrane operator. This is significant because these paths determine the action of the membrane operator, as explained in Sec. III B. An edge i cut by the dual membrane of the magnetic membrane operator $C^k(m_1)$ has its edge label g_i multiplied by a factor $g(\text{s.p.}(m_1) - v_i)^{-1} k g(\text{s.p.}(m_1) - v_i)$ (or the inverse), where v_i is the vertex on the direct membrane that is attached to i. These factors have the form $g(t)^{-1} h g(t)$, where each path t now intersects with the green membrane operator $C^h(m_2)$. We must therefore find the commutation relation of such a path label operator $g(t)$ with the membrane operator.

We already saw how a magnetic membrane operator affects the label of paths that pierce the membrane when we looked at the charge flux braiding. From the charge braiding calculation we know that the label of a path t that starts at the common start point and intersects the outer membrane changes from $g(t)$ to $hg(t)$, where h is the label of the outer membrane operator being intersected [see Eq. (16)]. As discussed previously, this path element $g(t)$ appears in the action of the other (inner) membrane operator. If the inner membrane has label k, the membrane operator acts on an edge cut by the membrane by multiplying the edge label by $g(t)^{-1} k g(t)$, where t is the path from the start point to that edge. Under commutation with the outer membrane, when $g(t)$ changes to $hg(t)$, this action becomes multiplication by $g(t)^{-1} h^{-1} k h g(t)$, which is equivalent to the action of an unbraided membrane of label $h^{-1}kh$. Therefore, we see that the label of one of the flux tubes is conjugated by braiding. As we expect, the conjugacy class of the flux is invariant under braiding, but the flux element within the conjugacy class can be changed.

It is worth noting that if we had not deformed one membrane to pull it entirely through the other, some of the paths from the start point would not pierce the other membrane and so would be unaffected by the commutation relation. This means that the action of the membrane in the region from the start point to the intersection of the membrane is unaltered. This reflects the fact that a membrane operator moves the loop excitation associated to it. Before the intersection, the membrane operator is moving the excitation before it has braided, so its label is the original label of the loop. After the intersection, braiding has occurred and so the label of the membrane (and the excitation) has changed. The precise point at which braiding has occurred is somewhat arbitrary in an anyon theory (although we can guarantee whether braiding has occurred if the excitations start and end in the same position). Similarly, the choice of location for the membranes is somewhat arbitrary when the membrane operators act on the ground state because we can deform the membranes without affecting their action, and so we can change the location where the membrane operators intersect by deforming the membranes. This reflects the freedom in considering at which point during the motion the braiding transformation is applied (although if the excitations start and end in the same position, then the membrane operators will definitely intersect if braiding occurs, regardless of how we deform the membranes).

Having obtained the braiding relation, it is useful to consider how braiding affects a linear combination of magnetic membrane operators with label within a certain conjugacy class, such as $\sum_h \alpha_h C^h(m)$. If the magnetic membrane operator is an equal superposition of operators labeled by each element of a conjugacy class, then the conjugation of the labels by the braiding only permutes the labels within the conjugacy class, which has no effect when the coefficient for each element is the same. Therefore, the overall membrane operator transforms trivially under braiding. For a general superposition, the conjugation (and so permutation of the labels) does affect the operator and so the braiding is nontrivial. These conditions match the conditions for the start point of the membrane operator to be unexcited or excited. A magnetic operator with an unexcited start point is an equal superposition of magnetic operators with labels within a conjugacy class, and so is unaffected by braiding through other magnetic excitations. On the other hand, a magnetic operator with an excited start point will transform nontrivially when it braids through some other magnetic excitations. This is because, if the start point is excited, the magnetic excitation carries a pointlike charge, which enables it to braid nontrivially with other magnetic excitations when passed through them. Note that the same condition does not hold for the outer membrane operator, which can affect the inner membrane operator even if it does not have an excited start point. This is because we can shrink the inner loop to a point before braiding it without affecting the braiding relation, whereas the looplike character of the outer loop is essential for the braiding.

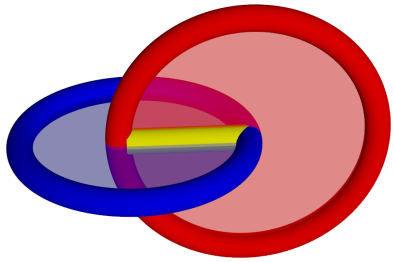

FIG. 19. Two linked loops may have an energetically costly linking string between them, here indicated by the short (yellow) string.

It is important to note that the precise form of the braiding relation depends on the orientation of the loops involved. Flipping a magnetic excitation is equivalent to changing its label from h to h^{-1}. Therefore, if we were to flip the orientation of the outer membrane from our earlier calculation, then the label of the inner membrane would change from k to hkh^{-1} under braiding rather than changing to $h^{-1}kh$. Flipping the orientation of the inner one does not change the expression because the transformation is the same when we invert both sides: $k^{-1} \to h^{-1}k^{-1}h \Rightarrow k \to h^{-1}kh$. Therefore, if the orientation of both loops is flipped, the braiding transformation is

$$k \to hkh^{-1}. \tag{18}$$

3. Linking

In addition to the nontrivial loop-loop braiding, there is another feature of loop excitations not present for point excitations. Two loop excitations may be *linked*. In this case, depending on the labels of the two excitations, there may be an energetically costly "linking string" that joins the two loops. This situation is indicated in Fig. 19. As we show in Sec. S-IV A 4 in the Supplemental Material [20], this linking string is present between two linked magnetic excitations when their labels do not commute. If the two loops are labeled by g and h and their membranes have the same start point, then the two loops are linked by a string with a label similar to $ghg^{-1}h^{-1}$. The exact label depends on the relative orientations of the two loops and which path we choose to use to define the flux of the linking string (so g or h could appear with an inverse in the label of the linking string, or the label could be conjugated by g or h).

This linking string indicates that there is an obstruction to pushing the two loops through one another and so pushing them through results in an energetically costly linking string. One way of viewing this is that the two strings are unable to pass through each other. Therefore, instead of the loops being pushed through each other, one is deformed to accommodate the other, as shown in Fig. 20. In Fig. 20, part of one of the loops envelops the other one and folds back on itself, as seen in the bottom right of the figure (this becomes the pink string in the lower left of the figure). We can consider this part of the two loops as the linking string. It is possible to work out the flux label of the linking string from this picture by writing a path that links with the thin section as a combination of the paths defining our two original fluxes (recall from Sec. IV B 1 that a flux tube is defined along with a path linking with that flux tube, which measures the flux value). A more complete

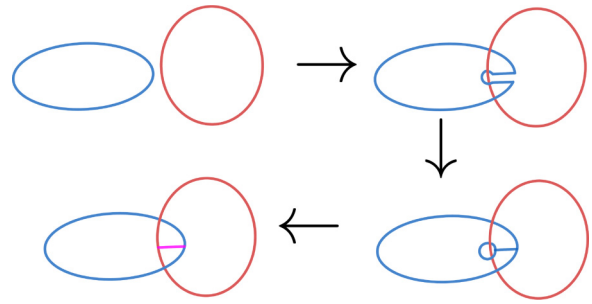

FIG. 20. Given two loops (blue and red here) that cannot pass through each other, we can push them together. To do this we must deform the boundary of one of the loops (second figure). The deformation then encloses the other loop (third figure). We can consider this deformed section of the loop as a new object, which is the linking string (colored pink in the fourth figure), whose flux label will depend on the labels of the two linked loops.

argument for this (in terms of generic fluxes, rather than in terms of this specific model) is given in Ref. [24].

The presence of the linking string indicates that further relative motion of the two loops is nontrivial because such motion will move the string (the position of which can be detected through the energy terms). For example, we can consider rotating one of the loops by a full rotation. This would be a trivial motion if the loops were unlinked. However, when the loops are linked, the linking string will follow this rotation, as shown in Fig. 21, indicating that the motion is nontrivial. In order to implement this rotation, we make the direct membrane paths (the paths that we defined when constructing the membrane operator) spiral outwards, wrapping around the linking (blue) loop. If we wanted to write the label of these paths in terms of the label of an unwrapped path, we would gain a factor that accounts for the flux of the blue loop. This in turn affects the action of the membrane operator, changing the effective label of parts of the membrane operator by conjugation by the flux of the blue loop.

4. Three-loop braiding

It has become clear [25,26] that when considering loops, the simple case where two loops pass through each other (two-loop braiding, shown in the left side of Fig. 15) that we have described so far does not fully describe the general topological properties of loops. A more general example of braiding is where two loops pass through each other while both loops are

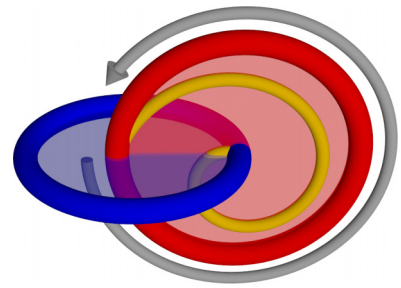

FIG. 21. Rotating a linked loop drags the linking string and conjugates the label of part of the membrane of the rotating loop.

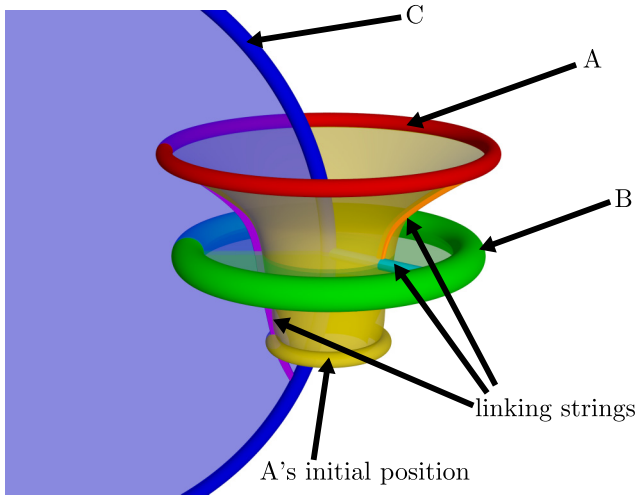

FIG. 22. An example of three-loop braiding. The open strings (orange, purple, and cyan) are possible linking strings.

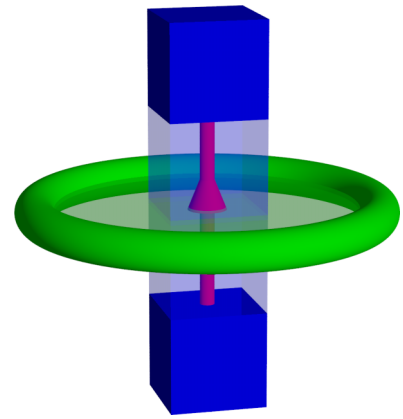

FIG. 23. Schematic of blob-loop braiding. The blue cubes (dark gray in grayscale) represent the blob excitations at the ends of the ribbon operator (whose ribbon is represented by the translucent cuboid and the arrow). The ribbon operator moves one of the blob excitations through the looplike excitation produced by an E-valued membrane operator applied on the translucent (green) membrane.

linked to a third loop (see Fig. 22). This is known as three-loop [25] or necklace braiding [27].

In this model, however, the result of three-loop braiding is similar to that of the ordinary braiding. The only difference is that the two loops may also drag linking strings with the third loop. This is shown in Fig. 22. The transformation of the loop labels is otherwise the same as in the ordinary case. One exception is that the linking string of two magnetic excitations can cancel the confining string of a confined blob excitation (provided that the labels of the linking string and blob excitation agree, as described in Sec. S-IV A 4 in the Supplemental Material [20]), which enables those blob excitations to move and braid freely while attached to a linked flux, which they would not normally be able to do.

C. Loop-blob braiding

So far we have considered the excitations that are described by the group G. The final nontrivial braiding is between the two types of excitation that are associated to the group E, the E-valued loops and blob excitations. In this case it is easy to find the braiding relations by looking at the effect of the blob ribbon operator on the surface measured by the operator that produces the loop. We consider a situation where the blob excitation passes through the loop excitation. To implement this situation on our lattice, we apply both an E-valued membrane operator and a blob ribbon operator whose path intersects with that membrane, as shown in Fig. 23.

In order to compute the braiding relation, we compare the situation where we first create the loop and then push the blob through, thus performing the braiding move, with the one where we push the blob through empty space before producing the loop. The relevant commutation relation is shown in Fig. 24.

As we saw in Sec. III D, the blob ribbon operator with label e multiplies the labels of the plaquettes pierced by its path by e or e^{-1}, depending on the relative orientation of the plaquette and ribbon. This action is not sensitive to the presence of the E-valued loop excitation and so the blob ribbon operator is unaffected by the commutation. On the other hand, the membrane operator for the loop excitation is affected by the action of the blob ribbon operator. Recall that the E-valued membrane operator measures the surface element of the membrane on which it is applied. This surface element, $\hat{e}(m)$, is a product of the elements of individual plaquettes: $\hat{e}(m) = \prod_{\text{plaquettes in } m} \hat{e}^{\pm 1}_{\text{plaquette}}$, where the $\pm$ accounts for the relative orientation of the surface and plaquette. We defined the blob ribbon operator to intersect the membrane, and so it will affect the label of one of the plaquettes in this product. If the blob ribbon operator pierces the membrane m through a plaquette q, then the label e_q of that plaquette is multiplied by e or e^{-1}, depending on the relative orientation of the plaquette and the ribbon. This in turn means that the contribution $e_q^{\pm 1}$ of the plaquette to the surface m will be multiplied by e or e^{-1}, depending on the relative orientation of the membrane and the ribbon. The orientation of the membrane matters rather than that of the plaquette because the ± 1 in the expression for the

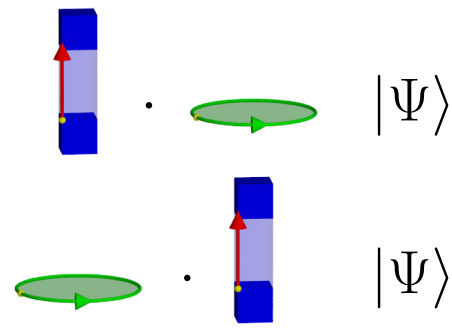

FIG. 24. In order to determine the blob-loop braiding relations, we compare the situation shown in the top line, where we first apply an E-valued membrane operator and then a blob ribbon operator that intersects with that membrane, to the situation shown in the bottom line, where we apply the operators in the opposite order. Here $|\psi\rangle$ is any state with no other excitations near the support of the two operators (e.g., a ground state).

surface label accounts for the relative orientation of plaquette and membrane (if the plaquette is antialigned with the membrane, the inverse in e_q^{-1} converts a factor of e from the ribbon operator into e^{-1} if the orientation of the ribbon opposes the plaquette but matches the membrane, or vice versa if the orientation of the ribbon matches the plaquette but opposes the membrane). If the orientation of the membrane matches the orientation of the blob ribbon operator, $e_q^{\pm 1}$ will be multiplied by e^{-1}. This indicates that $\hat{e}(m)B^e(t) = B^e(t)e^{-1}\hat{e}(m)$ in this case. Then, considering the basis operator for our space of E-valued membrane operators labeled by an irrep γ of E [as defined in Eq. (12)], the commutation relation with the blob ribbon operator $B^e(t)$ is given by

$$\begin{aligned} B^e(t)L^\gamma(m)|GS\rangle &= B^e(t)\sum_{e'\in E}\gamma(e')\delta(e', \hat{e}(m))|GS\rangle \\ &= \sum_{e'\in E}\gamma(e')\delta(e', e\hat{e}(m))B^e(t)|GS\rangle \\ &= \sum_{e'\in E}\gamma(e')\delta(e^{-1}e', \hat{e}(m))B^e(t)|GS\rangle \\ &= \sum_{e''=e^{-1}e'}\gamma(ee'')\delta(e'', \hat{e}(m))B^e(t)|GS\rangle \\ &= \gamma(e)\sum_{e''\in E}\gamma(e'')\delta(e'', \hat{e}(m))B^e(t)|GS\rangle, \end{aligned}$$

where we used the fact that E is Abelian to take γ as a 1D irrep and separate $\gamma(ee'')$ into $\gamma(e)$ and $\gamma(e'')$. Therefore,

$$B^e(t)L^\gamma(m)|GS\rangle = \gamma(e)L^\gamma(m)B^e(t)|GS\rangle. \tag{19}$$

Having the E-valued membrane operator on the left of the product (and the blob ribbon operator on the right) corresponds to the unbraided case (because in this case the blob excitation moved before the loop excitation is present), so the braiding of our two excitations results in accumulating a phase of $\gamma(e)$. A similar argument holds in the case where the membrane operator and blob ribbon operator are antialigned, except that we should replace e by its inverse.

It is worth noting that the blob excitations with label not in the kernel of ∂ (that is the confined blob excitations, as we saw in Sec. III D) braid nontrivially with the condensed E-valued loop excitations (those with trivial representation of the kernel), while those with label in the kernel braid trivially with them. This is because the condensed E-valued loop excitations have trivial representation of the kernel: $\gamma(e_K) = 1$ for e_K in the kernel. Therefore, the phase gained is 1 when a condensed loop braids with an unconfined blob (which carries a label in the kernel). This matches our expectation that only the confined excitations can braid nontrivially with the condensed excitations.

D. Summary of braiding when $\triangleright$ is trivial

For convenience, we summarize the excitations that braid nontrivially with each other in Table II. We can see that the excitations split into two sets. The electric and magnetic excitations (the excitations corresponding to the group G) braid nontrivially with each other and the blob and E valued loop excitations (the excitations corresponding to E) braid nontrivially with each other, but there is no nontrivial braiding between the two sets.

TABLE II. A summary of which excitations braid nontrivially in case 1, where $\triangleright$ is trivial. A tick indicates that at least some of the excitations of each type braid nontrivially with each other, while a cross indicates that there is no nontrivial braiding between the two types. Notice that the table has a block-diagonal structure, with nontrivial braiding only in the blocks.

Nontrivial	Magnetic			E-valued
Braiding?	Electric	flux	Blob	loop
Electric	✗	✓	✗	✗
Magnetic flux	✓	✓	✗	✗
Blob	✗	✗	✗	✓
E-valued loop	✗	✗	✓	✗

V. RIBBON AND MEMBRANE OPERATORS IN THE FAKE-FLAT CASE

Now that we have considered the first of our special cases, where $\triangleright$ is trivial, we move on to another of our special cases (case 3). We consider the case where our groups G and E, as well as our maps $\triangleright$ and ∂, are completely general, but we restrict our Hilbert space to only allow fake-flat configurations. Many of the features of the excitations are common between the two cases, so we will examine the differences between them rather than repeating our previous discussion entirely.

A. Electric excitations

The electric excitations are unchanged by taking $\triangleright$ nontrivial. Just as in the $\triangleright$ trivial case, we measure the value of a path and assign a weight according to the value of the path. This creates two pointlike excitations at the ends of the path. The operators are best labeled by irreps of the group G, with nontrivial irreps giving the excitations and the trivial irrep giving the identity operator. The excitations labeled by irreps with a nontrivial restriction to the image of ∂ are confined.

B. E-valued loop excitations

Next we consider the E-valued loop excitations, which are produced by membrane operators that measure the surface label of a membrane:

$$L^{\vec{\alpha}}(m) = \sum_{e\in E}\alpha_e\delta(\hat{e}(m), e).$$

Here $\hat{e}(m)$ is the surface label of the membrane m and the α_e are a general set of coefficients. This operator has the same form as the corresponding operator for the $\triangleright$ trivial case. However, there is a slight difference when we consider our irrep basis for the space of E-valued membrane operators [see Eq. (12) for the $\triangleright$ trivial case]. Because our group E may now be non-Abelian, the irreps are generally not 1D. This means that our basis for the E-valued membrane operators must include the matrix indices for those irreps, so that our

general basis operator takes the form

$$L^{\mu,a,b}(m) = \sum_{e\in E}[D^{\mu}(e)]_{ab}\delta(\hat{e}(m), e), \tag{20}$$

where μ is an irrep of E, and a and b are the matrix indices.

In addition to this slight difference in the presentation of the basis operators, we also have some physical differences compared to the $\triangleright$ trivial case. When $\triangleright$ is nontrivial, whenever we measure a surface we must specify a base point with respect to which we measure that surface label [4]. Because the membrane operator for the E-valued loop excitations involves measuring a surface, we must specify a base point for the measurement. We call that base point the start point of our membrane operator. Similarly to the start point of the magnetic membrane operator, this start point may be excited by the action of the E-valued membrane operator. Recall from Sec. II that a vertex transform at the base point of a surface affects the value of that surface, with A_v^g taking the surface label from e to $g \triangleright e$. This means that the vertex term (which is made of a sum of vertex transforms) at the start point of our membrane operator may not commute with our membrane operator, which may result in the vertex being excited (while the other vertex terms are still left unexcited). Whether the start point vertex is excited or not depends on whether the coefficients of $\delta(\hat{e}(m), e)$ are a function of the $\triangleright$ classes of E, where two elements e_1 and e_2 are in the same $\triangleright$ class if there exists a $g \in G$ such that $e_2 = g \triangleright e_1$ (this is an equivalence relation). If the coefficient for each element $e \in E$ is equal to the coefficient for each element related by the $\triangleright$ action, such as $g \triangleright e$, then the start point is not excited. On the other hand, if for each $\triangleright$ class the coefficients for the elements within that $\triangleright$ class sum to zero, then the start point is excited. We note that the irrep basis given in Eq. (20) does not provide a good description for this phenomenon, because the coefficients $[D^{\mu}(e)]_{ab}$ given by the matrix elements of an irrep do not transform in a particular way under an $\triangleright$ action, and this action can even cause mixing between irreps. Generally, to get membrane operators which either definitely excite the start point or definitely leave it unexcited, we must consider linear combinations of the basis operators given in Eq. (20).

In addition to the start point, we also need to be careful when determining the boundary of the surface, which supports the looplike excitation. The boundary of the surface always starts and ends at the start point of the membrane operator because this start point is the base point of the surface. This means that if we nucleate a looplike excitation at the start point and then try to move it away from the start point, part of the boundary still connects to the start point, as shown in Fig. 25. This section of the boundary is attached to the start point and the edges in this section appear twice in the boundary, with opposite orientation each time (see Sec. S-I C in the Supplemental Material of Ref. [15] for more details about the boundary of surfaces), just like a whiskering path of the type considered in Sec. I D of Ref. [14] (also shown in Fig. 4). For this reason, we will refer to such a section of boundary as a whiskered section. As we showed in Sec. S-I C of the Supplemental Material of Ref. [15], the edges along such sections of boundary may be excited if E is non-Abelian (whereas if E is Abelian these edges are never excited). Whether these edges are excited by a particular membrane operator or not depends on the coefficients associated to that membrane operator. For an E-valued membrane operator

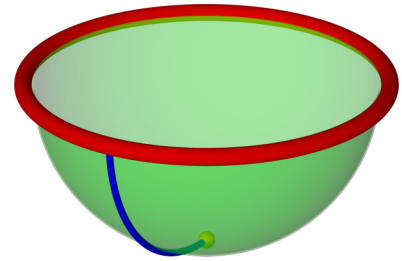

FIG. 25. The boundary of the surface (green) measured by the membrane operator starts and ends at the start point (yellow sphere). If this start point is away from the naive boundary of the membrane (represented by the red torus) there may be a line of excited edges (blue path) connecting the start point to the looplike excitation because the surface label measured by the membrane operator generally transforms nontrivially under such edge transforms when E is non-Abelian. This indicates that for some looplike excitations there is an energetic cost to moving the excitation away from the start point.

$$L^{\vec{\alpha}}(m) = \sum_{e\in E}\alpha_e\delta(\hat{e}(m), e)$$

with a general set of coefficients α_e, the edges on the whiskered section of boundary are left unexcited if the coefficients are a function of conjugacy class, so that $\alpha_e = \alpha_{fef^{-1}}$ for all $e, f \in E$. For example, if the coefficients are given by the characters of an irrep μ of E (which are invariant under conjugation), then the edges will be unexcited. On the other hand, the edges will be excited if the coefficients within each conjugacy class sum to zero. One important thing to note is that if the start point is not excited, then the edges from the start point to the loop are not excited either (as we may expect because the start point becomes unimportant when it is unexcited). To see this, we note that if the start point is unexcited, then the coefficients of the membrane operator are invariant under the $\triangleright$ action: $\alpha_e = \alpha_{g\triangleright e}$ for all $g \in G$ and $e \in E$. In particular, this means that the coefficients are invariant under an action of the form $\partial(f)\triangleright$ for any $f \in E$: $\alpha_e = \alpha_{\partial(f)\triangleright e}$. However, because of the Peiffer condition (2), $\partial(f) \triangleright e = fef^{-1}$. That is, the $\triangleright$ action from an element in $\partial(E)$ is equivalent to conjugation. Therefore, if the coefficient is invariant under any $\triangleright$ action, it is also invariant under conjugation, and so if the start point is unexcited then so are any edges on the whiskered section of the boundary.

This idea that there may be a string of excited edges from the start point to the looplike excitation is significant for the behavior of the excitation. If the edges are not excited, then it indicates that we can move the looplike excitation created by the membrane operator without dragging any excitations from the start point. That is, the excitation is not confined. On the other hand, if the edges are excited, then we cannot move the looplike excitation away from the start point without incurring an energy cost. This means that the excitation is confined. However, note that the additional energy cost is associated to a confining string which connects the loop to the start point. This additional energy does not depend on the size of the loop itself. As we discuss in Sec. IX A (although we do not

consider the fake-flat case in that section, we would expect a similar result), the looplike excitations of this model can also carry pointlike charge (which is balanced by the charge carried by the start point). The fact that the confining energy cost depends on the separation of the loop and start point (rather than the area of the membrane enclosed by the loop) suggests that it is the pointlike charge that is confined, rather than the looplike charge. This is further supported by the fact that the membrane operators that do not produce an excitation at the start point never produce confined looplike excitations.

C. Blob excitations

The blob excitations are changed significantly by taking $\triangleright$ nontrivial and enforcing fake flatness at the level of the Hilbert space. First, as we saw in Sec. III D, in the $\triangleright$ trivial case some of the blob ribbon operators excite the plaquettes along their length (and would still do so when we take $\triangleright$ to be nontrivial). These confined ribbon operators must be thrown out in the fake-flat case because they violate fake flatness. This means that the labels of the blob ribbon operators are restricted to lie in the kernel of ∂. Second, the action of each blob ribbon operator is more complicated. In addition to the path between the centers of blobs, we must specify a path on the lattice from a privileged vertex, called the start point of the operator, to the base points of each affected plaquette. We call this path the direct path, and call the original path (which pierces the affected plaquettes) the dual path. We can either have a single direct path that runs through each of these base points (so that the path to each base point is an extension of the path to the previous base point), or instead have a set of paths, one for each pierced plaquette. Now, instead of simply multiplying the plaquette labels by e or e^{-1}, the blob ribbon operator left multiplies the label of each plaquette p pierced by the dual path by $g(\text{s.p.} - v_0(p))^{-1} \triangleright e$ or right multiplies the plaquette elements by the inverse, where $[\text{s.p.} - v_0(p)]$ is the path from the start point of the ribbon operator to the base point of the affected plaquette and $g(\text{s.p.} - v_0(p))$ is the corresponding group element. As in the $\triangleright$ trivial case, whether the element or its inverse are used depends on the orientation of the plaquette with respect to the dual path of the blob ribbon operator, with the inverse used if the plaquette aligns with the dual path. A simple example of this action is shown in Fig. 26.

The way the direct path affects the action of the blob ribbon operator is similar to how the direct path affects the action of the magnetic ribbon in (2+1)D (as we saw in Ref. [15]), except that instead of conjugation by the path element we have this $\triangleright$ action. If we were allowed blob ribbon operators labeled by a general element of E (rather than just an element in the kernel of ∂), the precise path chosen for this direct path would be significant. This is because when we deform a path t over a fake-flat surface, while keeping the start and end points fixed, the path label $g(t)$ is altered by a factor of the form $\partial(f)$ for some $f \in E$. When E is general, this additional factor of $\partial(f)$ causes a nontrivial difference in expressions of the form $g(t)^{-1} \triangleright e$, such as those which appear in the action of the blob ribbon operator. Specifically, from the Peiffer conditions [Eqs. (1) and (2) in Sec. II] we have $(\partial(f)g(t)^{-1}) \triangleright e = f[g(t)^{-1} \triangleright e]f^{-1}$. However, when we restrict the element e labeling the blob ribbon operator to be in the kernel of ∂, we also ensure that e is in the center of the group E. To see that elements in the kernel of ∂ are also in the center of E, we again use the Peiffer conditions. Given that e_k is an element of the kernel of ∂, the second Peiffer condition [Eq. (2)] tells us that

$$e_k f e_k^{-1} = \partial(e_k) \triangleright f = 1_G \triangleright f = f \Rightarrow e_k f = f e_k \ \forall\ f \in E.$$

That is, elements in the kernel must commute with all elements of E. We also note that if e_k is an element of the kernel, then so is $g \triangleright e_k$ for any $g \in G$. This is because $\partial(g \triangleright e_k) = g\partial(e_k)g^{-1} = gg^{-1} = 1_G$, from the first Peiffer condition [Eq. (1)]. Therefore, for any element e_k in the kernel of ∂, $g \triangleright e_k$ is also in the kernel of ∂ and so is in the center of E. This means that in our earlier expression, $f[g(t)^{-1} \triangleright e]f^{-1}$ is equal to $g(t)^{-1} \triangleright e$ when e is in the kernel, and so the additional factor of $\partial(f)$ from deforming the path t is irrelevant, at least when we act on states that obey fake flatness. Therefore, when we restrict our blob excitations to the nonconfined ones, which are labeled by elements of the kernel of ∂, the precise choice of paths from the start point to the base points of the affected plaquettes does not matter. This insensitivity to the path is only for smooth deformation over fake-flat regions, so if the lattice supports noncontractible cycles then different choices of path may give different actions for the ribbon operator, with these different actions being equivalent to taking different labels for all or part of the ribbon operator.

Much as we saw with the magnetic excitation in (2+1)D, this dependence of the action of the blob ribbon operator on the value of (sections of) the direct path may lead to the blob ribbon operator exciting the start point of the operator. This is because vertex transforms at the start point can affect the path label of the direct path. As we show in Sec. S-I B 2 of the Supplemental Material [20], the start-point vertex is not excited if the ribbon operator is an equal superposition of all

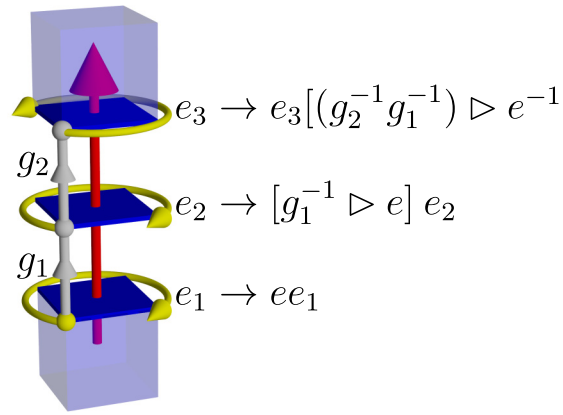

FIG. 26. When $\triangleright$ is nontrivial, the effect of the blob ribbon operator on a plaquette depends on the (inverse of the) path label for a path from a designated start point of the operator (yellow sphere labeled s.p.) to the base point of the plaquette (the gray sphere attached to each plaquette). As in the $\triangleright$ trivial case, the orientation of the plaquette (indicated by the curved yellow arrows) determines whether the plaquette label is left multiplied by e or right multiplied by e^{-1}.

the ribbon operators labeled by elements in an $\triangleright$ class (the sets of elements related by the $\triangleright$ action), but is excited if the coefficients for the elements in each $\triangleright$ class sum to zero.

D. Condensation and confinement

In Sec. III E, we discussed the pattern of confinement and condensation exhibited by the excitations of the higher-lattice gauge theory model when $\triangleright$ is trivial. In addition, we explained that for any pair of groups G and E that form a valid crossed module with $\triangleright$ trivial, there is a family of crossed modules (and so lattice models) differentiated from each other by different maps ∂ (assuming that the two groups can support different homomorphisms ∂). In each family, the model described by the crossed module for which ∂ maps only to the identity of G is an "uncondensed model" where there is no condensation or confinement present. Then the transition to other models described by the same groups G and E (but different ∂) is a condensation-confinement transition. When $\triangleright$ is nontrivial, however, the picture is less clear. This is because, given a model described by an arbitrary crossed module, we cannot necessarily construct a corresponding uncondensed model. To see this, consider a generic crossed module $(G, E, \partial, \triangleright)$. Now suppose that E is a non-Abelian group. This means that there are some pairs of elements $e, f \in E$ such that $efe^{-1} \neq f$. From the Peiffer condition (2) (see Sec. II), this means that $\partial(e) \triangleright f \neq f$ for this pair. However, there is condensation and confinement when $\partial(E)$ is not the trivial group (as we discussed in the $\triangleright$ trivial case in Sec. III E and will describe in the fake-flat case later in this section). If there were an "uncondensed" model with $\partial \to 1_G$, then $\partial(e) \triangleright f \neq f$ from the non-Abelian nature of the group E implies that $1_G \triangleright f \neq f$. However, this is incompatible with the definition of $\triangleright$ as a group homomorphism from G to endomorphisms on E (see Sec. II), because this definition means that the identity element 1_G should be mapped to the identity map on E. Therefore, there is no such crossed module and so no "uncondensed" model corresponding to the pair of groups G and E. Because the Hilbert space is fixed by the lattice and the groups G and E, for a model described by a general crossed module there does not seem to be a corresponding uncondensed model with the same Hilbert space (at least not in the space of higher-lattice gauge theory models, though there may well be another model giving the "uncondensed" phase). This means that we are unable to describe the general model in terms of a condensation-confinement transition in this work. However, we can still describe the pattern of confinement (i.e., which excitations cost energy to separate from their antiparticle) and condensation (i.e., which operators act equivalently to "local" operators on the ground state), which we aim to do briefly in this section.

The first excitations to consider are the electric excitations, some of which are confined due to their ribbon operators exciting the edge terms along the ribbon. These excitations have the same pattern of confinement as in the $\triangleright$ trivial case considered in Sec. III E. Namely, the confined electric ribbon operators $\sum_g \alpha_g \delta(\hat{g}(t), g)$ have coefficients which satisfy $\sum_{e\in E} \alpha_{\partial(e)g} = 0$ for all $g \in G$ and the unconfined ribbon operators have coefficients which satisfy $\alpha_{\partial(e)g} = \alpha_g$ for all $g \in G$ and $e \in E$ (while general ribbon operators can be split into contributions from the two cases and leave the edges along the ribbon in a superposition of excited and unexcited states).

We next consider the blob excitations. Some of these, namely, those created by blob ribbon operators with label outside the kernel of ∂, would be confined, but because the mechanism for this confinement is the violation of the plaquette terms that enforce fake flatness, these ribbon operators must be excluded from the fake-flat model.

So far, this pattern of confinement is the same as for the $\triangleright$ trivial case described in Sec. III E. However, unlike in that case, some of the E-valued loops are also confined, as we described in Sec. V B. That is, the E-valued membrane operators

$$\sum_{e\in E} \alpha_e \delta(\hat{e}(m), e)$$

whose coefficients α_e are sensitive to conjugation (i.e., α_e does not equal $\alpha_{fef^{-1}}$ for some pair $e, f \in E$) may produce an excited string (in addition to the loop excitation itself) as the loop is moved away from the start point of the membrane. In particular, if the coefficients satisfy $\sum_{f\in E} \alpha_{fef^{-1}} = 0$ for each $e \in E$, then the string is definitely excited (whereas the string is definitely not excited if $\alpha_e = \alpha_{fef^{-1}}$ for all $e, f \in E$). As we noted in Sec. V B, this confinement appears to correspond to confinement of the pointlike charge carried by the loop excitation, rather than of the looplike charge, because the confinement energy does not depend on the area of the loop, and the confinement can only occur when the start point of the membrane is excited (an excited start point seems to indicate the presence of a nontrivial pointlike charge, as we are able to show in Sec. IX A 1 for the less general case where ∂ maps to the center of G and E is Abelian).

Next, we consider the pattern of condensation evident in the model in this fake-flat case (case 3 from Table I). By this, we mean that we want to look at which excitations can be produced by operators that are local to the excitation itself. That is, condensed pointlike excitations can be produced by operators that act only on a few degrees of freedom near the excitations, and condensed looplike excitations can be produced by operators near the loops (which have linear extent, so the operators need not be local in the traditional sense). Because we are unable to construct the magnetic excitations when we restrict to fake flatness, the only condensed excitations remaining are E-valued loop excitations. Just as in the $\triangleright$ trivial case, the condensed E-valued loop excitations are those that are produced by membrane operators which are not sensitive to surface elements in the kernel of ∂. This is because if the membrane operator is only sensitive to $\partial(\hat{e}(m))$ (i.e., is not sensitive to the kernel of ∂), then it has the same action as an electric ribbon operator measuring the boundary label (whereas a membrane operator sensitive to the kernel of ∂ can resolve information not obtainable from the boundary path element).

One interesting fact about this pattern of condensation is that it can coexist with the confinement of the E-valued loop excitations. Recall that the condition for the E-valued loop excitation to be confined is that $\sum_{f\in E} \alpha_{fef^{-1}} = 0$ for all $e \in E$. This is not mutually exclusive with the condition that the excitation is condensed [$\alpha_e = \alpha_{ee_k}$ for any $e \in E$ and $e_k \in \ker(\partial)$]. For example, consider a crossed module of

the form ($G, E = G, \partial = \mathrm{id}, \triangleright \to$ conj.), for which the two groups G and E are the same, with ∂ being the identity map, while $\triangleright$ maps to conjugation (i.e., $g \triangleright e = geg^{-1}$). In this case, the only element of the kernel of ∂ is the identity element $1_G = 1_E$. Therefore, any E-valued membrane operator will satisfy the condensation condition (i.e., any coefficients α_e satisfy $\alpha_e = \alpha_{ee_k}$ for all e_k in the kernel of ∂, because e_k can only be the identity element). This means that any coefficients satisfying the confinement condition $\sum_{f\in E} \alpha_{fef^{-1}} = 0$ for this crossed module will also trivially satisfy the condensation condition. How can it be that an excitation is simultaneously confined and condensed? This is because, as we discussed previously in this section, it is the pointlike charge carried by the excitation that is confined. On the other hand, the way we have defined condensation means that the condensation must be of the looplike charge: we have shown that the loop excitation can be produced by an operator local to the excitation (which has linear extent), but this does not mean that the pointlike charge can be produced locally in a pointlike sense (i.e., with support only on a few degrees of freedom). This fact demonstrates that in future study of condensation and confinement in (3+1)D, we must be careful to consider what exactly we mean by condensation or confinement, and which charges (not just excitations) undergo condensation.

VI. BRAIDING IN THE FAKE-FLAT CASE

Next we discuss the braiding relations in this special case, case 3 from Table I, in which we restrict to fake-flat configurations. The fact that we are unable to include the magnetic excitations (because they violate fake flatness) means that the braiding relations are rather simple. Indeed, the only remaining nontrivial braiding is between the E-valued loop excitations and the blob excitations. Just as in the (2+1)D case considered in Ref. [15], however, the signatures of the magnetic excitations are still present in the ground states of manifolds with noncontractible cycles, which can have labels outside of $\partial(E)$. Before we discuss the braiding proper, we will briefly describe how the excitations transform as they are moved around such noncontractible cycles.

A. Moving excitations around noncontractible cycles

The first type of excitation that we wish to consider moving around a noncontractible cycle is the electric excitation. The transformation obtained by moving an electric excitation around such a cycle is the same in the (3+1)D case as in the (2+1)D case considered in Ref. [15]. Namely, if we compare an electric ribbon operator applied on a path s to one that is applied on the path $s \cdot t$ obtained by concatenating the original path with a noncontractible closed path t is

$$S^{R,a,b}(s \cdot t) = \sum_{c=1}^{|R|} [D^R(\hat{g}(t))]_{cb} S^{R,a,c}(s), \tag{21}$$

where $S^{R,a,b}(s \cdot t)$ is the electric ribbon operator labeled by irrep R of G and matrix indices a and b. We see that there is mixing between different electric ribbon operators labeled by the same irrep R, with this mixing controlled by the matrix $D^R[\hat{g}(t)]$ representing the path element $\hat{g}(t)$ in irrep R. The path element $\hat{g}(t)$ is an operator, and the ground states are not typically eigenstates of this operator even for closed paths t.

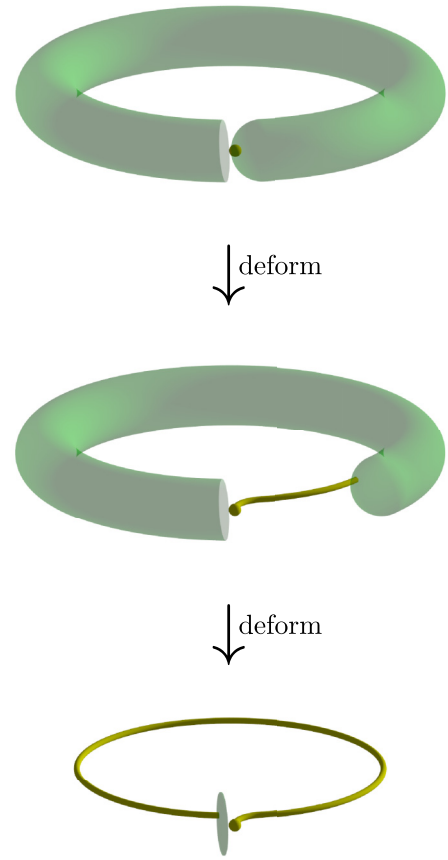

FIG. 27. Given an E-valued membrane operator (green) wrapping around a closed cycle, we can deform the section wrapping around the cycle and shrink it down to nothing. This just leaves a whiskering string (yellow) connecting the start point (yellow sphere) to the small part of the membrane remaining (the green disk in the final image).

In a similar way, we can find how the E-valued looplike excitations transform as they are moved around a noncontractible cycle. In order to do so, we compare E-valued membrane operators applied on two membranes m and m' which are the same except that m' is whiskered around the noncontractible cycle t. This is because the membrane operators are topological, and so a membrane traveling around the cycle can be deformed by shrinking the section of the membrane around the cycle down to nothing, so that only a whiskering path t remains, as shown in Fig. 27. Then the E-valued membrane operator $L^{\mu,a,b}(m')$ applied on this whiskered membrane is given by

$$L^{\mu,a,b}(m') = \sum_{e\in E} [D^\mu(e)]_{ab} \delta(e, \hat{e}(m')),$$

where μ is the irrep of E labeling the membrane operator (and a and b are the matrix indices labeling the operator). The surface element $\hat{e}(m')$ can be written in terms of the surface element of the unwhiskered membrane m using the rules for whiskering surfaces given in Ref. [4]. We have

$$\hat{e}(m') = \hat{g}(t) \triangleright \hat{e}(m),$$

where t is the closed cycle, which is also the path [s.p.(m') − s.p.(m)] between the start points of the two membranes. Then we have

$$\begin{aligned} L^{\mu,a,b}(m') &= \sum_{e\in E}[D^{\mu}(e)]_{ab}\delta(e,\hat{e}(m')) \\ &= \sum_{e\in E}[D^{\mu}(e)]_{ab}\delta(e,\hat{g}(t)\triangleright\hat{e}(m)) \\ &= \sum_{e\in E}[D^{\mu}(e)]_{ab}\delta(\hat{g}(t)^{-1}\triangleright e,\hat{e}(m)) \\ &= \sum_{e'=\hat{g}(t)^{-1}\triangleright e\in E}[D^{\mu}(\hat{g}(t)\triangleright e')]_{ab}\delta(e',\hat{e}(m)). \end{aligned} \quad (22)$$

The matrix $D^{\mu}(\hat{g}(t)\triangleright e')$ can be considered as the matrix representation for element e' in a new irrep, $\hat{g}(t)\triangleright\mu$. Therefore, we see that moving the E-valued loop excitation around the path t mixes the irreps related by this $\triangleright$ action. We say that irreps related by the action of $g\triangleright$ for some $g\in G$ belong to the same $\triangleright$-Rep class of irreps.

The final type of excitation to consider passing around a noncontractible cycle is the blob excitation. Recall from Sec. V C that the action of a blob ribbon operator $B^{e}(r)$ on a plaquette p pierced by the ribbon r is (choosing the plaquette to be aligned with r for simplicity)

$$B^{e}(r):e_p = e_p\{g(\text{s.p.}(r)-v_0(p))^{-1}\triangleright e^{-1}\}.$$

Taking the path s.p.$(r)-v_0(p)$ to be $t\cdot s$, where t is a closed noncontractible cycle, we can write this action as

$$\begin{aligned} B^{e}(r):e_p &= e_p[g(t\cdot s)^{-1}\triangleright e^{-1}] \\ &= e_p\{[g(s)^{-1}g(t)^{-1}]\triangleright e^{-1}\} \\ &= e_p\{g(s)^{-1}\triangleright[g(t)^{-1}\triangleright e^{-1}]\} \end{aligned}$$

which is the same as the action of a blob ribbon operator that does not wrap around the cycle (so that the path [s.p.$(r)-v_0(p)$] is just s) except with e replaced by $g(t)^{-1}\triangleright e$. Note that here we have taken the direct path of the ribbon operator to wrap around the noncontractible cycle, but not the dual path. If we also let the dual path wrap around the cycle, then the plaquettes pierced by s obtain two factors acting on the plaquette label, one from the ribbon before it wraps the cycle (corresponding to the label e) and one from the ribbon after it wraps the cycle [corresponding to the label $g(t)^{-1}\triangleright e$ as above].

B. Loop-blob braiding

Compared to the loop-blob braiding that we saw in Sec. IV C, the loop-blob braiding in this special case is slightly more complicated. This is because the action of the ribbon and membrane operators involved now depends on the values of various paths on the lattice. For example, as we saw in Sec. V C, the blob ribbon operator multiplies plaquette elements by a group element $\hat{g}[\text{s.p.}-\text{v}_0(\text{p})]^{\text{l}-1}\triangleright\text{e}$ which depends on the label of a path. This label is really an operator because the value of the path label depends on what state we are acting on. In particular, the ground state does not have a definite value of this label, instead being made up of a linear combination of states with different path labels. Because of this, we may expect that the braiding does not generally give us a definite result and that the braiding relation may depend on such operator-valued labels. However, as with the braiding of the flux tubes that we saw in Sec. IV B 2, the braiding relations are simple for particular cases where the start points of the operators match. Therefore, we are most interested in these same start-point commutation relations. To understand these, it will be useful to first discuss the interpretation of the blob and loop excitations in 2-gauge theory.

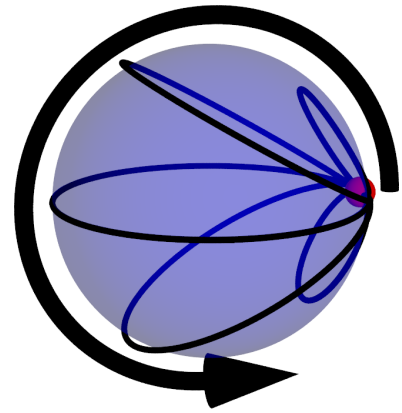

FIG. 28. (Copy of Fig. 25 from Ref. [14]) The 2-holonomy of a surface (in this case a sphere) can be measured by a transport process. A small loop is created at the base point (the small red sphere), then dragged over the surface (the larger blue sphere), as indicated by the arrow.

Similar to lattice gauge theory, it is useful to consider the gauge invariants of higher-lattice gauge theory, which can be built from quantities associated to closed loops and surfaces [4]. In addition to the "1-flux" of loops, which is also present in ordinary gauge theory, we have the "2-flux" or 2-holonomy of closed surfaces. The 2-flux itself, described by an element of E, is not a gauge-invariant quantity. However, the 2-flux of a closed surface is only changed within certain equivalence classes of elements by the gauge transforms [4] (as we will see for tori and spheres in Secs. S-V B and S-V D in the Supplemental Material [20]), and so these classes in E are gauge invariant, with the identity element in particular belonging to a class of its own. This means that the 2-flux is still a useful quantity. In this model, the blob excitations are associated to nontrivial 2-flux on a surface enclosing the blob excitation. The boundary of the excited blob is itself a surface with nontrivial 2-flux because an excited blob by definition has a nontrivial surface label on its boundary. To measure this 2-flux, we must pass a loop over the closed surface whose 2-flux we wish to measure. When we measure the 2-flux, we must specify the base point with respect to which we measure the 2-flux. The choice of base point is equivalent to a gauge choice, so choosing a different base point can give a different element for the 2-flux, within the same $\triangleright$ class (i.e., the new element is related to the old one by a $\triangleright$ action). Once we have chosen the base point, our measurement loop must be nucleated at that base point before being passed over the surface, as shown in Fig. 28. In this model, the E-valued loop excitations measure 2-flux, as we can see from the fact that the corresponding measurement operators assign a weight to each possible surface label.

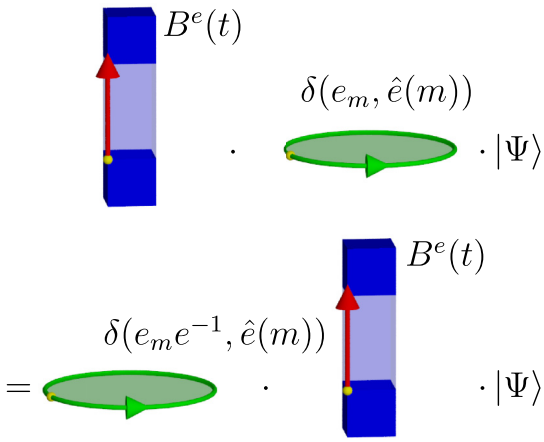

FIG. 29. The result of loop-blob braiding ($|\psi\rangle$ is a state with no excitations near the two operators).

This idea about measuring a 2-flux has important ramifications for our braiding. We have seen that the blob excitations are nontrivial 2-fluxes and the E-valued loop excitations measure surface elements, so these loop excitations can measure the 2-flux of the blob excitations. This is why there is nontrivial braiding between these two types of excitation. When we compare the situation where the loop excitation is passed over the blob to the situation where it is not (i.e., we compare the braided case to the unbraided case), we measure the 2-flux of the blob excitation. However, the blob ribbon operator produces excitations that have definite 2-flux only with respect to the start point of the blob ribbon operator. Similarly, the E-valued loop measures 2-flux with respect to the start point of the membrane operator that creates the loop excitation. Therefore, we expect a definite braiding relation when the start point for our blob ribbon operator matches the start point for our E-valued loop membrane operator. Note that when $\triangleright$ is trivial, the start points lose meaning (we do not need a direct path for the blob ribbon operators and the surface does not need a base point for the E-valued loop) and the loop can be nucleated at any point before being passed over the blob excitation (rather than at the specified start point of the blob ribbon operator). This is why the braiding is simple when $\triangleright$ is trivial (as discussed in Sec. IV C) and it is not necessary to fix the positions of the start points in that case.

While we have discussed braiding of the blobs and the loops so far in terms of passing the loop over the blob, we can equally move the blob excitation through the loop instead. These are equivalent, but it is slightly easier to calculate the latter situation. The relevant commutation relation to calculate this braiding relation is shown in Fig. 24. Again, we must ensure that the start points of each operator are in the same location.

The result of this same-site braiding, where we pass a ribbon operator $B^e(t)$ through an E-valued membrane operator $\delta(e_m, \hat{e}(m))$, is then

$$B^e(t)\delta(e_m, \hat{e}(m)) = \delta(e_m e^{-1}, \hat{e}(m))B^e(t),$$

as illustrated in Fig. 29 (and proven in Sec. S-IV B in the Supplemental Material [20]). The operators $\delta(e_m, \hat{e}(m))$ for each label $e_m \in E$ form a basis for our space of E-valued membrane operators, but we want to consider the commutation of one of the basis operators labeled by an irrep of E instead. We have that

$$\begin{aligned} &B^e(t)\sum_{e_m\in E}[D^\alpha(e_m)]_{ab}\delta(\hat{e}(m), e_m) \\ &= \sum_{e_m\in E}[D^\alpha(e_m)]_{ab}\delta(\hat{e}(m), e_m e^{-1})B^e(t) \\ &= \sum_{e'=e_m e^{-1}\in E}[D^\alpha(e'e)]_{ab}\delta(\hat{e}(m), e')B^e(t) \\ &= \sum_{e'\in E}\sum_{c=1}^{|\alpha|}[D^\alpha(e')]_{ac}[D^\alpha(e)]_{cb}\delta(\hat{e}(m), e')B^e(t) \\ &= \sum_{c=1}^{|\alpha|}[D^\alpha(e)]_{cb}\sum_{e'\in E}[D^\alpha(e')]_{ac}\delta(\hat{e}(m), e')B^e(t). \end{aligned} \tag{23}$$

If α is a 1D representation the braiding therefore results in the accumulation of a phase of $\alpha(e)$. If α is higher dimensional, then it would seem that there is mixing between the different matrix indices. However, recall from Sec. V C that in order to ensure fake flatness we restricted the label e of the blob ribbon operators to be in the kernel of ∂ and therefore the center of E. The matrix representation of an element of the center is a scalar multiple of the identity from Schur's lemma, so we can write $[D^\alpha(e)]_{cb} = \delta_{cb}[D^\alpha(e)]_{11}$ (where the index 1 could be replaced with any index). This means that the braiding relation 23 simplifies to

$$\begin{aligned} &B^e(t)\sum_{e_m\in E}[D^\alpha(e_m)]_{ab}\delta(\hat{e}(m), e_m) \\ &\quad= [D^\alpha(e)]_{11}\sum_{e'\in E}[D^\alpha(e')]_{ab}\delta(\hat{e}(m), e')B^e(t), \end{aligned} \tag{24}$$

so again we only accumulate a phase $[D^\alpha(e)]_{11}$ (this matrix element must be a phase because the matrix is diagonal and unitary, and in fact the matrix element can be used to define an irrep of the kernel of ∂).

We see that the braiding relation between the E-valued loops and blob excitations is similar to the result we found for the braiding of magnetic fluxes and charges that we discussed in Sec. IV B 1, except that in this case the irrep labels the looplike, rather than pointlike, excitation.

C. Summary of braiding in the fake-flat case

In Table III, we summarize the braiding in the fake-flat case by indicating which excitations can braid nontrivially. Note that when we enforce fake flatness on the level of the Hilbert space, there are no magnetic excitations, although we can still have nontrivial flux labels around noncontractible loops on manifolds that are not simply connected (e.g., the 3-torus).

VII. RIBBON AND MEMBRANE OPERATORS IN THE CASE WHERE $\partial \to$ CENTER(G) AND E IS ABELIAN

So far, we have examined the excitations of the higher-lattice gauge theory model in two cases. First, we looked at the case where $\triangleright$ is trivial, where we can find all of the excitations

TABLE III. A summary of the nontrivial braiding in the fake-flat case. In the fake-flat case, there are no magnetic excitations and the nontrivial braiding between excitations only involves the blob excitations and E-valued loops. However, there are nontrivial results from moving excitations around handles (noncontractible cycles), which can support nontrivial 1-flux.

Nontrivial braiding?	Electric	Blob	E-valued loop	Around handle
Electric	✗	✗	✗	✓
Blob	✗	✗	✓	✓
E-valued loop	✗	✓	✗	✓

of the model. However, in this case the membrane operators corresponding to the 2-gauge field (labeled by the group E) are simple, and produce no excitations at the start point of the corresponding operators. Second, we looked at the case where $\triangleright$ is general, but where we restrict our Hilbert space to the fake-flat subspace, thus having to exclude the magnetic excitations. This gave us more interesting excitations from our 2-gauge field, allowing the E-valued membrane operators and blob ribbon operators to produce additional excitations at the start points of the operators. However, excluding the magnetic excitations removes the interesting features from the 1-gauge field excitations. In the following sections, we consider a generalization of the $\triangleright$ trivial case, which will allow us to keep all of the excitations while also gaining many of the features from the $\triangleright$ general case. This means that we will be able to see how the magnetic excitation interacts with the more general 2-gauge excitations. We consider the case where E is Abelian and ∂ maps onto the center of G (case 2 in Table I). Note that this case includes the $\triangleright$ trivial case as a subcase, so this is a strict generalization of the situation considered in Secs. III and IV.

In this case, many of the features of the general crossed module (but fake-flat) case are preserved, despite our restrictions on the crossed module. The electric, E-valued loop and blob excitation creation operators are all the same as in the general crossed module (but fake-flat) case (see Sec. V), except that we also allow blob ribbon operators with labels outside the kernel of ∂ and the irreps that label the basis E-valued membrane operators are 1D. Because of this, we will not describe the operators that produce these excitations again. On the other hand, we can include excitations analogous to the magnetic excitations from the $\triangleright$ trivial case. The membrane operators that produce these magnetic excitations are significantly altered from the $\triangleright$ trivial case that we considered in Sec. III B, however. This alteration of the membrane operators is necessary to ensure that each membrane operator commutes with the various energy terms, apart from those near the boundary of the membrane. The magnetic membrane operators affect the edge labels in the same way as in the $\triangleright$ trivial case, but they also affect the plaquette labels near the membrane. Recall that to specify our magnetic membrane we had to define a dual membrane, with the operator changing the labels of the edges cut by the dual membrane, and a direct membrane, with paths on the direct membrane controlling how the cut edges were changed (see Fig. 7). As well as edges, the dual membrane cuts through the plaquettes between these edges (such as the vertical plaquettes in Fig. 30). In this new case, the magnetic membrane operator changes the label of the "cut" plaquettes if their base points lie on the direct membrane. We say that plaquettes whose base points lie on the direct membrane are based on the direct membrane. The action of the operator on these plaquettes depends on paths on the direct lattice, in a similar way to the action on the edges. Given a cut plaquette based on the direct membrane, the action of the membrane operator on the plaquette depends on the label of a path from the start point of the membrane to the base point of the plaquette. An example of this type of path is shown in Fig. 30. We denote the group element assigned to the path between the start point and the base point of plaquette p by $g[\text{s.p.} - \text{v}_0(\text{p}))]$, where s.p. is the privileged start point of the membrane operator and $v_0(p)$ is the base point of the plaquette p. If p is cut by the dual membrane and based on the direct membrane, then its label is changed from e_p to $\{g[\text{s.p.} - v_0(p)]^{-1} h g[\text{s.p.} - v_0(p)]\} \triangleright e_p$. As we mentioned previously, the magnetic membrane operator only acts on a cut plaquette in this way if the plaquette is based on the direct membrane. That is, if the plaquette has its base point away from the direct membrane, then the label of the plaquette is not affected by this $\triangleright$ action. It may seem arbitrary that the plaquette label is only changed in this way if its base point is on the direct membrane. However, this is analogous to the action of vertex transforms, which only affect plaquettes that are based at the vertex on which we apply the transform (except instead of only affecting surfaces based at the vertex, the membrane operator affects surfaces based on that surface). Indeed, we demonstrate that closed magnetic membrane operators are closely related to the vertex transforms in Secs. S-II D and S-II E of the Supplemental Material [20].

The $\triangleright$ action on the plaquettes is not the only additional feature to the magnetic membrane operator in this new special case. Changing some of the edge labels by multiplication and plaquette labels by this $\triangleright$ action leaves the blob conditions for blobs cut by the dual membrane unsatisfied (recall that the blob condition enforces that the total surface label of the blob is trivial). To correct this and ensure that the membrane operator commutes with the blob energy terms near the bulk of the membrane, blob ribbon operators (of the type considered in Sec. V C) are added to the membrane operator. For every plaquette that is entirely on the direct membrane (not cut by the dual membrane, but instead lying flat on the direct membrane), we have one such blob ribbon operator associated to that plaquette. We call the associated plaquette the base plaquette for that blob ribbon operator. The blob ribbon operators all start at the same privileged blob, which we call blob 0 and must define when specifying the magnetic membrane operator. The blob ribbon operators end at the blob that is connected to the base plaquette and cut by the dual membrane, as shown in Fig. 31. The label of this blob ribbon operator, for a base plaquette b on the direct membrane and with orientation away from the dual membrane (downwards in Fig. 31, as shown in Fig. 32), is given by $f(b) = \{g[\text{s.p.} - v_0(b)] \triangleright e_b\}\{[h^{-1} g(\text{s.p.} - v_0(b))]\} \triangleright e_b^{-1}]$, where e_b is the label of the base plaquette and $v_0(b)$ is the base point of the plaquette. If the plaquette has the opposite orientation, we must invert the

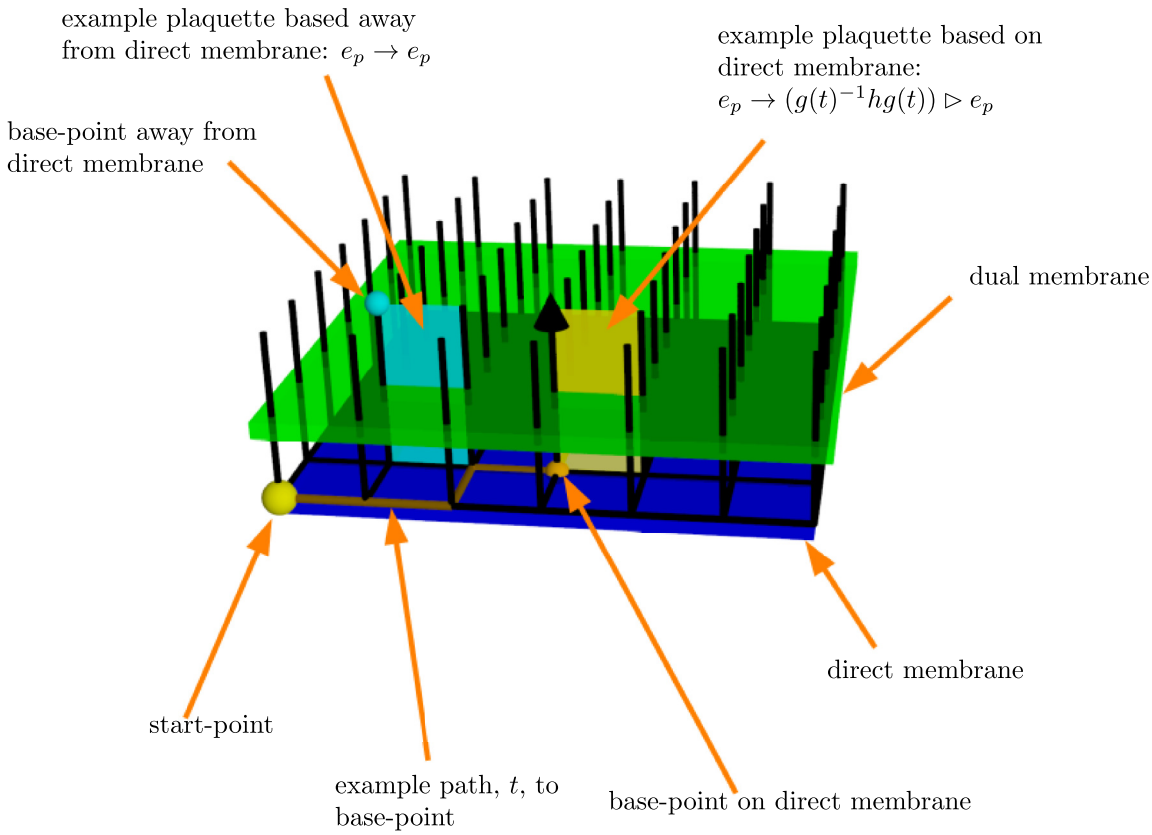

FIG. 30. In addition to changing the edges cut by the dual membrane, when $\triangleright$ is nontrivial the magnetic membrane operator affects the plaquettes cut by the dual membrane if their base points lie on the direct membrane.

label e_b in this expression. After incorporating this additional action for the magnetic membrane operator, we write the total magnetic membrane operator [denoted by $C_T^h(m)$, where T indicates that it is the total operator] as

$$C_T^h(m) = C_{\triangleright}^h(m) \prod_{\text{plaquette } b \in m} B^{f(b)}(\text{blob } 0 \to \text{blob } b), \quad (25)$$

where blob b is the blob attached to base plaquette b and cut by the dual membrane (note, however, that the same blob may be attached to multiple base plaquettes). In Eq. (25), $C_{\triangleright}^h(m)$ performs the action of the membrane operator on the edges and the $\triangleright$ action on the plaquettes, while the $B^{f(b)}(\text{blob } 0 \to \text{blob } b)$ operators are the added blob ribbon operators (see Sec. V C for a description of blob ribbon operators).

Even with these modifications, the magnetic membrane operator still excites more energy terms than in the $\triangleright$ trivial case (i.e., more than just the boundary plaquettes and potentially the start-point vertex). First, the privileged blob, blob 0, is not generally left in an energy eigenstate. This is because the blob ribbon operators that we added to the magnetic membrane all originate in this blob and so change the surface label of the blob, from 1_E in the ground state to $[h \triangleright \hat{e}(m)^{-1}]\hat{e}(m)$, where $\hat{e}(m)$ is the total surface label of the direct membrane. $\hat{e}(m)$ is an operator, which means that blob 0 is not generally left in an energy eigenstate. Second, the edges around the boundary of the direct membrane are potentially excited. This is because the labels of the added blob ribbon operators depend on the labels of the plaquettes on our direct membrane. Edges in the bulk of the membrane are attached to two plaquettes on the membrane and so the edge transform affects the blob ribbon operators associated with both plaquettes. These effects on the labels of the two ribbon operators (together with a contribution from the edge transform on the plaquettes cut by the dual membrane) cancel out, so that the edge transform commutes with the membrane operator, as we show in Sec. S-I D 3 of the Supplemental Material [20]. On the other hand, edges on the boundary of the membrane are only attached to one plaquette on the membrane, so there is no such cancellation. These boundary edges are therefore not generally left in an energy eigenstate.

A. Condensation and confinement

In the previously considered $\triangleright$ trivial (see Sec. III E) and fake-flat cases (see Sec. V), we saw that many of the excitations are confined, meaning that it costs energy to separate a pair of excitations, in addition to the energy required to produce the pair. We also found that other particle types are condensed, meaning that they can be produced by local operators (local to the excitation, in the sense discussed in Sec. III E) and so carry trivial topological charge. The pattern of condensation and confinement in the $\partial \to \text{center}(G)$ case is the same as in the $\triangleright$ trivial case discussed in Sec. III E. The blob excitations with label not in the kernel of ∂ are confined, as are the electric excitations labeled by irreps of

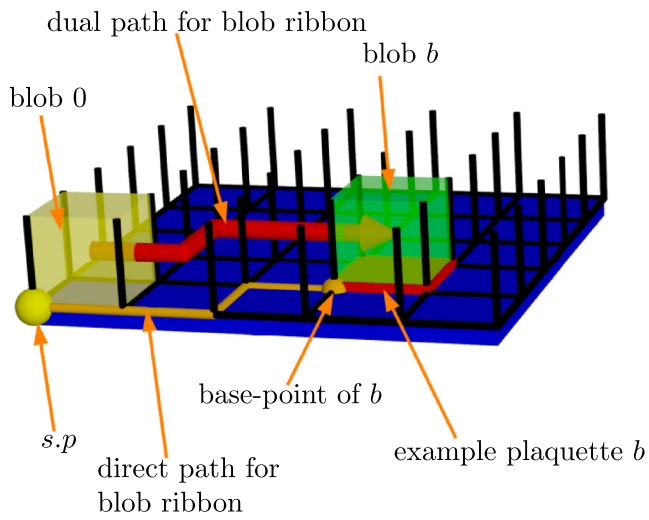

FIG. 31. When we define the magnetic membrane operator $C_T^h(m)$, we must include blob ribbon operators. There is one blob ribbon operator per plaquette on the direct membrane (which is represented by the large blue surface here, while the dual membrane is omitted and would be above this surface, cutting through the vertical edges). Here we show an example, corresponding to the plaquette b (red square). The dual path for the blob ribbon operator runs from the privileged blob 0 to the blob, blob b, which is attached to the plaquette b and cut by the dual membrane (not shown for clarity, but it would be above the direct membrane and bisect the vertical edges). The direct path for the ribbon operator runs from the start point of the membrane, s.p, to the base point of plaquette b.

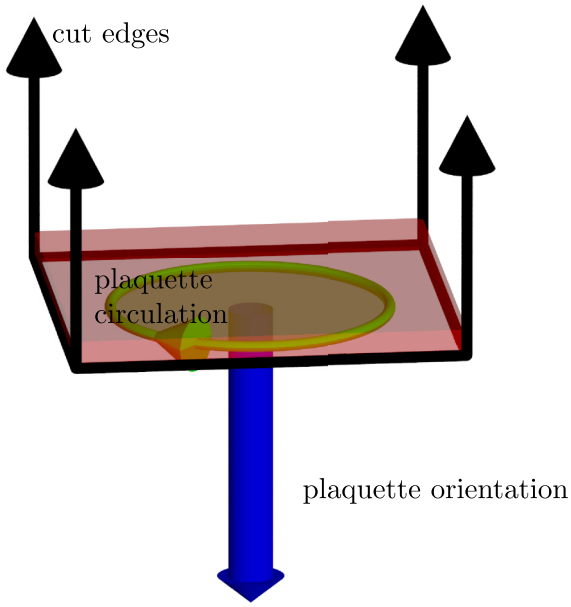

FIG. 32. We consider the case where the plaquettes on the membrane point downwards, away from the cut edges. To obtain the case where some of the plaquettes point upwards, we must invert the labels of those plaquettes. Note that the orientation of the plaquette is related to the circulation by the right-hand rule.

G that have nontrivial restriction to the subgroup $\partial(E)$ of G. On the other hand, the condensed excitations are the magnetic excitations with label in the image of ∂ and the E-valued loops that are labeled by irreps of E which are trivial on the kernel of ∂. These properties, along with the other properties of the excitations in this case, are summarized in Fig. 33.

VIII. BRAIDING IN THE CASE WHERE $\partial \to$ CENTER(G) AND E IS ABELIAN

Now that we have described the membrane and ribbon operators that produce our excitations, we can consider the braiding relations of these excitations. Any braiding not involving the magnetic excitations is the same as in the fake-flat case described in Sec. VI. Namely, there is nontrivial braiding between the blob excitations and the E-valued loops, with the same start-point braiding resulting in an accumulation of phase. The result is a phase, rather than the more general transformation given in Eq. (23) for the case considered in Sec. VI B, because the irreps of E are 1D when E is Abelian.

Unlike for the fake-flat case, we can find the magnetic excitations and so describe their braiding relations. However, rather than using the magnetic membrane operator directly, it is convenient when considering braiding to combine the magnetic membrane operator with an E-valued membrane operator. We multiply the magnetic membrane operator by an E-valued membrane operator such as $\delta(e_m, \hat{e}(m))$, acting before the magnetic membrane operator. That is, we construct membrane operators of the form $C_T^h(m)\delta(e_m, \hat{e}(m))$, which we denote by $C_T^{h,e_m}(m)$. We note that combining the magnetic membrane operator with this E-valued membrane operator in this way does not excite regions of the lattice not already excited by the magnetic membrane operator, because both membrane operators only cause excitations near the boundary of the membrane, and possibly at blob 0 and the start point of the membrane. We will shortly explain why we perform this combination of membrane operators (in essence, it gives the looplike excitation a well-defined 2-flux), but before we discuss this we shall consider the combination of the membrane operators in more detail.

In order to combine the magnetic and E-valued membrane operators, there are some details that we must specify. The first of these is the relative orientation of the two membrane operators. We take the orientation of the E-valued membrane operator to point away from the dual membrane of the magnetic membrane operator. The second detail is more subtle. In addition to combining this E-valued membrane operator with the magnetic membrane operator, we move blob 0 and the start point of the membrane operator so that they are displaced slightly away from the membrane itself, as shown in Fig. 34. We do this because the E-valued membrane may cause an excitation at the start point, which would prevent us from using the topological nature of the magnetic membrane operator to deform the membrane. It is not necessary to move blob 0 in this way, but it will be convenient when considering topological charge to have a clear separation between the pointlike excitations (blob 0 and the start point) and the looplike excitation at the boundary of the membrane. A third detail is our convention for the overall orientation of the total membrane operator. Because we have displaced the start

Electric

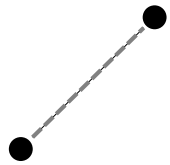

- Pointlike
- Labelled by irreps of G
- Internal space described by matrix indices
- Confined if nontrivial restriction of irrep to $\partial(E)$

Magnetic

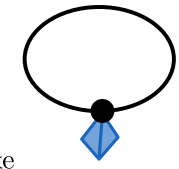

- Looplike
- Labelled by conjugacy classes of G
- Internal space within conjugacy class
- Condensed if conjugacy class in $\partial(E)$

Blob

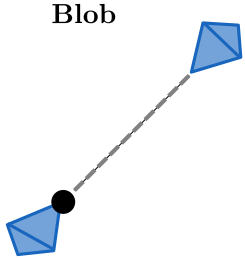

- Pointlike
- Labelled by $\triangleright$-classes of E
- Internal space within class
- Confined if class not in $\ker(\partial)$

E-valued loop

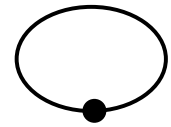

- Looplike
- Labelled by $\triangleright$-Rep classes of irreps of E
- Internal space within class
- Condensed if nontrivial restriction to $\ker(\partial)$

FIG. 33. A summary of the excitations in the E Abelian, $\partial \to \text{center}(G)$ case.

point away from the membrane in a particular direction, it is sensible to define the orientation of the membrane to be consistent with this displacement. That is, we imagine that the loop excitation is nucleated at the start point and moves away from the start point along the membrane. Therefore, the loop excitation would be oriented downwards in Fig. 34, matching the orientation of the E-valued membrane operator.

Having considered these details about the combined membrane operator, we now explain why this combination was useful. As we mentioned in Sec. VII, the action of the magnetic membrane operator generally causes the privileged blob, blob 0, of the membrane to acquire a nontrivial 2-flux (nontrivial surface label). However, this surface label is given in terms of an operator [the surface label $\hat{e}(m)$ of the membrane itself] and so is not well defined. Including the E-valued membrane operator ensures that the 2-flux of the privileged blob 0 after the action of the magnetic membrane operator is well defined. Giving blob 0 a definite 2-flux is significant because we expect the looplike excitation to also carry a nontrivial 2-flux to balance the 2-flux of blob 0, and we expect the value of this 2-flux to be important in braiding relations. As we show in Sec. S-IV C of the Supplemental Material [20], the surface label of blob 0 after the action of the combined membrane operator (with displaced start point, which does affect the label) is given by $e_m^{-1}[h^{-1} \triangleright e_m]$. As we show in Sec. S-IV C [see Eq. (S105)] [20], the 2-flux of the loop excitation labeled by h and e_m is given by

$$\tilde{e}_m = e_m\left[h^{-1} \triangleright e_m^{-1}\right], \tag{26}$$

which is the inverse of the 2-flux carried by blob 0. Due to the fact that the excitations produced by this combined membrane operator carry both ordinary magnetic flux and this 2-flux, we call the combined membrane operator a "higher-flux membrane operator" and call the excitations higher-flux excitations. If we wish to instead consider the original magnetic membrane operator (without the attached E-valued membrane operator), we can simply sum over each value of e_m because this gives us a complete sum of projectors $\delta(e_m, \hat{e}(m))$. That is $\sum_{e_m \in E} \delta(e_m, \hat{e}(m)) = 1$ and so

$$\sum_{e_m \in E} C_T^{h,e_m}(m) = C_T^h(m). \tag{27}$$

Having constructed this higher-flux membrane operator, we can now use it to find the braiding relations involving the higher-flux excitations. Because the action of the higher-flux membrane operator on the edges is the same as that of the magnetic membrane operator from the $\triangleright$ trivial case, the braiding relation between the magnetic and electric excitations is the same as in that case (which is described in Sec. IV).

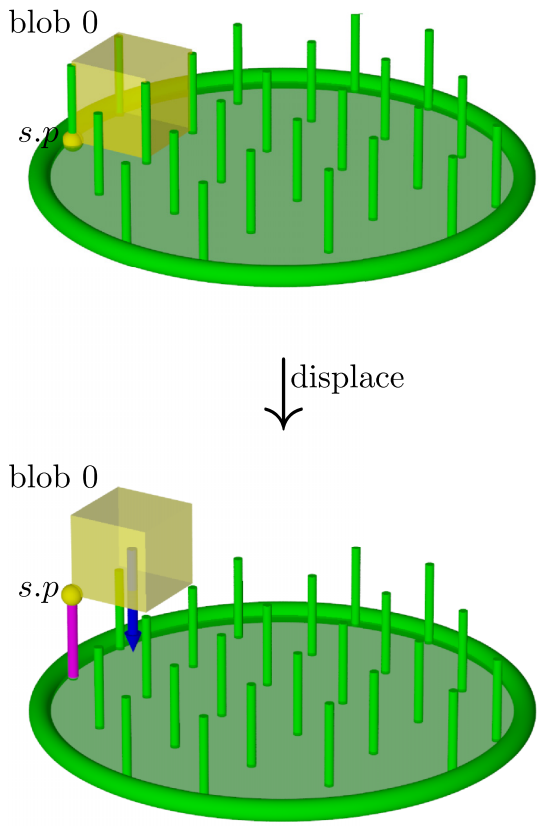

FIG. 34. Rather than place blob 0 and the start point (represented by the yellow cube and sphere, respectively) of the membrane operator on the direct membrane (green) itself, as in the upper image, we displace them away from the membrane as shown in the lower image. Then blob 0 and the start point are on the other side of the edges cut by the dual membrane (where the edges are represented by the green cylinders). This allows us to deform the membrane away from the start point and blob 0 (downwards in the figure) using the topological property of the magnetic and E-valued membrane operators which make up the higher-flux membrane operator.

However, as we will see shortly, the braiding between the higher-flux loop excitation and the other excitations is significantly altered. In particular, because the higher-flux excitations can carry a nontrivial 2-flux, we expect nontrivial braiding relations with the E-valued loops, which measure 2-flux.

A. Braiding of the higher-flux excitations with blob excitations

The first braiding relation we examine is between the higher-flux excitations and the blob excitations. We consider a blob ribbon operator $B^e(t)$, applied on a ribbon t, piercing the membrane of a higher-flux membrane operator $C_T^{h,e_m}(m)$, applied on a membrane m. The ribbon t intersects the membrane m at a plaquette q, as shown in Fig. 35. Note that the orientation of the operators is significant. We first look at the case where the blob ribbon operator pierces the direct membrane of the magnetic membrane operator before the dual membrane. If the membrane is oriented downwards, as in Fig. 35 (note that the pointlike excitation is above the loop) then the ribbon is oriented upwards (at the point of intersection at least).

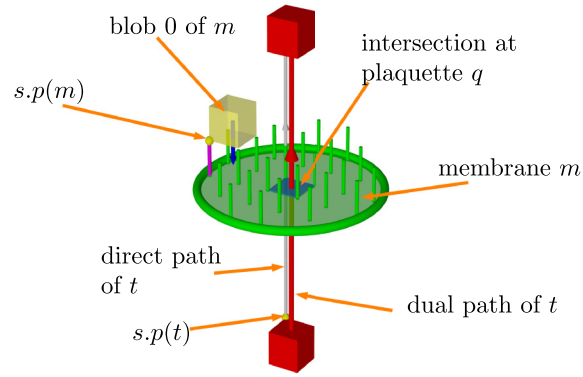

FIG. 35. We consider a blob ribbon operator $B^e(t)$ (between the two red blobs) that passes through a higher-flux membrane operator $C_T^{h,e_m}(m)$ (where m is shown in green). The ribbon t pierces the membrane m through a plaquette q (blue square).

We have seen in previous cases that braiding is frequently well defined only when the start points of the membrane and ribbon operators match. However, we shall first examine the general case where the start points are arbitrary. As usual, we can relate the braiding relation to a commutation relation between the two operators. We compare the case where the magnetic membrane is produced first, and then the blob excitation moved through it, to the reverse case. We find that, as demonstrated in Sec. S-IV C 1 in the Supplemental Material [20],

$$\begin{aligned} &B^e(t)C_T^{h,e_m}(m)|GS\rangle \\ &\quad = C_T^{h,e_m\{\hat{g}(\mathrm{s.p.}(m)-\mathrm{s.p.}(t))\triangleright e\}}(m)B^e(t_1') \\ &\qquad \times B^{\{\hat{g}(\mathrm{s.p.}(t)-s.p.(m))h^{-1}\hat{g}(\mathrm{s.p.}(t)-s.p(m))^{-1}\}\triangleright e}(t_2')|GS\rangle. \end{aligned} \quad (28)$$

In this expression, we note that the original ribbon operator is split into two parts, on ribbons t_1' and t_2', which transform differently under the braiding. Here t_1' starts at the original origin of ribbon t and ends at blob 0 of the membrane m (corresponding to the part of the ribbon before the intersection with the membrane, except that it is diverted to end at blob 0 of m), while t_2' starts at blob 0 and ends at the original end of ribbon t (corresponding to the part of the ribbon after the intersection), as shown in Fig. 36. We therefore see that, under commuta-

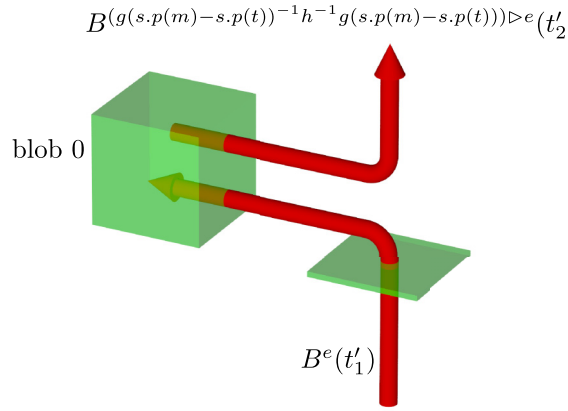

FIG. 36. The blob ribbon operators after commutation.

tion, the ribbon t is diverted to pass through blob 0 of the membrane, and after passing through this blob it changes label from e to $\{\hat{g}(\text{s.p.}(t) - \text{s.p.}(m))h^{-1}\hat{g}(\text{s.p.}(t) - \text{s.p.}(m))^{-1}\} \triangleright e$.

The fact that the label of the blob ribbon operator before the intersection is unaffected by the commutation relation is perhaps unsurprising because this part of the operator corresponds to the motion of the blob excitation before it braids with the magnetic excitation and so before it has undergone its transformation. This can be seen from the fact that the blob ribbon operator actually creates two excitations and the one which is not moved should not be affected by the other one moving through the loop excitation. Another thing to note is that, as long as the blob ribbon operator is not confined, we can deform the ribbons of the blob ribbon operators without changing their action, as long as we keep the end points fixed. Because of this, it does not matter at which plaquette q our magnetic membrane and blob ribbon operators intersect.

In addition to the transformation undergone by the blob ribbon operator, the E label of the higher-flux excitation changes from e_m to $e_m\{\hat{g}(\text{s.p.}(m) - \text{s.p.}(t)) \triangleright e\}$. This transformation of the E label of the membrane operator is simply the standard braiding relation between a blob excitation and an E-valued membrane, as we saw in Sec. VI. We note that this result and the other results given in this section are proven fully in Sec. S-IV C 1 in the Supplemental Material [20].

If we give the magnetic membrane operator and the blob ribbon operator the same start point, the braiding relation that we explained above simplifies and we are able to remove the operator $\hat{g}(\text{s.p.}(m) - \text{s.p.}(t))$ from the relation. We move the start points together, without moving them through the higher-flux membrane (which would alter the commutation relations found so far). In this case the blob label goes from e before the braiding to $h^{-1} \triangleright e$ afterwards (at least in the part after the intersection) and the E label of the higher-flux membrane operator goes from e_m beforehand to $e_m e$. If we had used the opposite orientation, obtained by reversing the direction of the blob ribbon operator, instead the blob label e becomes $h \triangleright e$ and the membrane label e_m becomes $e_m[h \triangleright e^{-1}]$. Again, this result is proven in Sec. S-IV C 1 of the Supplemental Material [20].

If we want to consider the braiding of the original magnetic excitation, produced by the membrane operator $C^h(m) = \sum_{e_m \in E} C^{h,e_m}(m)$, we simply need to sum over the E-valued label e of the higher-flux membrane operator. Then we have, from Eq. (28),

$$\begin{aligned}
&B^e(t)C_T^h(m)|GS\rangle \\
&\quad = \sum_{e_m \in E} B^e(t)C_T^{h,e_m}(m) \\
&\quad = \sum_{e_m \in E} C_T^{h,e_m\{\hat{g}(\text{s.p.}(m)-\text{s.p.}(t)\}\triangleright e]}(m)B^e(t_1') \\
&\qquad \times B^{\{\hat{g}(\text{s.p.}(t)-\text{s.p.}(m)]h^{-1}\hat{g}(s.p(t)-s.p(m)]^{-1}\}\triangleright e}(t_2')|GS\rangle \\
&\quad = \sum_{e_m'=e_m\{\hat{g}(\text{s.p.}(m)-\text{s.p.}(t)]\triangleright e\}} C_T^{h,e_m'}(m)B^e(t_1) \\
&\qquad \times B^{\{\hat{g}(\text{s.p.}(t)-\text{s.p.}(m)]h^{-1}\hat{g}(\text{s.p.}(t)-\text{s.p.}(m)]^{-1}\}\triangleright e}(t_2')|GS\rangle \\
&\quad = C_T^h(m)B^e(t_1) \\
&\qquad \times B^{\{\hat{g}(\text{s.p.}(t)-\text{s.p.}(m)]h^{-1}\hat{g}(\text{s.p.}(t)-\text{s.p.}(m)]^{-1}\}\triangleright e}(t_2')|GS\rangle, \quad (29)
\end{aligned}$$

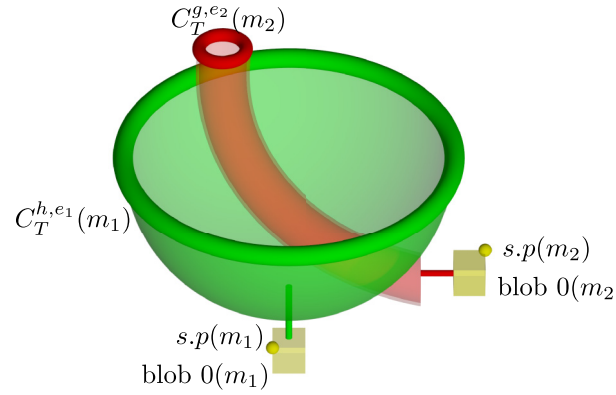

FIG. 37. We consider the braiding move where we pull one higher-flux loop excitation (small red torus) through another (large green torus). This can be implemented using higher-flux membranes applied on the (green and red) membranes in the figure. If we first apply the membrane operator $C_T^{h,e_1}(m_1)$ on the larger (green) membrane, then $C_T^{g,e_2}(m_2)$ on the narrower (red) membrane, then we are considering the case where we first produce the larger (green) loop excitation then move the smaller (red) one through it. Comparing this to the opposite order of operators gives us the braiding relation.

from which we see that the magnetic excitation is unchanged by the braiding, whereas the blob excitation is affected in the same way as in the braiding with the higher-flux excitation.

B. Braiding with other higher-flux excitations

Next, we consider the braiding between two higher-flux excitations. As we described in Sec. IV A 2, there are two kinds of braiding for loops. The first, which we call permutation, involves moving two loops around each other without passing through one another. The other, which we term braiding, involves passing one though the other. As we discussed in Sec. IV A 2, the permutation move is trivial in this model. Therefore, we just consider the braiding move. In this motion, shown in Fig. 37, one of the magnetic loop excitations (indicated by a small red ring) is moved along the red surface and through another loop (indicated by a large green loop attached to a large green surface). To calculate the braiding relation we apply membrane operators on these surfaces and examine the commutation relations between the membrane operators.

We define the membrane operators as indicated in Fig. 37, but then we use the topological nature of the magnetic membrane operators to pull m_2 through m_1 (as we did in the $\triangleright$ trivial case in Sec. IV B 2), while keeping the start point and blob 0 fixed. In Sec. S-IV C 2 in the Supplemental Material [20],

we show that this leads to the commutation relation

$$C_T^{g,e_2}(m_2)C_T^{h,e_1}(m_1)|GS\rangle = C_T^{h,e_1[g((1)-(2))\triangleright\{(h_{[2-1]}\triangleright e_2^{-1})[(h_{[2-1]}g^{-1})\triangleright e_2]\}]}(m_1)C_{\triangleright}^{h_{[2-1]}gh_{[2-1]}^{-1}}(m_2)$$
$$\times\left(\prod_{\substack{\text{plaquette}\\ p\in m_2}} B^{[h_{[2-1]}^{-1}\triangleright e_{p|2}][(g^{-1}h_{[2-1]}^{-1})\triangleright e_{p|2}^{-1}]}((2)-(1))B^{e_{p|2}[(h_{[2-1]}g^{-1}h_{[2-1]}^{-1})\triangleright e_{p|2}^{-1}]}((1)-p)\right)$$
$$\times\,\delta(h_{[2-1]}\triangleright e_2,\hat{e}(m_2))|GS\rangle, \tag{30}$$

where $g((1)-(2))$ is the path element for the path between the two start points of the membranes and

$$h_{[2-1]} = g((1)-(2))^{-1}hg((1)-(2)) = g((2)-(1))hg((2)-(1))^{-1}. \tag{31}$$

To simplify the expression, we used $e_{p|2}$ to denote the label of the plaquette p when we move its base point to the start point of m_2. This quantity is equivalent to $g[\text{s.p.}(m_2)-v_0(p)]\triangleright e_p$. Furthermore, we used $B^{\cdots}[(2)-(1)]$ to denote a blob ribbon operator that runs from blob 0 of m_2 to blob 0 of m_1 and $B^{\cdots}[(1)-p]$ to denote a blob ribbon operator running from blob 0 of m_1 to the blob on m_2 that is attached to plaquette p. These blob ribbon operators may seem complicated, but the situation is analogous to the braiding of blob ribbon operators with the magnetic membranes. Each of the blob ribbon operators that we added to the magnetic membrane operator has a similar commutation relation with the magnetic membrane operator as an ordinary blob ribbon operator. Namely, the blob ribbon operator splits into two parts, one that runs from blob 0 of m_2 to blob 0 of m_1 and one which runs from blob 0 of m_1 to the final destination of the original blob ribbon operator. The only difference from the ordinary blob ribbon operator braiding is that the label of the blob ribbon operator is an operator (depending on the label of a plaquette on m_2), which causes an additional apparent change to the label even for the part of the blob ribbon operator before the intersection. However, this does not reflect a real change to the blob ribbon operators before the intersection. This is because we can combine the blob ribbon operators that pass from blob 0 of m_2 to blob 0 of m_1 into a single blob ribbon operator, and use $\delta(h_{[2-1]}\triangleright e_2,\hat{e}(m_2))$ to fix its label in terms of e_2 instead of an operator. As shown in Sec. S-IV C 2 in the Supplemental Material [20], this gives us

$$C_T^{g,e_2}(m_2)C_T^{h,e_1}(m_1)|GS\rangle = C_T^{h,e_1(g((1)-(2))\triangleright\{(h_{(2-1)}\triangleright e_2^{-1})[(h_{[2-1]}g^{-1})\triangleright e_2]\}]}(m_1)C_{\triangleright}^{h_{[2-1]}gh_{[2-1]}^{-1}}(m_2)B^{e_2[g^{-1}\triangleright e_2^{-1}]}((2)-(1))$$
$$\times\left(\prod_{\substack{\text{plaquette}\\ p\in m_2}} B^{e_{p|2}[(h_{[2-1]}g^{-1}h_{[2-1]}^{-1})\triangleright e_{p|2}^{-1}]}((1)-p)\right)\delta(h_{[2-1]}\triangleright e_2,\hat{e}(m_2))|GS\rangle. \tag{32}$$

Now the section of blob ribbon operator between blob 0 of each membrane, which is the part of the ribbon operator before the intersection of the membranes, is labeled by $e_2[g^{-1}\triangleright e_2^{-1}]$. This is the same label as it would have if we combined the blob ribbons on these sections in the absence of the second higher-flux membrane $C_T^{h,e_1}(m_1)$. That is, this part of the blob ribbon operator is unaffected by the braiding, as we may expect given that this section of ribbon operator is the part before the intersection of the membranes. We can contrast this with the sections of the blob ribbon operators after the intersection (which should be affected by the braiding) which have their labels changed from

$$e_{p|2}\left[g^{-1}\triangleright e_{p|2}^{-1}\right]$$

to

$$e_{p|2}\left[\left(h_{[2-1]}g^{-1}h_{[2-1]}^{-1}\right)\triangleright e_{p|2}^{-1}\right].$$

We see that the only change is that we replace g with $h_{[2-1]}g^{-1}h_{[2-1]}^{-1}$. This matches how the label g of the higher-flux membrane operator transforms under braiding [as we see from the operator $C_{\triangleright}^{h_{[2-1]}gh_{[2-1]}^{-1}}(m_2)$ in Eq. (32)]. That is, the labels of the blob ribbon operators after the intersection (i.e., after braiding) are the labels we expect given the label of the magnetic part of the membrane operator after intersection.

Apart from this splitting of the blob ribbon operators at the intersection of the membranes, we see that the labels of the two membrane operators change (as we mentioned previously for g). We have that

$$\begin{aligned} h &\to h,\\ e_1 &\to e_1\big(g((1)-(2))\triangleright\big\{\big(h_{[2-1]}\triangleright e_2^{-1}\big)\\ &\qquad\times\,[(h_{[2-1]}g^{-1})\triangleright e_2]\}\big),\\ g &\to h_{[2-1]}gh_{[2-1]}^{-1},\\ e_2 &\to h_{[2-1]}\triangleright e_2. \end{aligned}$$

As usual for our braiding, when the start points of the operators are not the same, we have operators in our braiding relations. When we take the start points to be the same, these relations simplify to

$$\begin{aligned} h &\to h,\\ e_1 &\to e_1\left[h\triangleright e_2^{-1}\right][(hg^{-1})\triangleright e_2],\\ g &\to hgh^{-1},\\ e_2 &\to h\triangleright e_2. \end{aligned} \tag{33}$$

This removes any operators from the labels, so that we have definite braiding. Note that the transformation of the 1-flux

labels (h and g) is the same as for the braiding of two magnetic excitations in the $\triangleright$-trivial case, as given in Eq. (18) in Sec. IV B 2, replacing k with g (that equation in particular because we used the specific orientation of the loops also used to find that equation). However, the expression for the change of the E labels is not so easy to interpret. It is easier to understand these results if we change variables, from the surface labels of the membranes to the 2-fluxes possessed by the looplike excitations, as we discussed at the start of Sec. VIII. The 2-flux of the loop excitation $\tilde{e}_1$ is related to the 1-flux label h and the surface label e_1 of the membrane operator by $\tilde{e}_1 = e_1[h^{-1} \triangleright e_1^{-1}]$. Therefore, we define

$$\tilde{e}_1 = e_1\big[h^{-1} \triangleright e_1^{-1}\big],$$
$$\tilde{e}_2 = e_2\big[g^{-1} \triangleright e_2^{-1}\big].$$

Then, from our braiding relations in Eqs. (33), under braiding these 2-fluxes transform according to

$$\begin{aligned}
\tilde{e}_1 &\to e_1\big[h \triangleright \tilde{e}_2^{-1}\big]\big[h^{-1} \triangleright e_1^{-1}\big]\tilde{e}_2 \\
&= \tilde{e}_1\big[h \triangleright \tilde{e}_2^{-1}\big]\tilde{e}_2, \\
\tilde{e}_2 &\to [h \triangleright e_2]\big[(hg^{-1}h^{-1}) \triangleright \big(h \triangleright e_2^{-1}\big)\big] \\
&= h \triangleright \big(e_2\big[g^{-1} \triangleright e_2^{-1}\big]\big) \\
&= h \triangleright \tilde{e}_2. \qquad (34)
\end{aligned}$$

This means that the product of the two fluxes transforms as

$$\tilde{e}_1\tilde{e}_2 \to \tilde{e}_1[h \triangleright \tilde{e}_2^{-1}]\tilde{e}_2[h \triangleright \tilde{e}_2] = \tilde{e}_1\tilde{e}_2$$

under the braiding, which indicates that the product of these 2-fluxes is conserved.

Putting this together, we can see that the 1-fluxes and 2-fluxes of the looplike excitations transform as

$$((g, \tilde{e}_2), (h, \tilde{e}_1)) \to \big(\big(h, \tilde{e}_1\tilde{e}_2\big[h \triangleright \tilde{e}_2^{-1}\big]\big), (hgh^{-1}, h \triangleright \tilde{e}_2)\big)$$

under braiding, where the fact that one loop is moved past the other during the braiding is represented by swapping the order of their labels in the brackets.

We also wish to work out the inverse transformation, which describes the reversed braiding process. Denoting the result of the forward transformations as primed versions, we have from Eqs. (34)

$$\begin{aligned}
&\tilde{e}_2' = h \triangleright \tilde{e}_2, \quad \text{with } h' = h \Rightarrow \tilde{e}_2 = h'^{-1} \triangleright \tilde{e}_2', \\
&g' = hgh^{-1} \Rightarrow g = h'^{-1}g'h', \\
&\tilde{e}_1' = \tilde{e}_1\big[h \triangleright \tilde{e}_2^{-1}\big]\tilde{e}_2 \Rightarrow \tilde{e}_1 = \tilde{e}_1'\tilde{e}_2'\big[h'^{-1} \triangleright \tilde{e}_2'^{-1}\big].
\end{aligned}$$

The inverse transformation is therefore

$$\begin{aligned}
&((h', \tilde{e}_1'), (g', \tilde{e}_2')) \\
&\quad \to \big((h'^{-1}g'h', h'^{-1} \triangleright \tilde{e}_2'), \big(h', \tilde{e}_1'\tilde{e}_2'h'^{-1} \triangleright \tilde{e}_2'^{-1}\big)\big). \qquad (35)
\end{aligned}$$

This matches the braiding proposed in Ref. [28] for higher gauge theory based on discussions of the loop braid group. It is important to note that the braiding depends on the result of fusing the two excitations. Given two loops with 1-flux and 2-flux given by $(h, \tilde{e}_1)$ for the first loop and $(g, \tilde{e}_2)$ for the second loop, there are many possible fusion products. The fact that the products of 1-fluxes $hg \to hgh^{-1}h = hg$ (swapping the order after braiding to account for the swapping of loop positions) and of 2-fluxes $\tilde{e}_1\tilde{e}_2$ are conserved indicates that these are the total 1-flux and 2-flux of the combined loops, and so we have obtained the braiding when they fuse to give the labels $(hg, \tilde{e}_1\tilde{e}_2)$. We could equally have considered the braiding in a different situation, such as when the start points of the two operators are in different positions, for which the loops $(h, \tilde{e}_1)$ and $(g, \tilde{e}_2)$ fuse to give different total quantum numbers than $(hg, \tilde{e}_1\tilde{e}_2)$.

As we did when considering the braiding of the higher-flux with the blob excitation, we can also consider the braiding of our original magnetic excitation, before we pinned an additional E-valued loop to it. As described by Eq. (27), we can obtain the original magnetic membrane operators from the higher-flux membrane operators by summing over all possible elements of e for the E label. That is, we consider

$$\begin{aligned}
C_T^g(m_2)C_T^h(m_1)|GS\rangle &= C_T^g(m_2)\sum_{e_2\in E}\delta(e_2, \hat{e}(m_2))C_T^h(m_1)\sum_{e_1\in E}\delta(e_1, \hat{e}(m_1))|GS\rangle \\
&= \sum_{e_2\in E}\sum_{e_1\in E} C_T^{g,e_2}(m_2)C_T^{h,e_1}(m_1)|GS\rangle.
\end{aligned}$$

Using Eq. (30), we see that this gives us

$$\begin{aligned}
C_T^g(m_2)C_T^h(m_1)|GS\rangle = \sum_{e_1\in E}\sum_{e_2\in E} &C_T^{h,e_1[g((1)-(2))\triangleright\{(h_{[2-1]}\triangleright e_2^{-1})[(h_{[2-1]}g^{-1})\triangleright e_2]\}]}(m_1)C_{\triangleright}^{h_{[2-1]}gh_{[2-1]}^{-1}}(m_2) \\
&\times\left(\prod_{\substack{\text{plaquette}\\ p\in m_2}} B^{[h_{[2-1]}^{-1}\triangleright e_{p|2}][(g^{-1}h_{[2-1]}^{-1})\triangleright e_{p|2}^{-1}]}((2)-(1))B^{e_{p|2}[(h_{[2-1]}g^{-1}h_{[2-1]}^{-1})\triangleright e_{p|2}^{-1}]}((1)-p)\right) \\
&\times \delta(h_{[2-1]} \triangleright e_2, \hat{e}(m_2))|GS\rangle.
\end{aligned}$$

Then we have

$$\sum_{e_1\in E} C_T^{h,e_1[g[(1)-(2)]\triangleright\{(h_{[2-1]}\triangleright e_2^{-1})[(h_{[2-1]}g^{-1})\triangleright e_2]\}]}(m_1) = C_T^h(m_1)$$

because summing over e_1 gives us an equal sum over all Kronecker deltas $\delta(\hat{e}(m_1), e)$, regardless of the actual value of e_2. This gives us

$$C_T^g(m_2)C_T^h(m_1)|GS\rangle = \sum_{e_1\in E}\sum_{e_2\in E} C_T^h(m_1)C_{\triangleright}^{h_{[2-1]}gh_{[2-1]}^{-1}}(m_2) \times \left(\prod_{\substack{\text{plaquette}\\ p\in m_2}} B^{[h_{[2-1]}^{-1}\triangleright e_{p|2}][(g^{-1}h_{[2-1]}^{-1})\triangleright e_{p|2}^{-1}]}((2)-(1))B^{e_{p|2}[(h_{[2-1]}g^{-1}h_{[2-1]}^{-1})\triangleright e_{p|2}^{-1}]}((1)-p)\right) \times \delta(h_{[2-1]}\triangleright e_2, \hat{e}(m_2))|GS\rangle.$$

We can similarly use the sum over $e_2 \in E$ to remove the other Kronecker delta. We have

$$\sum_{e_2\in E}\delta(h_{[2-1]}\triangleright e_2, \hat{e}(m_2)) = 1$$

because $h_{[2-1]}\triangleright e_2$ runs over all $e \in E$. This gives us the final result

$$C_T^g(m_2)C_T^h(m_1)|GS\rangle = \sum_{e_1\in E}\sum_{e_2\in E} C_T^h(m_1)C_{\triangleright}^{h_{[2-1]}gh_{[2-1]}^{-1}}(m_2) \times \left(\prod_{\substack{\text{plaquette}\\ p\in m_2}} B^{[h_{[2-1]}^{-1}\triangleright e_{p|2}][(g^{-1}h_{[2-1]}^{-1})\triangleright e_{p|2}^{-1}]}((2)-(1))B^{e_{p|2}[(h_{[2-1]}g^{-1}h_{[2-1]}^{-1})\triangleright e_{p|2}^{-1}]}((1)-p)\right)|GS\rangle. \tag{36}$$

Then looking at the effect of braiding on the G-valued label, we see that the result is simply conjugation of one of the magnetic flux labels by the other. The labels of the blob ribbons corresponding to m_2 are also changed before and after the intersection of the two membranes. Just as we discussed for the higher-flux membrane operators earlier in this section, the label after the intersection reflects the change to the label g of the membrane operator applied on m_2, while the change to the label before the intersection is only an apparent change due to the operator label.

C. Braiding with E-valued loops

The final braiding relation to consider is the braiding between these higher-flux excitations and the E-valued loops. We can obtain this relation from the calculation for two higher-flux membrane operators in the previous section because the E-valued loops are simply higher-flux excitations with trivial G label. We therefore simply need to take the special case of that calculation when one of the G elements is 1_G. Rather than repeating the full equations, we will only present the results in the same-start-point braiding case.

First we consider the case where the red excitation shown in Fig. 37 is a higher-flux excitation, produced by a membrane operator $C_T^{g,e_{\text{mag}}}(m_2)$, while the green excitation is a pure E-valued loop, labeled by e_m. In this case the label of the E-valued loop transforms as $e_m \to e_m e_{\text{mag}}^{-1}[g^{-1}\triangleright e_{\text{mag}}]$ under the braiding, while the labels of the magnetic membrane operator are unaffected by the braiding. When we change to consider our irrep basis for the E-valued loops [given in Eq. (12)] this transformation gives us a phase of

$$\gamma\left(e_{\text{mag}}^{-1}[g^{-1}\triangleright e_{\text{mag}}]\right)^{-1}, \tag{37}$$

where γ is the irrep of E labeling the E-valued loop. Note that if we consider the ordinary magnetic excitation by averaging over e_{mag}, the braiding relation is different for each value of e_{mag}, so the different terms in the sum accumulate different transformations. This is part of the reason why it was necessary to consider the higher-flux membrane instead of the magnetic one in the first place. The result of this different transformation for the different E labels is that, even if the excitation is initially an ordinary magnetic excitation, with an equal superposition of the different E labels, it will not necessarily remain so after braiding, instead becoming an uneven superposition of the different higher-flux excitations, with labels coupled to the state of the E-valued loop.

Now we consider the opposite case where the E-valued loop passes through the magnetic one. In this case, the red excitation from Fig. 37 is a pure E-valued loop excitation produced by the membrane operator $\delta(\hat{e}(m_2), e_m)$, while the green excitation is a higher-flux loop excitation produced by the membrane operator $C_T^{h,e_1}(m_1)$. In this case the label e_m of the E-valued loop transforms as $e_m \to h\triangleright e_m$ under the braiding, while the labels of the higher-flux operator are again unaffected by the braiding move. In our irrep basis for the E-valued membrane operators, this transformation actually changes the irrep γ labeling the membrane operator to a different irrep $h^{-1}\triangleright\gamma$ in the same $\triangleright$-Rep class of irreps [where two irreps of E, α and β, are in the same $\triangleright$-Rep class if there exists a $g \in G$ such that $\alpha(g\triangleright e) = \beta(e)$ for all $e \in E$]. This suggests that the irreps of E are not by themselves good labels for the topological charge because the irreps are not invariant under braiding, and instead the $\triangleright$-Rep classes should be important (although the condensation further affects the topological charge). However, as we see in Sec. IX A 1, the pointlike charge of the looplike excitations actually depends on how the coefficients of the membrane operator transform under the $\triangleright$ action, and so this topological charge has some dependence on quantities within the $\triangleright$ class as well. We will discuss the topological charge in more detail in Sec. IX.

TABLE IV. A summary of which excitations braid nontrivially in case 2, where the group E is Abelian and ∂ maps onto the center of G. A tick indicates that at least some of the excitations of each type braid nontrivially with each other, while a cross indicates that there is no nontrivial braiding between the two types.

Nontrivial	Higher			E-valued
braiding?	Electric	flux	Blob	loop
Electric	✗	✓	✗	✗
Higher flux	✓	✓	✓	✓
Blob	✗	✓	✗	✓
E-valued loop	✗	✓	✓	✗

D. Summary of braiding in this case

Table IV summarizes which types of excitation can have nontrivial braiding relations in the case where E is Abelian and ∂ maps to the center of G, where nontrivial braiding between the types of excitation is indicated by ticks. Note that the higher-flux excitations have potentially nontrivial braiding relations with every class of excitation.

IX. TOPOLOGICAL CHARGE

In Ref. [14] we explained the concept of topological charge and in Ref. [15] we presented a detailed construction of the measurement operators for topological charge in the (2+1)D case. To briefly restate our explanation from Ref. [14], topological charge is a quantity that is conserved, so that the only way to change the topological charge in a region is to apply an operator that connects this region to the rest of our lattice. Further conditions are imposed on the topological charge relevant to our model by requiring that the ground state is the topological vacuum. There is a significant difference between the (2+1)D and (3+1)D cases, however. Whereas we consider the topological charge in regions isomorphic to disks (or unions and differences of disks, like annuli) when there are only two spatial dimensions, there are more topologically distinct regions to consider when there are three spatial dimensions. For example, we have both topological balls and solid tori. The charge in these regions should be measured by operators on the surfaces of the regions, i.e., on spheres and tori. This variety of regions is related to our excitations. We have both pointlike and looplike excitations, both of which should carry topological charge. While we expect pointlike charges to be fully measured by spheres, the sphere has no features that would allow it to distinguish between a loop and a point. On the other hand, a torus has handles which can link with a looplike excitation and we expect this to allow the torus to distinguish between point particles and loops. We therefore expect that the loop excitations should carry a charge that is not measured by the sphere (in addition to some charge that can be measured by the sphere). Therefore, we need to include the toroidal measurement surfaces as well.

In order to measure the topological charge held within or without a particular surface, we follow a similar procedure to the one used for the (2+1)D case in Ref. [15], except that the boundary for our region is a surface rather than a path. We take our surface of interest and apply every closed membrane or ribbon operator that we can on this surface, before considering only the sums of these operators that will commute with the Hamiltonian. Combinations of ribbon and membrane operators can produce any linear operator on the Hilbert space. This is because we can consider ribbon and membrane operators that act only on a single edge or plaquette. An electric ribbon operator acting on a single edge can measure any value for that edge, while a magnetic membrane operator acting only on a single edge can multiply that edge by any group label. Together these allow us to freely control the label of any edge. Similarly, an E-valued membrane operator can measure the label of a single plaquette and a blob ribbon operator can multiply its label by any value. Combinations of these operators can therefore control the label of every edge and plaquette in the lattice. However, when we restrict to operators that commute with the Hamiltonian, we are left only with closed ribbon and membrane operators. This restriction of commuting with the Hamiltonian is because our measurement operator should not by itself produce or move topological charge.

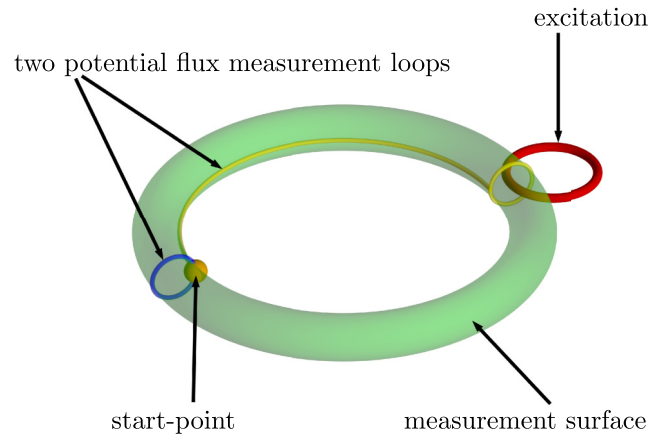

FIG. 38. If an excitation pierces the measurement surface, then the charge within the surface is ill defined. In the case shown in this figure, measuring the 1-flux along the two potential loops may give different results (to the point of not giving the same topological charge).

We consider this process of measuring the charge for spherelike and toruslike surfaces. Theoretically, we could do the same for an arbitrary surface. However, because the simple excitations of the model are either pointlike or looplike, it does not appear necessary to consider the charge measured by higher-genus surfaces. Nevertheless, this may not be the case and it would be interesting to construct the higher-genus measurement operators, but we leave this for future study. One subtlety with measuring a looplike excitation is that, because the loops are extended, the excitations may pierce the measurement surface and not be wholly contained within or without the surface. As an example, consider the situation shown in Fig. 38. As part of the measurement procedure, we must choose closed paths on which to measure any magnetic

flux enclosed by the torus. However, in the presence of excitations on the surface itself, two choices of loops to measure on (for example, the blue or yellow paths in the figure) would give different results. This is because different loops may or may not link with the excitation (the thicker red torus). Because both choices are supposed to measure the charge within the torus (the partially transparent green torus), this leads to a contradiction. If we want to measure the charge held within a surface without knowing what excitations are present and where they are, this presents a difficulty. Therefore, we include in our charge measurement operators a projector to the space where the surface has no excitations. This sidesteps the above issue, but it does mean that we cannot measure the charge of confined excitations (which always cause excitations on a surface enclosing them) using this procedure.

A. Topological charge within a sphere in the case where $\partial \to$ center(G) and E is Abelian

Before we look at the charge measured by a torus, which is sensitive to both looplike and pointlike charge, we will first examine the charge measured by a sphere. We will do this in the case where E is Abelian and ∂ maps onto the center of G (case 2 in Table I), which includes the $\triangleright$ trivial case (case 1 in Table I) as a subcase. Because a sphere has no noncontractible cycles, the sphere should only be sensitive to pointlike charge. Nonetheless, the sphere charge is interesting, not only because it lets us look at the properties of point particles, but because loop excitations also possess pointlike charge. As we explained in the previous section, to measure the charge within a sphere we first project to the case where there are no excitations on the measurement surface. Then we consider which independent closed ribbon and membrane operators we can apply on this surface.

While it may seem that we can independently apply ribbon operators around any closed loop on the surface of the sphere, this is not the case. Any ribbon operators are either topological or confined (or can be written as a linear combination of ribbon operators of the two types), as we show in Sec. S-II in the Supplemental Material [20]. If a ribbon operator is confined, then applying it leads to excitations on the measurement surface, which we do not allow. On the other hand, if a ribbon operator is topological, then because all closed paths on the sphere are contractible on the spherical surface (and we do not allow excitations on the surface), the ribbon can be contracted to nothing without affecting the action of the ribbon operator. This means that applying a closed topological ribbon operator on the surface of the sphere is equivalent to applying the identity operator (at least in the subspace on which we apply measurement operators). Therefore, any ribbon operators that we are allowed to apply (the nonconfined ones) act trivially.

This leaves us only with the membrane operators $C_T^h(m)$ and $L^e(m)$, where $C_T^h(m)$ is the total magnetic membrane operator defined in Sec. VII [see Eq. (25)] and $L^e(m)$ is the E-valued membrane operator $\delta(e, \hat{e}(m))$. We consider applying these two operators over the sphere. Although we apply both operators on the same sphere, when we define the membrane m for each operator to act on we need to define a start point for the membrane. It would seem that we could choose the start points of the membranes to be different for the two membrane operators, giving us many potential measurement operators. However, this is not the case because of the requirement that the total measurement operator commute with the energy terms on the sphere. As we have discussed previously, and prove in Sec. S-I D 3 in the Supplemental Material for this work [20] and Sec. S-I C in the Supplemental Material for Ref. [15], both the magnetic membrane operator and E-valued membrane operator commute with the vertex transforms except those at the start points. If the two operators have different start points, then each must individually commute with their specific start-point vertex transform (rather than their combination having to commute with a mutual start-point transform). However, when a membrane operator commutes with the start-point vertex transforms, the start point of the operator becomes arbitrary. That is, if the start point is not excited we can move the start point without affecting the action of the membrane operator because parallel transport of a vertex is equivalent to applying a vertex transform (see Sec. S-I D 4 in the Supplemental Material [20] for a proof of this for the magnetic membrane operator and Sec. S-I C in the Supplemental Material of Ref. [15] for a proof for the E-valued membrane operator). This means that we can move the start points to be in the same location anyway, without affecting the action of the two membrane operators. Therefore, without loss of generality, we can consider the two start points of the membrane operators to be in the same location.

The most general operator we can apply is a linear combination of terms with the form $C_T^h(m)L^e(m)$ for different labels h and e, where m is the spherical membrane that we are measuring the charge within. We might also consider products that include multiples of one or more of the two types of operators, such as $C_T^h(m)L^e(m)L^f(m)C_T^g(m)$. However, because the two types of operator commute, we can always collect the separate instances of each type of operator, to give us terms like $C_T^h(m)C_T^g(m)L^e(m)L^f(m)$. Then we can use the algebra of the membrane operators to combine them, which just gives us $\delta(e, f)C_T^{hg}(m)L^e(m)$ for the above example. This is just an example of a linear combination of terms of the form $C_T^h(m)L^e(m)$, so we only need consider such terms. We take the membrane m to be oriented inwards to match the orientation of the surface label of the direct membrane used in $C_T^h(m)$. Taking the opposite orientation would be equivalent to using e^{-1} instead of e. We also do not displace blob 0 and the start point of $C_T^h(m)$ and $L^e(m)$ from the membrane, contrary to the approach used in Sec. VIII when considering the braiding of the higher-flux excitations. This choice does not matter because the fact that we enforce the start point and blob 0 to be unexcited by the combined action of the measurement operator means that we can freely move the start point and blob 0 around without affecting the total action of the measurement operator. Moving the start point is equivalent to applying a vertex transform at the start point, which is trivial when the start point is unexcited, and we show in Sec. S-I D 5 of the Supplemental Material [20] that moving blob 0 is trivial when that blob is unexcited.

Having found that the operator we apply must have the form $\sum_{h\in G}\sum_{e\in E}\alpha_{h,e}C_T^h(m)L^e(m)$, where $\alpha_{h,e}$ are a set of coefficients, we next have to find which coefficients lead to the operator commuting with the energy terms on the sphere. In Sec. S-V D of the Supplemental Material [20], we show

that requiring commutation with the energy terms leads to two types of restrictions for the coefficients. Some of these restrictions enforce that the coefficient $\alpha_{h,e}$ must be zero for certain labels [i.e., certain pairs of label (h, e) for $C_T^h(m)L^e(m)$ are disallowed], while other conditions mean that the coefficients of two pairs (h_1, e_1) and (h_2, e_2) must be the same (i.e., $\alpha_{h_1,e_1} = \alpha_{h_2,e_2}$). As a shorthand, we write $(h_1, e_1) \overset{S}{\sim} (h_2, e_2)$ for two pairs that are subject to this latter type of restriction (must have equal coefficients). Then the restrictions that we find are

$$h \triangleright e = e, \tag{38}$$

$$\partial(e) = 1_G, \tag{39}$$

$$h \overset{S1}{\sim} \partial(f)h \; \forall \; f \in E, \tag{40}$$

and

$$(h, e) \overset{S2}{\sim} (ghg^{-1}, g \triangleright e) \; \forall \; g \in G. \tag{41}$$

The two equivalence relations $\overset{S1}{\sim}$ and $\overset{S2}{\sim}$ together form the equivalence relation $\overset{S}{\sim}$, where any pairs of labels (h_1, e_1) and (h_2, e_2) related by $\overset{S}{\sim}$ must have equal coefficients. We can write $\overset{S}{\sim}$ explicitly as

$$(h, e) \overset{S}{\sim} (\partial(f)ghg^{-1}, g \triangleright e), \tag{42}$$

for each $g \in G$ and $f \in E$ [i.e., (h, e) is in the same equivalence class as (h', e') if there exists any $g \in G$ and $e \in E$ such that $(h', e') = (\partial(f)ghg^{-1}, g \triangleright e)$]. Given all of these conditions for our measurement operators, we can construct a basis for the space of allowed measurement operators. As we show in Sec. S-V D of the Supplemental Material [20], one such basis is given by a set of operators labeled by two objects. The first object, C, is a $\triangleright$ class of the kernel of ∂. A $\triangleright$-class of the kernel is a subset of the kernel consisting of elements related by the equivalence relation $e \overset{\triangleright}{\sim} f$ if there exists a $g \in G$ such that $g \triangleright e = f$. It is convenient to pick a representative element r_C for each such class C. Then we define the centralizer of the class C as $Z_{\triangleright,r_C} = \{ h \in G \mid h \triangleright r_C = r_C \}$. The second object that labels our basis operators is a class within this centralizer, this time described by the equivalence relation

$$h \overset{Z_{\triangleright,r_C}}{\sim} xhx^{-1}\partial(w) \tag{43}$$

for any elements $x \in Z_{\triangleright,r_C}$ and $w \in E$. Note that this equivalence relation is similar to $\overset{S}{\sim}$, in that it gives the same form of relation, but only for elements $x \in Z_{\triangleright,r_C}$ (for which $x \triangleright r_C = r_C$) rather than general elements $g \in G$. The basis operator corresponding to a particular $\triangleright$ class C of the kernel and equivalence class D [defined by Eq. (43)] of the associated centralizer is

$$T^{D,C}(m) = \sum_{q \in Q_C} \sum_{d \in D} C_T^{qdq^{-1}}(m) L^{q \triangleright r_C}(m),$$

where Q_C is a set of elements of G that move us between the elements of the $\triangleright$ class C, so that each element $e_i \in C$ has a unique $q_i \in Q_C$ such that $e_i = q_i \triangleright r_C$. As we show in Sec. S-V D of the Supplemental Material [20], any element $g \in G$ can be uniquely decomposed as a product of an element of Q_C and an element of $Z_{\triangleright,r_C}$. We can use this basis of operators to construct the projectors to definite topological charge within the sphere. These projectors are given by

$$T^{R,C}(m) = \frac{|R|}{|Z_{\triangleright,r_C}|} \sum_{D \in (Z_{\triangleright,r_C})_{cl}} \chi_R(D) T^{D,C}(m), \tag{44}$$

where R is an irrep of the quotient group $Z_{\triangleright,r_C}/\partial(E)$ with dimension $|R|$ and $(Z_{\triangleright,r_C})_{cl}$ is the set of classes in the centralizer defined by the equivalence relation (43). Note that the character χ_R of irrep R is independent of the element $d \in D$ [because characters are a function of conjugacy class, and R being an irrep of the quotient group means that it is also insensitive to factors of $\partial(w)$ from Eq. (43)]. In Sec. S-V D of the Supplemental Material [20] we prove that the operators defined by Eq. (44) are indeed projectors and are orthogonal and complete in our space.

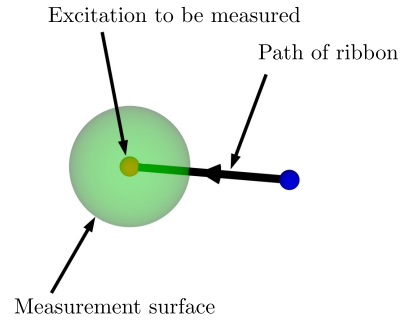

FIG. 39. We measure the charge held at the end of an electric ribbon, using our spherical surface (large green sphere).

1. The pointlike charge of simple excitations

Having worked out the projectors for the charges, it will be instructive to use them to check the topological charge of some of our simple excitations (those produced by single ribbon or membrane operators). To do this we try enclosing these charges with our measurement operators.

We first consider measuring the charge of an electric excitation at the end point of a ribbon operator. To do this, we first need to create our electric excitation, by applying an electric ribbon operator to our ground state. Considering a ribbon operator labeled by irrep X of G and matrix indices a and b, we obtain the state

$$\sum_{g \in G} [D^X(g)]_{ab} \delta(\hat{g}(t), g) |GS\rangle.$$

Next we want to measure this charge, by applying a measurement operator, as shown in Fig. 39. Therefore, we want to calculate

$$\begin{aligned} &T^{R,C}(m) \sum_{g \in G} [D^X(g)]_{ab} \delta(\hat{g}(t), g) |GS\rangle \\ &= \frac{|R|}{|Z_{\triangleright,r_C}|} \sum_{D \in (Z_{\triangleright,r_C})_{cl}} \chi_R(D) \sum_{d \in D} \sum_{q \in Q_C} C_T^{qdq^{-1}}(m) \\ &\quad \times \delta(\hat{e}(m), q \triangleright r_C) \sum_{g \in G} \delta(\hat{g}(t), g) [D^X(g)]_{ab} |GS\rangle. \end{aligned}$$

The operator $\delta(\hat{e}(m), q \triangleright r_C)$ commutes with $\delta(\hat{g}(t), g)$, so we can commute $\delta(\hat{e}(m), q \triangleright r_C)$ all the way to the right, so that it acts directly on the ground state. Then we have

$$\delta(\hat{e}(m), q \triangleright r_C)|GS\rangle = \delta(1_E, q \triangleright r_C)|GS\rangle$$

because m is a sphere, and any contractible sphere in the ground state must have a surface label of 1_E due to the blob energy terms. We can write $\delta(q \triangleright r_C, 1_E)$ as $\delta(r_C, 1_E) = \delta(C, \{1_E\})$ (using the fact that the identity is invariant under the $\triangleright$ action and so is the only element of its $\triangleright$ class). Therefore, we find that the result of measurement is zero unless the class that we are trying to measure is the trivial one. This is as we expect because the electric excitations do not possess nontrivial 2-flux.

Having found that the class C must be trivial for a nonzero result, we can also simplify the other mathematical objects appearing in the projector. When $r_C = 1_E$, we have that $h \triangleright 1_E = 1_E \ \forall\, h \in G$, which implies that $Z_{\triangleright, r_C} = G$ and the quotient group $Z_{\triangleright, r_C}/\partial(E)$ is simply $G/\partial(E)$. In addition, the set Q_C is the trivial group containing just the identity element, so we may drop the sum over $q \in Q_C$. Then the result of our measurement is

$$\begin{aligned}
&\delta(C, \{1_E\})\frac{|R|}{|G|}\sum_{D\in(Z_{\triangleright,r_C})_{cl}}\chi_R(D)\sum_{d\in D}C_T^d(m)\sum_{g\in G}\delta(\hat{g}(t), g)[D^X(g)]_{ab}|GS\rangle \\
&\quad = \delta(C, \{1_E\})\frac{|R|}{|G|}\sum_{d\in G}\sum_{g\in G}\chi_R(d)[D^X(g)]_{ab}C_T^d(m)\delta(\hat{g}(t), g)|GS\rangle.
\end{aligned}$$

Then we just need to find the commutation relation between $C_T^d(m)$ and $\delta(\hat{g}(t), g)$. The calculation of this is analogous to the calculation performed to find the braiding relation between the electric and magnetic excitations (see Sec. IV B 1), except that we have the opposite orientation of the magnetic membrane operator. We find that

$$C_T^d(m)\delta(\hat{g}(t), g)|GS\rangle = \delta(\hat{g}(t-m)d\hat{g}(t-m)^{-1}\hat{g}(t), g)C_T^d(m)|GS\rangle,$$

where $\hat{g}(t-m)$ is shorthand for $\hat{g}(\text{s.p.}(t) - \text{s.p.}(m))$, the path element for the path from the start point of t to the start point of m. We also have that $C_T^d(m)|GS\rangle = |GS\rangle$ because the sphere is contractible and the operator is topological (so that we can deform the operator to nothing). Using these results in our previous expression gives

$$T^{R,C}(m)\sum_{g\in G}[D^X(g)]_{ab}\delta(\hat{g}(t), g)|GS\rangle = \delta(C, \{1_E\})\frac{|R|}{|G|}\sum_{d\in G}\sum_{g\in G}\chi_R(d)[D^X(g)]_{ab}\delta(\hat{g}(t), \hat{g}(t-m)d^{-1}\hat{g}(t-m)^{-1}g)|GS\rangle.$$

We then rewrite $\hat{g}(t-m)d\hat{g}(t-m)^{-1}$ as d' and replace the sum over the dummy index d with a sum of d'. Noting that the character χ_R is a function of conjugacy class, so that $\chi_R(d') = \chi_R(d)$, we then see that

$$\begin{aligned}
T^{R,C}(m)\sum_{g\in G}[D^X(g)]_{ab}\delta(\hat{g}(t), g)|GS\rangle &= \delta(C, \{1_E\})\frac{|R|}{|G|}\sum_{d'\in G}\sum_{g\in G}\chi_R(d')[D^X(g)]_{ab}\delta(\hat{g}(t), d'^{-1}g)|GS\rangle \\
&= \delta(C, \{1_E\})\frac{|R|}{|G|}\sum_{d'\in G}\sum_{g'=d'^{-1}g\in G}\chi_R(d')[D^X(d'g')]_{ab}\delta(\hat{g}(t), g')|GS\rangle \\
&= \delta(C, \{1_E\})\frac{|R|}{|G|}\sum_{d',g'\in G}\sum_{c=1}^{|X|}\sum_{e=1}^{|R|}[D^R(d')]_{ee}[D^X(d')]_{ac}[D^X(g')]_{cb}\delta(\hat{g}(t), g')|GS\rangle.
\end{aligned}$$

We now want to use the orthogonality relations for irreps of a group to simplify this. There is a slight complication in that X is an irrep of G whereas R is an irrep of $G/\partial(E)$. However, R induces a representation R_G of G defined by $R_G(g) = R[\tilde{g}\partial(E)]$, where $\tilde{g}\partial(E)$ is the coset which g belongs to. Therefore, each matrix from R is copied $|\partial(E)|$ times in R_G. Given that R is an irrep of $G/\partial(E)$, R_G must also be irreducible (as a representation of G). This is because the same matrices appear in the two representations R and R_G, so if R cannot be reduced to a block-diagonal form then neither can R_G. Then we can use R_G instead of R and apply the standard irrep orthogonality relations to obtain

$$\begin{aligned}
&T^{R,C}(m)\sum_{g\in G}[D^X(g)]_{ab}\delta(\hat{g}(t), g)|GS\rangle \\
&\quad = \delta(C, \{1_E\})\frac{|R|}{|G|}\sum_{g'\in G}\frac{|G|}{|R|}\delta_{ec}\delta_{eb}\delta(\overline{R}_G, X) \\
&\qquad \times [D^X(g')]_{cb}\delta(\hat{g}(t), g')|GS\rangle \\
&\quad = \delta(C, \{1_E\})\delta(R_G, \overline{X})\sum_{g'\in G}[D^X(g')]_{cb} \\
&\qquad \times\ \delta(\hat{g}(t), g')|GS\rangle. \qquad (45)
\end{aligned}$$

We see that the final result of applying the measurement operator is that we recover our original electric operator acting on the ground state, multiplied by $\delta(C, \{1_E\})\delta(R_G, \overline{X})$. This indicates that the charge of the excitation is $(\{1_E\}, \overline{X})$. If the irrep X corresponds to a confined excitation, none of our measurement operators will give a nonzero result because R_G

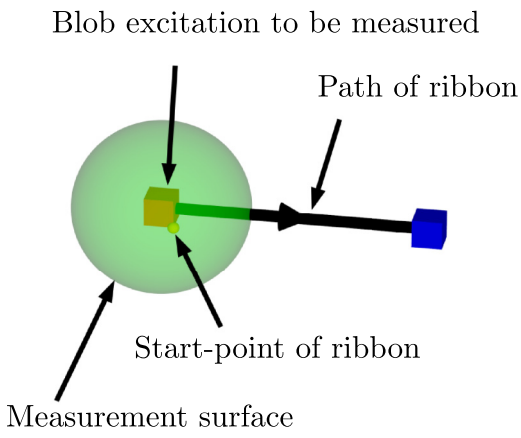

FIG. 40. We measure the topological charge of the blob excitation at the start of the blob ribbon operator.

derives from an irrep of the quotient group, and so cannot have a nontrivial restriction to the image of ∂. This is a result of our requirement that we project out the states that have excitations on the measurement membrane itself, which naturally precludes the measurement of any confined excitations.

We can similarly check the charge of a blob excitation. We expect that the corresponding charge will be labeled by a nontrivial class C because this class is associated to the 2-flux measured by the measurement operator. We may think that because the blob excitation can have an excited vertex, in addition to the excited blob, that this means that the representation labeling the charge should be nontrivial, just like with the electric excitation. However, we will see that the vertex excitation does not in this case result in a nontrivial representation. We measure the topological charge of the blob excitation at the start of the path of a blob ribbon operator, as indicated in Fig. 40. We choose to measure the charge of the excitation at the start of the ribbon, rather than the end as we did with the electric excitation, because this will highlight the fact that the excited vertex enclosed by the measurement surface does not lead to a nontrivial representation R.

We consider measuring the charge of a blob excitation produced by the blob ribbon operator

$$\sum_{e\in[\tilde{e}]_\triangleright} \alpha_e B^e(t),$$

where $[\tilde{e}]_\triangleright$ is the $\triangleright$ class containing $\tilde{e}$, which is defined by

$$e \in [\tilde{e}]_\triangleright \iff \exists g \in G \text{ s.t. } e = g \triangleright \tilde{e}. \tag{46}$$

In order to measure the charge, we apply a measurement operator $T^{R,C}$ on the state produced by acting with the blob ribbon operator on the ground state. That is, we examine a state

$$\begin{aligned} &T^{R,C}(m) \sum_{e\in[\tilde{e}]_\triangleright} \alpha_e B^e(t)|GS\rangle \\ &= \frac{|R|}{|Z_{\triangleright,r_C}|} \sum_{D\in(Z_{\triangleright,r_C})_{cl}} \chi_R(D) \sum_{d\in D}\sum_{q\in Q_C} C_T^{qdq^{-1}}(m) \\ &\quad\times \delta(\hat{e}(m), q \triangleright r_C) \sum_{e\in[\tilde{e}]_\triangleright} \alpha_e B^e(t)|GS\rangle, \end{aligned} \tag{47}$$

where α_e is a set of coefficients that we keep general, so that we can show that the topological charge does not depend on the coefficients within the $\triangleright$ class, only on the class itself.

From a calculation analogous to the one for braiding between higher-flux excitations and blob excitations in Sec. VIII A, we know that

$$\begin{aligned} &C_T^{qdq^{-1}}(m)\delta(\hat{e}(m), q \triangleright r_C)B^e(t)|GS\rangle \\ &\quad= B^e(\text{start}(t) - \text{ blob } 0) \\ &\qquad\times B^{[g(m-t)^{-1}qdq^{-1}g(m-t)]\triangleright e}(\text{blob } 0 - \text{end}(t))C_T^{qdq^{-1}}(m) \\ &\qquad\times \delta(\hat{e}(m), [q \triangleright r_C]\{\hat{g}(\text{s.p.}(m) - \text{s.p.}(t)) \triangleright e^{-1}\})|GS\rangle, \end{aligned} \tag{48}$$

where all of the blob ribbon operators have the same start point as t and $g(m-t)$ is shorthand for the path element $g[\text{s.p.}(m) - \text{s.p.}(t)]$. Then, because the membrane m is contractible, its surface element must be the identity in the ground state. Therefore, we have

$$\begin{aligned} &\delta(\hat{e}(m), [q \triangleright r_C]\{\hat{g}(\text{s.p.}(m) - \text{s.p.}(t)) \triangleright e^{-1}\})|GS\rangle \\ &\quad= \delta([q \triangleright r_C]\{\hat{g}(\text{s.p.}(m) - \text{s.p.}(t)) \triangleright e^{-1}\}, 1_E)|GS\rangle. \end{aligned} \tag{49}$$

Substituting the relations from Eqs. (48) and (49) into Eq. (47), we have

$$\begin{aligned} &T^{R,C}(m) \sum_{e\in[\tilde{e}]_\triangleright} \alpha_e B^e(t)|GS\rangle \\ &= \frac{|R|}{|Z_{\triangleright,r_C}|} \sum_{D\in(Z_{\triangleright,r_C})_{cl}} \chi_R(D) \sum_{d\in D}\sum_{q\in Q_C}\sum_{e\in[\tilde{e}]_\triangleright} \alpha_e \\ &\quad\times B^e(\text{start}(t) - \text{blob } 0)B^{[g(m-t)^{-1}qd]\triangleright r_C}(\text{blob } 0 - \text{end}(t)) \\ &\quad\times \delta(q \triangleright r_C, \hat{g}(m-t) \triangleright e)|GS\rangle, \end{aligned} \tag{50}$$

where we used the Kronecker delta to rewrite the label of the second blob ribbon operator in terms of r_C. But then d is an element of $Z_{\triangleright,r_C}$, so $d \triangleright r_C = r_C$. This means that $[\hat{g}(m-t)^{-1}qd] \triangleright r_C = [\hat{g}(m-t)^{-1}q] \triangleright r_C$. Then the Kronecker delta enforces that $q \triangleright r_C = \hat{g}(m-t) \triangleright e$, so that

$$\begin{aligned} [\hat{g}(m-t)^{-1}q] \triangleright r_C &= \hat{g}(m-t)^{-1} \triangleright (q \triangleright r_C) \\ &= \hat{g}(m-t)^{-1} \triangleright [\hat{g}(m-t) \triangleright e] \\ &= e. \end{aligned}$$

Substituting this into Eq. (50), we see that the result of our measurement is

$$\begin{aligned} &T^{R,C}(m) \sum_{e\in[\tilde{e}]_\triangleright} \alpha_e B^e(t)|GS\rangle \\ &= \frac{|R|}{|Z_{\triangleright,r_C}|} \sum_{D\in(Z_{\triangleright,r_C})_{cl}} \chi_R(D) \sum_{d\in D}\sum_{q\in Q_C}\sum_{e\in[\tilde{e}]_\triangleright} \alpha_e \\ &\quad\times B^e(\text{start}(t) - \text{ blob } 0)B^e(\text{blob } 0 - \text{end}(t)) \\ &\quad\times \delta(q \triangleright r_C, \hat{g}(m-t) \triangleright e)|GS\rangle. \end{aligned}$$

We see that the labels of the two sections of the blob ribbon operator are the same, and so we can recombine them into a single ribbon operator applied on the original ribbon t. We

then have

$$T^{R,C}(m)\sum_{e\in[\tilde{e}]_\triangleright}\alpha_e B^e(t)|GS\rangle = \frac{|R|}{|Z_{\triangleright,r_C}|}\sum_{D\in(Z_{\triangleright,r_C})_{cl}}\chi_R(D)\sum_{d\in D}\sum_{q\in Q_C}\sum_{e\in[\tilde{e}]_\triangleright}\alpha_e \times B^e(t)\delta(q\triangleright r_C, \hat{g}(m-t)\triangleright e)|GS\rangle.$$

Next, note that if the Kronecker delta

$$\delta(q\triangleright r_C, \hat{g}(m-t)\triangleright e)$$

is satisfied, then e and r_C must be in the same $\triangleright$ class [they are related by the action of $q^{-1}\hat{g}(m-t)$], and so we can extract $\delta([\tilde{e}]_\triangleright, C)$ from the Kronecker delta to obtain

$$T^{R,C}(m)\sum_{e\in[\tilde{e}]_\triangleright}\alpha_e B^e(t)|GS\rangle = \frac{|R|}{|Z_{\triangleright,r_C}|}\sum_{D\in(Z_{\triangleright,r_C})_{cl}}\chi_R(D)\sum_{d\in D}\sum_{q\in Q_C}\sum_{e\in[\tilde{e}]_\triangleright}\alpha_e \times B^e(t)\delta([\tilde{e}]_\triangleright, C)\delta(q\triangleright r_C, \hat{g}(m-t)\triangleright e)|GS\rangle.$$

In addition, the dummy variable q now only appears in the expression

$$\delta(q\triangleright r_C, \hat{g}(m-t)\triangleright e).$$

However, provided that r_C and e are in the same $\triangleright$ class [as enforced by $\delta([\tilde{e}]_\triangleright, C)$], there is precisely one value of $q\in Q_C$ that satisfies $q\triangleright r_C = \hat{g}(m-t)\triangleright e$, and so we can remove the sum over q along with the Kronecker delta, to obtain

$$T^{R,C}(m)\sum_{e\in[\tilde{e}]_\triangleright}\alpha_e B^e(t)|GS\rangle = \delta([\tilde{e}]_\triangleright, C)\frac{|R|}{|Z_{\triangleright,r_C}|}\sum_{d\in Z_{\triangleright,r_C}}\chi_R(d)\sum_{e\in[\tilde{e}]_\triangleright}\alpha_e B^e(t)|GS\rangle.$$

Next, we wish to use orthogonality of characters to find the irrep R. To do so, we note that the character of the trivial irrep is one for all elements, and so

$$\sum_{d\in Z_{\triangleright,r_C}}\chi_R(d) = \sum_{d\in Z_{\triangleright,r_C}}\chi_R(d)\chi_{1_{\mathrm{Rep}}}(d^{-1}).$$

The index d appears only in this expression, and so we can use orthogonality of characters to write

$$T^{R,C}(m)\sum_{e\in[\tilde{e}]_\triangleright}\alpha_e B^e(t)|GS\rangle = \delta([\tilde{e}]_\triangleright, C)\frac{|R|}{|Z_{\triangleright,r_C}|}\left(\sum_{d\in Z_{\triangleright,r_C}}\chi_R(d)\chi_{1_{\mathrm{Rep}}}(d^{-1})\right) \times\sum_{e\in[\tilde{e}]_\triangleright}\alpha_e B^e(t)|GS\rangle = \delta([\tilde{e}]_\triangleright, C)\frac{|R|}{|Z_{\triangleright,r_C}|}\left(\delta(R,1_{\mathrm{Rep}})|Z_{\triangleright,r_C}|\right)\sum_{e\in[\tilde{e}]_\triangleright}\alpha_e B^e(t)|GS\rangle$$

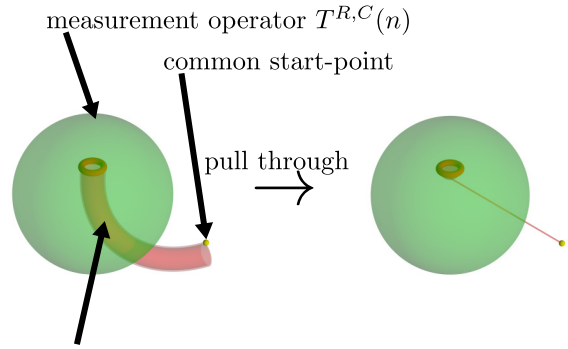

FIG. 41. We measure the spherical charge of an E-valued loop. To simplify the calculation, we deform the E-valued membrane to pull it inside the measurement operator, while keeping the start point outside.

$$= \delta([\tilde{e}]_\triangleright, C)\delta(R, 1_{\mathrm{Rep}})\sum_{e\in[\tilde{e}]_\triangleright}\alpha_e B^e(t)|GS\rangle. \quad (51)$$

This expression is just our original blob ribbon operator acting on the ground state, multiplied by $\delta([\tilde{e}]_\triangleright, C)\delta(R, 1_{\mathrm{Rep}})$. This indicates that our blob excitation has charge $([\tilde{e}]_\triangleright, 1_{\mathrm{Rep}})$. Note that because our measurement operator only runs over classes C in the kernel of ∂, if the blob ribbon operator is confined we will always get zero when we act with our measurement operator. We also note that the representation R is always the trivial representation, regardless of which set of coefficients α_e we have. This means that, as we stated earlier, even if the coefficients α_e are such that the blob ribbon operator excites the start-point vertex, this is not reflected in the charge of the excitation. The idea that the extra vertex excitation on an object may not correspond to an additional charge is something that is familiar from Kitaev's quantum double model in (2+1)D [16,29].

We previously mentioned that the looplike excitations of this model may also carry a pointlike topological charge that can be measured by the spherical measurement operators. As an example, consider the E-valued loop excitations (we also examine the higher-flux excitations, but this is left to Sec. S-V D 1 in the Supplemental Material [20] due to the increased mathematical complexity of the calculation). We wish to measure the topological charge of such a loop excitation using our spherical measurement operator, as shown in Fig. 41. Note that if the start point were inside the measurement sphere, the entire membrane operator would be wholly within the sphere (or could be deformed to be within the sphere), so the membrane operator would commute with any measurement operator applied on that sphere. Therefore, the measurement operator would just measure the charge of the ground state, i.e., the vacuum charge. This means that the combined pointlike charge of the start point and the loop excitation is trivial, and so any pointlike charge carried by the loop must be balanced by a charge belonging to the start point.

In order to find the charge of the looplike excitation, we want to calculate

$$T^{R,C}(n)\sum_{e\in E} a_e\delta(e,\hat{e}(m))|GS\rangle.$$

To do so, we must first evaluate

$$C_T^h(n)L^{e_n}(n)\delta(\hat{e}(m),e)|GS\rangle,$$

where h and e_n are stand ins for any label that can appear for the individual operators in our measurement operators. First, we note that $L^{e_n}(n)=\delta(\hat{e}(n),e_n)$ commutes with $\delta(\hat{e}(m),e)$ because both are diagonal in the configuration basis (the basis where each edge is labeled by an element of G and each plaquette is labeled by an element of E). On the other hand, $\delta(\hat{e}(m),e)$ does not commute with the magnetic membrane operator $C_T^h(n)$. We can see this by writing the surface element $\hat{e}(m)$ in terms of the constituent plaquettes, as

$$\hat{e}(m)=\prod_{p\in m}\hat{g}(\text{s.p.}(m)-v_0(p))\triangleright\hat{e}_p,$$

where e_p is the label of plaquette p and we have assumed each plaquette aligns with m (otherwise we must replace the plaquette label with the inverse). We see that this depends on the group element associated to the path $[\text{s.p.}(m)-v_0(p)]$ from the start point of the membrane to the base point of the plaquette. This path passes through the membrane n and so is affected by the magnetic membrane operator. As we prove in Sec. S-IV A 1 of the Supplemental Material [see Eq. (S72)] [20], such a path element satisfies the commutation relation

$$\begin{aligned}&\hat{g}(\text{s.p.}(m)-v_0(p))C_T^h(n)\\&=C_T^h(n)\hat{g}(\text{s.}p.(m)-\text{s.}p.(n))h^{-1}\hat{g}(\text{s.}p.(m)-\text{s.}p.(n))^{-1}\\&\times\hat{g}(\text{s.}p(m)-v_0(p)).\end{aligned}$$

Defining

$$h_{[m-n]}=\hat{g}(\text{s.}p.(m)-\text{s.}p.(n))h\hat{g}(\text{s.}p.(m)-\text{s.}p.(n))^{-1},$$

this leads to the surface label satisfying the commutation relation

$$C_T^h(n)\hat{e}(m)=h_{[m-n]}\triangleright\hat{e}(m)C_T^h(n),$$

so that

$$\begin{aligned}C_T^h(n)\delta(\hat{e}(m),e)&=\delta(h_{[m-n]}\triangleright\hat{e}(m),e)C_T^h(n)\\&=\delta\big(\hat{e}(m),h_{[m-n]}^{-1}\triangleright e\big)C_T^h(n).\end{aligned}$$

Then if we take the start points of m and n to be the same (which has no effect on the result because the start point of the measurement operator can be changed without affecting the measurement operator), this becomes

$$\begin{aligned}&C^h(n)L^{e_n}(n)\delta(\hat{e}(m),e)|GS\rangle\\&=\delta(\hat{e}(m),h^{-1}\triangleright e)C^hL^{e_n}(n)|GS\rangle\\&=\delta(\hat{e}(m),h^{-1}\triangleright e)\delta(e_n,1_E)|GS\rangle,\end{aligned}$$

where in the last line we used the fact that the contractible closed surface n must have trivial label in the ground state, while the magnetic membrane operator applied on n acts trivially on the ground state (again, because n is closed and contractible). We can then use this result to evaluate the action of the measurement operator, to obtain

$$\begin{aligned}&T^{R,C}(n)\sum_{e\in E}a_e\delta(e,\hat{e}(m))|GS\rangle\\&=\frac{|R|}{|Z_{\triangleright,r_C}|}\sum_{D\in(Z_{\triangleright,r_C})_{cl}}\chi_R(D)\sum_{d\in D}\sum_{q\in Q_C}\\&\quad\times C^{qdq^{-1}}(n)L^{q\triangleright r_C}(n)\sum_{e\in E}a_e\delta(e,\hat{e}(m))|GS\rangle\\&=\frac{|R|}{|Z_{\triangleright,r_C}|}\sum_{D\in(Z_{\triangleright,r_C})_{cl}}\chi_R(D)\sum_{d\in D}\sum_{q\in Q_C}\sum_{e\in E}a_e\\&\quad\times\delta(qd^{-1}q^{-1}\triangleright e,\hat{e}(m))\delta(e_n,1_E)|GS\rangle.\end{aligned}$$

Then $\delta(e_n,1_E)$ enforces that $C=\{1_E\}$ and so, just as with the calculation for the charge of the electric excitation, the groups involved in the projector simplify greatly. $Z_{\triangleright,r_C}$, the group of elements in G which stabilize r_C, becomes the whole group when $r_C=1_E$. This also means that the sum over representatives $q\in Q_C$ becomes trivial, with $q=1_G$ being the only element. This gives us

$$\begin{aligned}&T^{R,C}(n)\sum_{e\in E}a_e\delta(e,\hat{e}(m))|GS\rangle\\&=\delta(C,\{1_E\})\frac{|R|}{|G|}\sum_{d\in G}\chi_R(d)\sum_{e\in E}a_e\delta(d^{-1}\triangleright e,\hat{e}(m))|GS\rangle\\&=\delta(C,\{1_E\})\frac{|R|}{|G|}\sum_{d\in G}\chi_R(d)\sum_{e'=d^{-1}\triangleright e}a_{d\triangleright e'}\delta(e',\hat{e}(m))|GS\rangle\\&=\delta(C,\{1_E\})\frac{|R|}{|G|}\sum_{e'\in E}\left(\sum_{d\in G}\chi_R(d)a_{d\triangleright e'}\right)\delta(e',\hat{e}(m))|GS\rangle.\end{aligned}\tag{52}$$

Examining the term in parentheses, $(\sum_{d\in G}\chi_R(d)a_{d\triangleright e'})$, we see that treating $a_{d\triangleright e'}$ as a coefficient for d will result in this coefficient being decomposed into irreps of G, describing the way in which the group G acts on the coefficients by the $\triangleright$ action. Only the contribution from $\overline{R}$ survives, due to orthogonality of characters, meaning that the measurement only gives a nonzero result if the a coefficients contain the irrep $\overline{R}$. Therefore, the E-valued loop can have a nontrivial spherical topological charge labeled by a representation of G, depending on the choice of a coefficients. If the a coefficients are invariant under the $\triangleright$ action, so that $a_{d\triangleright e'}=a_{e'}$ for all $d\in G$ and $e\in E$, then the term in parentheses is zero unless R is the trivial irrep, because a must only contain the trivial irrep of G. We note that this is the same condition for the start point to be unexcited, as discussed in Sec. V B, and so if the start point is not excited then there is no pointlike charge for the loop (this is to be expected because if the start point is not excited then it should not carry a charge to be balanced by the loop). However, if $a_{d\triangleright e'}\neq a_{e'}$ in general, then there will be some contribution from a nontrivial irrep. In particular, if $\sum_{d\in G}a_{d\triangleright e'}=0$ for all $e'\in E$ (which is the condition for the start point to definitely be excited, as proven in Sec. S-I C of the Supplemental Material for Ref. [15]) then the contribution

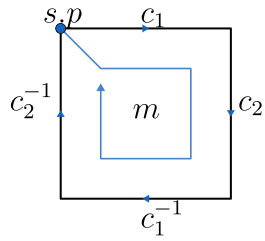

FIG. 42. The surface of the torus is conveniently represented by a square with periodic boundary conditions. The edges of this square (which are glued due to the periodic boundary conditions) are referred to as the seams of the torus. We apply electric ribbon operators along these seams to measure the noncontractible cycles of the torus and apply an E-valued membrane operator on the surface. We will also apply blob ribbon operators around the two cycles and a magnetic membrane operator over the surface. The edges cut by the dual membrane of the magnetic membrane point outwards from the page.

from the trivial irrep is proportional to

$$\sum_{d\in G} \chi_{1_{\mathrm{Rep}}}(d) a_{d\triangleright e'} = \sum_{d\in G} a_{d\triangleright e'} = 0$$

and so there is no contribution from the trivial charge measurement operator. This means that the pointlike charge is definitely nontrivial if the start point is excited.

B. Topological charge within a torus

Now we consider measuring the topological charge using a toroidal surface. To do this, we first choose such a surface to measure on. Then we project onto the space where the surface has no excitations on it, so that we only measure the charge if no objects intersect the surface itself. This is to avoid the case where a loop excitation is only partially inside the measurement surface because then we cannot unambiguously define the charge within the torus, as explained earlier in Sec. IX. A torus will allow us to measure both looplike and pointlike charge. One important thing to note is that the excitations that we measure need not lie inside the torus itself. Indeed, we measure the looplike charge of loop excitations that link with one of the cycles of the torus. For the meridian of the torus, those excitations will live inside the torus. However, the excitations that link with the longitude will be outside of the torus. This means that the torus surface can actually measure linklike excitations, made from loops outside the torus linking with those inside, rather than just looplike excitations.

The topological charges measured by the torus are more numerous and mathematically complicated to derive than those measured by the sphere. We therefore first consider the case where $\triangleright$ is trivial (case 1 from Table I) as an introduction. As illustrated in Fig. 42, we represent the torus surface as a rectangle with opposite sides identified. These sides are then one particular choice for the two independent cycles of the torus. We will choose to apply any membrane operators on this rectangle with the boundary at the cycles, before closing the rectangle by gluing the opposite edges. This leaves "seams" at the two cycles, which may have special properties because the action of the membrane operators on either side of the seam may not match. We can understand this by imagining taking a membrane operator applied on a rectangle and folding it up to glue the opposite edges together. There is no guarantee that a membrane operator acts the same on opposite sides of the rectangle, and this disparity may remain when we glue the sides together. We will see that this leads to additional joining conditions required to prevent additional excitations being present at these seams.

To find the measurement operators, we have to first project onto the case where the surface itself is not excited, then we see what degrees of freedom are left over. After projecting onto all of the plaquettes on the surface being flat, these two cycles of the torus are still left undetermined. We therefore apply two closed electric operators $\delta(\hat{g}(c_1), g_{c_1})$ and $\delta(\hat{g}(c_2), g_{c_2})$, where c_1 and c_2 are the two cycles of the torus. We also apply a closed membrane operator $\delta(\hat{e}(m), e_m)$ on the torus, with the glued boundary of this torus being $c_1 c_2 c_1^{-1} c_2^{-1}$.

Requiring fake flatness on the torus (this requirement follows from the plaquette terms) leads to the following constraint on the surface label e_m of the torus and the labels g_{c_1} and g_{c_2} of the two cycles:

$$\partial(e_m) g_{c_1} g_{c_2} g_{c_1}^{-1} g_{c_2}^{-1} = 1_G.$$

Together with the other conditions that we will discuss in this section, we prove this constraint in Sec. S-V A in the Supplemental Material [20]. We can use the fact that $\triangleright$ is trivial to rewrite this constraint in a simpler way. When $\triangleright$ is trivial, conjugating an element $\partial(e) \in \partial(E)$ by any element $g \in G$ is trivial because $g\partial(e)g^{-1} = \partial(g \triangleright e) = \partial(e)$ for all $g \in G$ and $e \in E$. Then defining $[g, h] = ghg^{-1}h^{-1}$, we can write the above constraint in various ways. For example, we have

$$\begin{aligned}
&\partial(e_m) g_{c_1} g_{c_2} g_{c_1}^{-1} g_{c_2}^{-1} = 1_G \\
&\quad\Rightarrow \partial(e_m) = g_{c_2} g_{c_1} g_{c_2}^{-1} g_{c_1}^{-1} = \left[g_{c_2}, g_{c_1}\right] \\
&\quad\Rightarrow \left(g_{c_2} g_{c_1}\right)^{-1} \partial(e_m) g_{c_2} g_{c_1} = g_{c_2}^{-1} g_{c_1}^{-1} g_{c_2} g_{c_1} \\
&\quad\Rightarrow \partial\left[\left(g_{c_2} g_{c_1}\right)^{-1} \triangleright e_m\right] = \left[g_{c_2}^{-1}, g_{c_1}^{-1}\right] \\
&\quad\Rightarrow \partial(e_m) = \left[g_{c_2}^{-1}, g_{c_1}^{-1}\right],
\end{aligned}$$

where in the fourth line we used one of the Peiffer conditions [Eq. (1) in Sec. II] and in the last line we used the fact that $\triangleright$ is trivial. We can also write the condition as

$$\partial(e_m)^{-1} = \left[g_{c_1}^{-1}, g_{c_2}^{-1}\right]. \tag{53}$$

Next we apply our magnetic membrane operator $C^h(m)$. Because we already projected to the subspace where the torus satisfies fake flatness, some of the details of the operator are arbitrary; in particular the set of paths on the direct membrane, which affect the action on the edges, can be freely chosen, as long as these paths do not cross the seams of the membrane (we take this convention because two choices of path that differ by a noncontractible cycle may give different results and this gives us a consistent way of choosing the paths).

Finally, we apply blob ribbon operators around the cycles, so that our measurement operator so far is given by

$$B^{e_{c_1}}(c_1) B^{e_{c_2}}(c_2) C^h(m) \delta(\hat{e}(m), e_m) \delta\left(\hat{g}(c_1), g_{c_1}\right) \delta\left(\hat{g}(c_2), g_{c_2}\right).$$

In principle, we could put closed blob ribbon operators anywhere on the membrane, rather than just on the cycles c_1 and c_2. However, any blob ribbon operators with label in the kernel of ∂ can be freely deformed on the surface without affecting the action of the ribbon operators because these operators are topological and there are no edge excitations on the surface (edge excitations in particular are relevant because we deform blob ribbon operators by applying edge transforms, which are trivial when the edges are unexcited). This means that any such blob ribbon operator that does not wrap around a noncontractible cycle may be contracted into nothing, while an operator that does wrap around a noncontractible cycle on the torus may be deformed to wrap around the chosen cycles c_1 and c_2 (if the ribbon operator wraps both cycles, or wraps one multiple times, we split it into multiple ribbon operators on the cycles). This is not true for the other blob ribbon operators (those with label outside the kernel) because they are confined and so are not topological. Instead, we find that this confinement leads to their position being fixed and their labels being restricted (as described in Sec. S-V A of the Supplemental Material [20]), in order not to create any excitations. This is because the magnetic membrane operator may create plaquette excitations on the seams of the torus, but these excitations can be removed if the confined blob ribbon operators lie along the seam and have appropriate labels to cancel the effect of the magnetic membrane operator. We cannot place confined ribbon operators elsewhere (away from these seams) without producing new excitations. The appropriate labels for blob ribbon operators $B^{e_{c_1}}(c_1)$ and $B^{e_{c_2}}(c_2)$, applied around the cycles c_1 and c_2, respectively, satisfy

$$\partial(e_{c_2}) = [g_{c_1}, h], \tag{54}$$

$$\partial(e_{c_1}) = [h, g_{c_2}]. \tag{55}$$

So far we have restricted the labels by requiring that our operator does not violate the plaquette conditions. However, we also need the combined operator to commute with the vertex and edge transforms on the surface so that the operator does not create vertex and edge excitations. This forces us to use linear combinations of operators with different labels. In particular, we show in Sec. S-V A of the Supplemental Material [20] that we need an equal sum of the operators with sets of labels in certain equivalence classes. If two sets of labels must appear with equal coefficients in the linear combination, we denote this with an equivalence relation. We find the relations

$$(g_{c_1}, g_{c_2}, h) \sim (x^{-1} g_{c_1} x, x^{-1} g_{c_2} x, x^{-1} h x) \ \forall\, x \in G, \tag{56}$$

$$g_{c_1} \sim \partial(e) g_{c_1} \ \forall\, e \in E, \tag{57}$$

$$g_{c_2} \sim \partial(e') g_{c_2} \ \forall\, e' \in E, \tag{58}$$

$$h \sim \partial(e'') h \ \forall\, e'' \in E. \tag{59}$$

These conditions show a striking resemblance to the relations that appear in the calculation of the ground-state degeneracy of the 3-torus in Ref. [4] and indeed they map perfectly onto them in the $\triangleright$ trivial case. This indicates that the number of topological charges we can measure within a 2-torus is the same as the ground-state degeneracy of the 3-torus in the $\triangleright$-trivial case, as found more generally in Ref. [19].

We can repeat this calculation for the special case (case 2 from Table I) where we only enforce that E is Abelian and $\partial \to \text{center}(G)$. Following the same argument as for the previous case (with full proofs given in Sec. S-V B in the Supplemental Material [20]), we obtain the restrictions

$$\partial(e_m) = [g_{c_2}, g_{c_1}]; \tag{60}$$

$$\partial(e_{c_2}) = [g_{c_1}, h]; \tag{61}$$

$$\partial(e_{c_1}) = [h, g_{c_2}]; \tag{62}$$

$$1_E = [h \triangleright e_m^{-1}]\, e_m e_{c_1}^{-1} [g_{c_1}^{-1} \triangleright e_{c_1}] e_{c_2}^{-1} [g_{c_2}^{-1} \triangleright e_{c_2}], \tag{63}$$

together with the equivalence relations

$$\begin{aligned}&((g_{c_1}, g_{c_2}, h), (e_{c_1}, e_{c_2}, e_m))\\ &\quad \sim (g(g_{c_1}, g_{c_2}, h) g^{-1}, g \triangleright (e_{c_1}, e_{c_2}, e_m))\end{aligned} \tag{64}$$

$$\begin{aligned}&(g_{c_1}, e_{c_2}, e_m)\\ &\quad \sim (\partial(e)^{-1} g_{c_1}, e_{c_2}[h \triangleright e]\, e^{-1}, e_m e^{-1} [g_{c_2}^{-1} \triangleright e])\end{aligned} \tag{65}$$

$$\begin{aligned}&(g_{c_2}, e_{c_1}, e_m)\\ &\quad \sim (\partial(r) g_{c_2}, e_{c_1}[h \triangleright r]\, r^{-1}, e_m r^{-1} [g_{c_1}^{-1} \triangleright r])\end{aligned} \tag{66}$$

and

$$(h, e_{c_1}, e_{c_2}) \sim (\partial(e)h, e_{c_1}[g_{c_2}^{-1} \triangleright e]\, e^{-1}, e_{c_2}[g_{c_1}^{-1} \triangleright e^{-1}]\, e). \tag{67}$$

These restrictions can again be mapped onto the ground-state conditions given in Ref. [4], as we demonstrate in Sec. S-V B in the Supplemental Material [20]. This indicates that again there are the same number of ground states on the 3-torus as there are charges that can be measured by the 2-torus. We note that this relationship between the ground-state degeneracy on the manifold $M \times S^1$ and the charge sectors measured by the surface M (with M in this case being the 2-torus $T^2 = S^1 \times S^1$ and $M \times S^1$ being the 3-torus) is something we may expect for a topological quantum field theory (TQFT) [30].

We can use these conditions for the measurement operators to produce a set of projection operators that span the space of allowed measurement operators, just as we did for the spherical topological charge. Each such projector then corresponds to a particular value of topological charge. We find that these projectors are labeled by certain mathematical objects that were used by Bullivant *et al.* [19] when examining the ground states of the higher lattice gauge theory model. Specifically, each projector is labeled by a class C of a particular space (to be described shortly) and an irrep R of a particular group. To define these objects, we must follow some of the workings from Ref. [19]. We note that some of our notation is slightly different from that paper, in order to match notation that we have previously used (and that was used in Ref. [4]). To understand C, we must first define boundary $\mathcal{G}$ colorings. These are sets of three elements (g_y, g_z, e_x), where $g_y, g_z \in G$ and $e_x \in E$. If this set satisfies $g_z = g_y^{-1} \partial(e_x^{-1}) g_z g_y$, it is called a boundary $\mathcal{G}$ coloring [19]. These sets are then divided into

classes, by the equivalence relation [19]

$$(g_y, g_z, e_x) \sim \big(a^{-1}\partial\big(b_2^{-1}\big)g_y a,\ a^{-1}\partial\big(b_1^{-1}\big)g_z a,\ a^{-1} \triangleright \big(b_1^{-1}\big(g_z \triangleright b_2^{-1}\big)e_x(g_y \triangleright b_1)b_2\big)\big), \quad (68)$$

for each $a \in G$ and $b_1, b_2 \in E$. Then the label C of the projector is one of these classes. The elements in C are denoted by $(c_{y,i}, c_{z,i}, d_{x,i})$ and $(c_{y,1}, c_{z,1}, d_{x,1})$ is called the representative element of the class (i is an index that runs from 1 to the size $|C|$ of the class C) [19].

Expressions similar to the right-hand side of Eq. (68) will appear frequently in this section, so we introduce some shorthand from Ref. [19], defining

$$g^{k;f} = k^{-1}\partial(f)^{-1}gk, \quad (69)$$

where g and k are elements of G and f is an element of E. We also introduce the notation from Ref. [19] that

$$e^{k,h_1,h_2;f_1,f_2} = k^{-1} \triangleright \Big(f_1^{-1}(h_2 \triangleright f_2)^{-1}e[h_1 \triangleright f_1]f_2\Big), \quad (70)$$

where k, h_1, and h_2 are elements of G and f_1 and f_2 are elements of E. Then using this notation, Eq. (68)n can be written as

$$(g_y, g_z, e_x) \sim \big(g_y^{a;b_2},\ g_z^{a;b_1}, e_x^{a,g_y,g_z;b_1,b_2}\big). \quad (71)$$

In addition to the boundary $\mathcal{G}$ colorings, Bullivant *et al.* introduce sets of three elements (g_x, e_y, e_z), where $g_x \in G$ and $e_y, e_z \in E$, with these sets of elements being called "bulk $\mathcal{G}$ colorings" [19]. These colorings are also divided into classes, this time using an equivalence relation that depends on the boundary coloring. The equivalence relation is [19]

$$(g_x, e_y, e_z) \underset{g_y,g_z}{\sim} (\partial(\lambda)g_x, [g_z \triangleright \lambda]e_y\lambda^{-1}, [g_y \triangleright \lambda]e_z\lambda^{-1})$$

for each $\lambda \in E$. The corresponding set of equivalence classes is denoted by $\mathfrak{B}_{g_y,g_z}$. Then for a class $\mathcal{E}_{g_y,g_z}$ in the set $\mathfrak{B}_{g_y,g_z}$, the elements in $\mathcal{E}_{g_y,g_z}$ are denoted by

$$(s_{x,i}, f_{y,i}, f_{z,i}),$$

for $i = 1, 2, \ldots, |\mathcal{E}_{g_y,g_z}|$. The element $(s_{x,1}, f_{y,1}, f_{z,1})$ is called the representative element for this class. A subset of these classes form a group called the stabilizer group of the class C, Z_C [19]:

$$Z_C := \big\{\mathcal{E}_C \in \mathfrak{B}_C | (c_{y,1}, c_{z,1}, d_{x,1}) = \big(c_{y,1}^{s_{x,1};f_{z,1}}, c_{z,1}^{s_{x,1};f_{y,1}} d_{x,1}^{s_{x,1},c_{y,1},c_{z,1};f_{y,1},f_{z,1}}\big)\big\},$$

where $\mathfrak{B}_C = \mathfrak{B}_{c_{y,1},c_{z,1}}$ and the subscript C in $\mathcal{E}_C$ is to remind us that $\mathcal{E}_C$ belongs to $\mathfrak{B}_C$ (and is interchangeable with the subscript $c_{y,1}, c_{z,1}$). The product for this group is defined so that the product of two classes $\mathcal{E}_C$ and $\mathcal{E}'_C \in Z_C$, $\mathcal{E}_C \cdot \mathcal{E}'_C$, is the equivalence class in $\mathfrak{B}_C$ whose representative element is

$$(s_{x,1}s'_{x,1}, f_{y,1}(s_{x,1} \triangleright f'_{y,1}), f_{z,1}(s_{x,1} \triangleright f'_{z,1})).$$

The label R of a projector to definite topological charge is an irrep of this stabilizer group.

Using the objects that we have discussed so far, we can finally define our projectors. First we define our product of individual membrane and ribbon operators:

$$Y^{(h,\, g_{c_1},\, g_{c_2},\, e_m,\, e_{c_1},\, e_{c_2}^{-1})}(m) = B^{e_{c_1}}(c_1)B^{e_{c_2}^{-1}}(c_2)C_T^h(m) \times \delta(\hat{e}(m), e_m)\delta\big(\hat{g}(c_1), g_{c_1}^{-1}\big)\delta\big(\hat{g}(c_2), g_{c_2}^{-1}\big). \quad (72)$$

Then we take appropriate linear combinations to construct the projector labeled by R and C:

$$P^{R,C}(m) = \sum_{i=1}^{|C|} \sum_{\substack{\mathcal{E}_{c_{y,i},c_{z,i}} \\ \in \mathfrak{B}_{c_{y,i},c_{z,i}}}} \sum_{m=1}^{|R|} \sum_{\lambda \in E} \delta\big(c_{y,i}, c_{y,i}^{s_{x,1};f_{z,1}}\big) \times \delta\big(c_{z,i}, c_{z,i}^{s_{x,1};f_{y,1}}\big)\delta\big(d_{x,i}, d_{x,i}^{s_{x,1},c_{y,i},c_{z,i};f_{y,1},f_{z,1}}\big) \times D^R_{m,m}\big(\big[\mathcal{E}_C^{\text{stab.}}\big]_{i,i}\big) \times Y^{(\partial(\lambda)s_{x,1},\, c_{y,i},\, c_{z,i},\, d_{x,i},\, [c_{z,i} \triangleright \lambda]f_{y,1}\lambda^{-1},\, [c_{y,i} \triangleright \lambda]f_{z,1}\lambda^{-1})}(m).$$

In this expression, $[\mathcal{E}_C^{\text{stab.}}]_{i,i}$ is the class in $\mathfrak{B}_C$ with representative element

$$\big(p_{x,i}^{-1}s_{x,1}p_{x,i},\ p_{x,i}^{-1} \triangleright \big(q_{z,i}^{-1}f_{z,1}(s_{x,1} \triangleright q_{z,i})\big), p_{x,i}^{-1} \triangleright \big(q_{y,i}^{-1}f_{y,1}[s_{x,1} \triangleright q_{y,i}]\big)\big),$$

where the p and q elements are defined as representatives which satisfy

$$(c_{y,1}, c_{z,1}, d_{x,1}) = \big(c_{y,i}^{p_{x,i};q_{z,i}}, c_{z,i}^{p_{x,i};q_{y,i}}, d_{x,i}^{p_{x,i},c_{y,i},c_{z,i};q_{y,i},q_{z,i}}\big)$$

and $(p_{x,1}, q_{y,1}, q_{z,1}) = (1_G, 1_E, 1_E)$ (that is the p and q move us around in the class C to get from element i to the representative element labeled by 1). In Sec. S-V C of the Supplemental Material [20] we perform the lengthy algebraic task of proving that the operators $P^{R,C}(m)$ labeled by the objects R and C form an orthogonal and complete set of projectors, indicating that the topological charges that we can measure with the torus are appropriately labeled by a class C of boundary $\mathcal{G}$ colorings and an irrep R of the corresponding stabilizer group.

X. CONCLUSION

In this work, we have discussed in detail the features of the higher-lattice gauge theory model in (3+1)D. We started by constructing the ribbon and membrane operators which create the simple excitations of the model. We found that there were two categories of excitation, those best labeled by objects related to the group G and those best labeled by objects related to the other group, E. The former type of excitation, consisting of pointlike electric excitations and looplike magnetic flux tubes, are analogous to the excitations we expect from ordinary lattice gauge theory. The other type, consisting of pointlike 2-gauge fluxes and looplike 2-gauge charges, are related to properties of the surfaces of the lattice, instead of paths. We then considered the braiding properties of these excitations. When the map $\triangleright$, defined as part of the crossed module, is trivial, these two types of excitations form separate sectors that do not have nontrivial braiding between them (only within each sector). However, when $\triangleright$ is nontrivial (although we had to restrict to the case where E is Abelian and ∂ maps to the center of G) some magnetic excitations acquire a 2-flux and can braid nontrivially with all other types of

excitation. This is reflected in the fact the membrane operator that produces the magnetic excitation must be modified to depend on the surface elements of the lattice.

Another feature that we looked at was the condensation of certain excitations, and the accompanying confinement of others. We found that this was controlled by the map ∂, with no condensation or confinement when ∂ maps only to the identity element (at least in the case where E is Abelian). By altering ∂ while keeping the groups fixed, we introduce condensation for some of the looplike (magnetic and E-valued loop) excitations while causing some of the pointlike (electric and blob) excitations to become confined. This can be thought of as a condensation-confinement transition, where the confined excitations are those that had nontrivial braiding with the condensed excitations. We also looked at the topological charge carried by the excitations, by constructing projectors to definite topological charge. The available charges depend on the surface of measurement, and we constructed the projectors for a spherical and toroidal surface. Similar to results found in Ref. [19], we found that the charges measured by the 2-torus surface matched the ground-state degeneracy on the 3-torus. We saw that these 2-torus surfaces generally measured links, rather than simple looplike excitations, suggesting that the number of inequivalent linklike excitations is equal to the ground-state degeneracy.

In Ref. [14], we already mentioned several potential avenues of interest for further study based on this work. Rather than repeat ourselves here, we would like to discuss one of these directions further. In this paper, we gave braiding relations in terms of the simple excitations produced by the membrane and ribbon operators. However, it would be useful to obtain the braiding relations and other properties in terms of the topological charge. To do so, it would first be necessary to find the fusion rules for the various topological charges. Because the topological charge depends on the measurement surface, we would need additional machinery to describe how different charges can fuse in a simple way. Once this has been done, we can consider a braiding process where the individual excitations are projected onto states of definite charge, and the overall system is similarly projected to definite total charge, in order to find the braiding relations satisfied by the charges [analogous to the approach used for (2+1)D theories]. In addition to better understanding this particular model, creating this machinery would give us a structure with which to study different models for topological phases in (3+1)D and understand what properties we expect. We note that, as mentioned in Ref. [14], from some preliminary calculations we can see that different torus charges can only fuse if they have the same value of a certain "threading flux," meaning that the quantum numbers passing through the two loops must be the same (for example, if they are linked to the same excitation). When this threading flux is nontrivial, we are considering the fusion of two looplike excitations while both are linked to another excitation. This means that the braiding of these charges would correspond to so-called "necklace braiding" [27] (or three-loop braiding [25]), meaning the braiding of two loops while linked to another. For general models this braiding can give different results compared to the usual two-loop braiding [25,26]. Therefore, having a structure in which to consider this process for generic (3+1)D topological models would be most useful.

Related to this idea, it would also be useful to understand better where the higher-lattice gauge theory models fit into the wider landscape of (3+1)D topological phases. It is conjectured that all (3+1)D bosonic topological phases with bosonic pointlike particles can be realized by Dijkgraaf-Witten theories [5]. This implies that the higher-lattice gauge theories should also be equivalent to lattice gauge theory, albeit with some additional nontopological content in the form of the condensed and confined excitations. It would be interesting to explicitly demonstrate this equivalence (or else disprove it), whether through a direct mapping or by considering the topological charges and other data as we described above and showing that they match between the two models. We have made some progress in this direction, but leave the results for future study.

In compliance with EPSRC policy framework on research data, this publication is theoretical work that does not require supporting research data.

ACKNOWLEDGMENTS

The authors would once again like to thank J. Faria Martins and A. Bullivant for helpful discussions about the higher-lattice gauge theory model. We are also grateful to P. Fendley for advice on the preparation of this series of papers. We acknowledge support from EPSRC Grant No. EP/S020527/1.

[1] K. Walker and Z. Wang, (3+1)-TQFTs and topological insulators, Front. Phys. **7**, 150 (2012).

[2] Y. Wan, J. C. Wang, and H. He, Twisted gauge theory model of topological phases in three dimensions, Phys. Rev. B **92**, 045101 (2015).

[3] D. J. Williamson and Z. Wang, Hamiltonian models for topological phases of matter in three spatial dimensions, Ann. Phys. **377**, 311 (2017).

[4] A. Bullivant, M. Calcada, Z. Kadar, P. Martin, and J. Faria Martins, Topological phases from higher gauge symmetry in 3+1D, Phys. Rev. B **95**, 155118 (2017).

[5] T. Lan, L. Kong, and X.-G. Wen, Classification of (3+1)D bosonic topological orders: The case when pointlike excitations are all bosons, Phys. Rev. X **8**, 021074 (2018).

[6] T. Lan and X.-G. Wen, Classification of 3 + 1D bosonic topological orders (II): The case when some pointlike excitations are fermions, Phys. Rev. X **9**, 021005 (2019).

[7] S. Doplicher, R. Haag, and J. E. Roberts, Local observables and particle statistics I, Commun. Math. Phys. **23**, 199 (1971).

[8] S. Doplicher, R. Haag, and J. E. Roberts, Local observables and particle statistics II, Commun. Math. Phys. **35**, 49 (1974).

[9] H. Pfeiffer, Higher gauge theory and a non-Abelian generalization of 2-form electrodynamics, Ann. Phys. **308**, 447 (2003).

[10] J. C. Baez and J. Huerta, An invitation to higher gauge theory, Gen. Relativ. Gravit. **43**, 2335 (2011).

[11] S. Gukov and A. Kapustin, Topological quantum field theory, nonlocal operators, and gapped phases of gauge theories, arXiv:1307.4793.

[12] A. Kapustin and R. Thorngren, Topological field theory on a lattice, discrete theta-angles and confinement, Adv. Theor. Math. Phys. **18**, 1233 (2014).
[13] A. Kapustin and R. Thorngren, *Higher Symmetry and Gapped Phases of Gauge Theories* (Springer, Cham, 2017), pp. 177–202.
[14] J. Huxford and S. H. Simon, Excitations in the higher-lattice gauge theory model for topological phases. I. Overview, Phys. Rev. B **108**, 245132 (2023).
[15] J. Huxford and S. H. Simon, Excitations in the higher-lattice gauge theory model for topological phases. II. The (2+1)-dimensional case, Phys. Rev. B **108**, 245133 (2023).
[16] A. Y. Kitaev, Fault-tolerant quantum computation by anyons, Ann. Phys. **303**, 2 (2003).
[17] M. Levin and X.-G. Wen, String-net condensation: A physical mechanism for topological phases, Phys. Rev. B **71**, 045110 (2005).
[18] H. Bombin and M. A. Martin-Delgado, A family of non-Abelian Kitaev models on a lattice: Topological condensation and confinement, Phys. Rev. B **78**, 115421 (2008).
[19] A. Bullivant and C. Delcamp, Excitations in strict 2-group higher gauge models of topological phases, J. High Energy Phys. 01 (2020) 107.
[20] See Supplemental Material at http://link.aps.org/supplemental/10.1103/PhysRevB.109.035152 for a collection of algebraic proofs that support the results in the main text.
[21] J. C. Baez, Higher Yang–Mills theory, arXiv:hep-th/0206130 v2.
[22] F. A. Bais, Flux metamorphosis, Nucl. Phys. B **170**, 32 (1980).
[23] M. Bucher, K.-M. Lee, and J. Preskill, On detecting discrete Cheshire charge, Nucl. Phys. B **386**, 27 (1992).
[24] M. G. Alford, K.-M. Lee, J. March-Russell, and J. Preskill, Quantum field theory of non-abelian strings and vortices, Nucl. Phys. B **384**, 251 (1992).
[25] C. Wang and M. Levin, Braiding statistics of loop excitations in three dimensions, Phys. Rev. Lett. **113**, 080403 (2014).
[26] S. Jiang, A. Mesaros, and Y. Ran, Generalized modular transformations in 3+1D topologically ordered phases and triple linking invariant of loop braiding, Phys. Rev. X **4**, 031048 (2014).
[27] A. Bullivant, A. Kimball, P. Martin, and E. C. Rowell, Representations of the necklace braid group: Topological and combinatorial approaches, Commun. Math. Phys. **375**, 1223 (2020).
[28] A. Bullivant, J. Faria Martins, and P. Martin, Representations of the loop braid group and Aharonov-Bohm like effects in discrete (3+1)-dimensional higher gauge theory, Adv. Theor. Math. Phys. **23**, 1685 (2019).
[29] A. Komar and O. Landon-Cardinal, Anyons are not energy eigenspaces of quantum double Hamiltonians, Phys. Rev. B **96**, 195150 (2017).
[30] M. F. Atiyah, Topological quantum field theory, Pub. Math. l'Institut Hautes Sci. **68**, 175 (1988).